



**Comparative approach to barnacle
adhesive-surface interactions**

Alessio Di Fino

A thesis submitted to Newcastle University in candidature for the
Degree of Doctor of Philosophy

School of Marine Science and Technology

February 2015

Abstract

Barnacles are considered to be one of the major marine fouling organisms. Their settlement behaviour has been investigated using mainly *Balanus amphitrite* as a model organism. To better understand the mechanisms involved during the colonisation of surfaces by cypris larvae we have investigated another species, *B. improvisus*, which is reported to have different surface preferences compared to *B. amphitrite*. This study aims to unravel the effects of surface physicochemical cues, in particular surface free energy (SFE), surface charge and elastic modulus on the settlement of cyprids of both species. The use of well-defined surfaces under controlled conditions further facilitates comparison of the results with *B. amphitrite*. Furthermore, since this phase of pre-settlement behaviour is characterised by temporary adhesive (footprint) deposition, considered to be fundamental to surface exploration and surface discrimination by cyprids, some of the chemistries used for the settlement assays were used to investigate temporary adhesive-surface interactions.

Cyprids were exposed to a series of model surfaces, namely self-assembled monolayers (SAMs) of alkanethiols with varying end-groups, homogeneously applied to gold-coated polystyrene Petri dishes. The settlement response was significantly higher on negatively charged SAMs and lower on positively charged surfaces, while intermediate settlement occurred on neutral SAMs. Furthermore, no effects were observed when data were plotted against surface free energy after 48 hr of exposure. Temporary adhesive on SAMs was investigated using imaging ellipsometry and atomic force microscopy. Relatively thick footprints with low wetting were found on positively charged surfaces. Settlement of both species was also low on these surfaces. Footprints were thinner and spread more on hydrophobic surfaces. The adhesion force of temporary adhesive measured with functionalised AFM tips was higher on hydrophobic and negatively charged surfaces for both species. Furthermore, PDMS-based surfaces were prepared varying the elastic modulus, keeping constant other parameters, settlement behaviour and strength of adhesion of juveniles and adults were tested.

We conclude that cyprid settlement behaviour of both species is influenced more by surface charge than SFE under controlled conditions. The temporary adhesives (footprints) of the two species had a stronger affinity for hydrophobic surfaces. Contrary

to previous reports, therefore, the settlement preferences and adhesive secretion of these two species are similar. Elastic modulus influences settlement, juveniles and adults removal of both species, although *B. improvisus* is more sensitive if compared with *B. amphitrite*. This finding will be important for understanding the mechanism of surface selection by cyprids and for the development of future antifouling technologies.

Acknowledgments

First and foremost I would like to thank my supervisor Prof. Tony Clare for his invaluable support throughout this project. From the guidance, suggestions and for providing the key concepts and practical insight that have been crucial to the development my research. It has been gratifying and an honour to work with you.

I am especially grateful to Nick Aldred for his daily help, in Newcastle and when I was abroad for collaborations, precise, professional and always critical. For all the effort in teaching me the English language (at least we have tried). I have been very lucky to work with you. Thank you Nick!!!

Thank you to Luigi Petrone for the time spent in the laboratory until late, teaching me the smart approach to the research without stop smiling.

Thanks must also go to all the colleagues and staff at the School of Marine Science and Technology (Newcastle University) for the company and the great support received. I would like to thank the Seacoat project which has given me the possibility to work into a fantastic European network. A special thank is for the colleagues of Linköping University, ETH Zurich, Heidelberg University and International Paint, with them I have had the possibility to learn new topics and methodologies.

Thank you to my family and friends that from Newcastle, Genoa and Bari made my life brighter. You have always been by my side, in all the places that I visited for the project, making me outward-looking and confident.

Finally, this research would not have been possible without the financial support from the Seventh Framework Programme FP7/2007–2013 under Grant Agreement number [237997] (SEACOAT).

Table of contents

Abstract.....	i
Acknowledgments.....	iii
List of Tables.....	viii
List of Figures.....	ix
Chapter 1. Fouling and adhesion.....	1
1.1 Introduction.....	1
1.2 Adhesion.....	5
1.3 Barnacles.....	7
1.3.1 The cyprid.....	9
1.3.2 Barnacle adhesives.....	12
1.4 Surface influence on barnacle adhesion.....	18
1.4.1 Surface chemistry.....	18
1.4.2 Topography.....	19
1.4.3 Biofilm.....	20
1.4.4 Larval age.....	21
1.5 Adult barnacle adhesion.....	21
1.6 Scope of the thesis.....	24
Chapter 2. Influence of surface charge and surface energy on the settlement behaviour of barnacles.....	25
2.1 Introduction.....	25
2.2 Materials and methods.....	28

2.2.1 Culture of cyprids of <i>B. amphitrite</i>	28
2.2.2 Culture of cyprids of <i>B. improvisus</i>	29
2.2.3 Substrata for settlement assays.....	30
2.2.4 Gold coating procedure.....	31
2.2.5 Self-assembled monolayer preparation.....	32
2.2.6 Infrared reflection-absorption spectroscopy – IRAS.....	34
2.2.7 Ellipsometry.....	34
2.2.8 Contact angle goniometry.....	34
2.2.9 Surface energy calculation.....	35
2.2.10 Stability tests.....	36
2.2.11 Data analysis.....	36
2.3 Results.....	37
2.3.1 Stability test in ASW.....	37
2.3.2 Effect of cyprid age.....	40
2.3.3 Determination of settlement assay method.....	41
2.3.4 Effect of container.....	42
2.3.5 Settlement assays using glass and polystyrene.....	43
2.3.6 Settlement in relation to Gibbs surface energy.....	43
2.3.7 Settlement in response to surface charge.....	44
2.4 Discussion.....	49
Chapter 3. Footprint characterisation.....	59
3.1 Introduction.....	59

3.1.1 Adsorption.....	61
3.1.2 Approach to the study.....	63
3.2 Materials and methods.....	67
3.2.1 Culture of cyprids.....	67
3.2.2 Footprints observation.....	67
3.2.3 Self assembled monolayer preparation.....	67
3.2.4 Imaging ellipsometry.....	68
3.2.5 Atomic force microscope.....	69
3.2.6 Scanning electronic microscope.....	70
3.2.7 Data analysis.....	70
3.3 Results and Discussion.....	70
3.3.1 Cyprid antennular, morphological observations.....	70
3.3.2 Microscopic observation of cyprid footprints.....	72
3.3.3 Imaging ellipsometry.....	72
3.3.4 Atomic force microscopy.....	80
Chapter 4. Effect of elastic modulus on surface selection and barnacle adhesion.....	90
4.1 Introduction.....	90
4.2 Material and methods.....	94
4.2.1 Settlement assay.....	94
4.2.2 Removal of juveniles under shear using a flow cell.....	95
4.2.3 Removal of adults by push off.....	96
4.2.4 Data analysis.....	96

4.2.5 Surfaces for settlement assays.....	97
4.2.6 Surface preparation.....	97
4.2.7 Elastic modulus calculation.....	99
4.2.8 Contact angle goniometry.....	100
4.3 Results.....	101
4.3.1 Settlement assay.....	101
4.3.2 Removal of juveniles by flow cell.....	102
4.3.3 Removal of adults using the push-off machine.....	103
4.3.4 Basal failure (percentage basis remaining on surface).....	104
4.3.5 Percentage coverage by adhesive.....	106
4.4 Discussion.....	107
Chapter 5. Discussion.....	114
5.1 Summary.....	114
5.2 Settlement behaviour.....	115
5.3 Footprint characterisation.....	115
5.4 Influence of elastic modulus.....	116
5.5 Final thoughts.....	117
Appendix.....	120
References.....	124

List of Tables

Table 1. Surface energy components for water, glycerol and diiodomethane in mJ m^{-2} (Good, 1993).	36
Table 2. Significant differences identified using Kruskal–Wallis/Dunn’s tests on data in Figure 20.	44
Table 3. The subset of samples used in each comparative experiment is indicated, as well as SAM thicknesses, contact angles measured with the three test liquids (γ_W , γ_{DIM} , γ_G), and surface energy parameters (γ_{LW} , γ_{AB} , γ^+ , γ^- , γ_s) calculated with the GvOC model, for all surfaces.	48
Table 4. Values of contact angles and surface energy for each SAM.	68
Table 5. Values of adhesion force (nN) recorded with functionalised tips for both species.	87
Table 6. Properties of mixtures of silicone-based surfaces used for cyprid settlement assays and removal assays with juveniles and adults of <i>B. amphitrite</i> and <i>B. improvisus</i> .	98
Table 7. Values of viscosity, elastic modulus, contact angle and surface energy for each surface.	101

List of Figures

Fig. 1 Representative fouling organisms with their scale size (Callow, 2012).	2
Fig. 2 Functional principles of biological attachment systems and physical effects involved. After Santos et al. (2013) from Gorb (2008).	5
Fig. 3 Mode of attachment of most investigated bio-fouling organisms, (a) mussel, (b) barnacle and (c) tubeworm (Fig. from Kamino, 2010).	7
Fig. 4 Life cycle of a thoracican barnacle showing the planktonic, planktobenthic and benthic stages.	8
Fig. 5 Antennule of <i>Balanus amphitrite</i> cyprid showing the 2 nd , 3 rd and 4 th segments (after Aldred and Clare 2008).	10
Fig. 6 <i>Balanus improvisus</i> : the 3rd segment of the cyprid antennules.	10
Fig. 7 Terminal and sub-terminal setae of the 4 th antennular segment of <i>Balanus improvisus</i> .	11
Fig. 8 Footprints of <i>B. amphitrite</i> stained by Coomassie Brilliant Blue-G- Colloidal Blue-silver (CBB-G).	13
Fig. 9 Footprint of <i>B. amphitrite</i> cyprid visualised on a -CH ₃ terminated SAM by imaging ellipsometry.	14
Fig. 10 Basal view of adult of <i>B. improvisus</i> attached to Plexiglas plate.	22
Fig. 11 Adult of (A) <i>B. amphitrite</i> and (B) <i>B. improvisus</i> .	24
Fig. 12: Schematic of the resistively-heated vacuum evaporation system for Ti and Au deposition, and the device for coating PS well plates. The initial and final positions are shown (horizontal and with the PS plates tilted at 30°, respectively). The plate rotates slowly around the vertical axis throughout the process.	32
Fig. 13 A gold-coated.PS 24-well plate and Falcon 1006 Petri dishes.	32
Fig. 14 Chemical structures of the thiols used for the preparation of the self-assembled monolayer surfaces.	34
Fig.15 IRAS spectra of N(CH ₃) ₃ ⁺ -terminated SAM in the region between 1600-1000 cm ⁻¹ before and after 4 days immersion in ASW.	38
Fig. 16 IRAS spectra of COOH-terminated SAM in the region between 1800-1100 cm ⁻¹ before and after 4 days immersion in ASW.	39
Fig. 17 IRAS spectra of CH ₃ -terminated SAM in the region between 3050-2750 cm ⁻¹ before and after 4 days immersion in ASW.	39
Fig. 18 IRAS spectra of OH-terminated SAM in the region between 3500-2700 cm ⁻¹ .	40

- Fig. 19 Mean percentage settlement (\pm standard error) of cyprids of *B. improvisus* 41
from 0- to 5-days-old in uncoated PS Petri dishes after 24 and 48 h in FSW
(salinity = 20). Results of Tukey pairwise comparisons are presented.
- Fig. 20 Mean percentage of cyprids (\pm standard error) (0-day-old) of *Balanus* 42
improvisus in FSW (salinity = 20) settled after 24, 48 and 72 h in (A) uncoated PS
24-well plates and (B) uncoated sealed Petri dishes.
- Fig. 21 Mean percentage settlement (\pm standard error) of (A) *B. amphitrite* in 43
FSW (salinity = 32) and (B) *B. improvisus* cyprids in FSW (salinity = 20) on glass
and polystyrene after 24 h and 48 h.
- Fig. 22 Mean percentage settlement of cyprids (\pm standard error) of (A) *B.* 44
amphitrite in FSW (salinity = 32) and (B) *B. improvisus* cyprids in FSW (salinity
= 32) settled on CH₃- and OH-terminated SAMs after 24 h and 48 h. Settlement
on the control PS was $13 \pm 2\%$ and $29 \pm 3\%$ after 24 and 48 h, respectively.
- Fig. 23 Mean percentage settlement (\pm standard error) of *B. improvisus* on SAMs 45
applied to 24 well plates with 2 mL FSW (salinity= 32) after 48 hr, where -CH₃ is
an abbreviation of HS(CH₂)₁₅CH₃, -OH = HS(CH₂)₁₆OH, -NH₃⁺ = HS(CH₂)₁₆NH₂,
-N(CH₃)₃⁺ = HS(CH₂)₁₁N(CH₃)₃⁺, -CO₂⁻ (TSA) = HSC₆H₄COOH, -CO₂⁻
(thioglycolic acid) = HSCH₂COOH and -CO₂⁻(MHA) = HS(CH₂)₁₆COOH. Tukey
pairwise comparisons are presented. Means that do not share a letter are
significantly different.
- Fig. 24 Settlement of cypris larvae of *B. improvisus* on SAMs applied to sealed 47
Petri dishes with 15 mL FSW (salinity=20) after 48 hr, where -CH₃ is an
abbreviation of HS(CH₂)₁₅CH₃, -OH = HS(CH₂)₁₆OH, -NH₃⁺ = HS(CH₂)₁₆NH₂, -
N(CH₃)₃⁺ = HS(CH₂)₁₁N(CH₃)₃⁺, -CO₂⁻ (TSA) = HSC₆H₄COOH, -PO₃²⁻ =
HS(CH₂)₁₁PO(OH)₂ and -SO₃⁻ = HS(CH₂)₁₁SO₃Na. Tukey pairwise comparisons
are presented. Means that do not share a letter are significantly different.
- Fig. 25 Settlement percentage of cypris larvae of *B. improvisus* used in this work 55
and *B. amphitrite* from a previous experiment (Petrone et al. 2011) where -CH₃ is
an abbreviation of HS(CH₂)₁₅CH₃, -OH = HS(CH₂)₁₆OH, -NH₃⁺ = HS(CH₂)₁₆NH₂,
-N(CH₃)₃⁺ = HS(CH₂)₁₁N(CH₃)₃⁺, -CO₂⁻ (TSA) = HSC₆H₄COOH.
- Fig. 26 Schematic of imaging ellipsometry with a sensitive CCD camera 65
- Fig. 27 Reflection of incident laser light from the sample (thin film on a reflecting 66
substrate). Changes of the incident elliptical polarization are caused by intrinsic
properties of the probed coating. (from Nanofilm EP3 ellipsometry Nanofilm
Technologie GmbH, Göttingen, Germany).
- Fig. 28 Lateral (A) and bottom (B) views of SEM micrographs of an antennule of 70
a cyprid of *B. improvisus* showing the attachment disc.
- Fig. 29 SEM micrographs of cypris antennules of (A) *B. amphitrite* (Aldred and 71
Clare, 2008) and (B) *B. improvisus* (this work).
- Fig. 30 Optical images of footprints stained by CBB-G for (A) *B. improvisus* and 72
(B) *B. amphitrite* cyprids.
- Fig. 31 Footprint trial (left) of *B. improvisus* cyprid and cross-section profile of a 74
single footprint visualized by imaging ellipsometry on a CH₃ -terminated SAM
surface.

Fig. 32 Footprint of cyprid of <i>B. amphitrite</i> on a CH ₃ -terminated SAM, with cross section (profile diagram) and overall 2-D distribution on the surface (map window) with the red bar indicating the cross section.	75
Fig. 33 3-D elaboration of cypris footprint (<i>B. amphitrite</i>) on CH ₃ -terminated SAM.	75
Fig. 34 Thickness (\pm standard error) of footprints from <i>B. amphitrite</i> and <i>B. improvisus</i> deposited onto different SAMs obtained by imaging ellipsometry. Results of Tukey pairwise comparisons are presented. Means that do not share a letter are significantly different.	76
Fig. 35 3-D maps of cypris footprints of <i>B. amphitrite</i> (A) and <i>B. improvisus</i> (B) on N(CH ₃) ₃ ⁺ -terminated SAM.	77
Fig. 36 Bar plot of footprints area (\pm standard error) of <i>B. amphitrite</i> (black) and <i>B. improvisus</i> (grey) deposited onto a series of SAMs. Data were obtained by imaging ellipsometry. Results of Tukey pairwise comparisons are presented.	78
Fig. 37 Cypris footprints of <i>B. amphitrite</i> (A) and <i>B. improvisus</i> (B) on CH ₃ -terminated SAM.	78
Fig. 38 Cyprid footprints of <i>B. amphitrite</i> (A) and <i>B. improvisus</i> (B) detected on OH-terminated SAM. Note that in B the footprint has two distinct height profiles.	79
Fig. 39 Cypris footprints of <i>B. amphitrite</i> (A) and <i>B. improvisus</i> (B) detected on CO ₂ ⁻ (MHA) -terminated SAM.	79
Fig. 40 Bar plot of the volume (\pm standard error) of footprints deposited onto different SAMs obtained by imaging ellipsometry elaboration. Results of Tukey pairwise comparisons are presented. Means that do not share a letter are significantly different.	80
Fig. 41 Footprint of (A) <i>B. amphitrite</i> imaged by AFM on CH ₃ -terminated SAM surface and (B) its 3-D representation.	82
Fig. 42 Graphics show pull-off AFM force measurements using a CH ₃ -SAM tip on cypris footprints of <i>B. amphitrite</i> (A) and <i>B. improvisus</i> (B). The means and standard deviations were calculated by fitting the histogram to a Gaussian distribution.	83
Fig. 43 Graphics show pull-off AFM force measurements using CO ₂ ⁻ (TSA)-terminated SAM tip on cypris footprints of <i>B. amphitrite</i> (A) and <i>B. improvisus</i> (B). The means and standard deviations were calculated by fitting the histogram to a Gaussian distribution.	84
Fig. 44 Graphics show pull-off AFM force measurements using N(CH ₃) ₃ ⁺ -SAM tips on cypris footprints of <i>B. amphitrite</i> (A) and <i>B. improvisus</i> (B). The means and standard deviations were calculated by fitting the histogram to a Gaussian distribution.	85
Fig. 45 Graphics show pull-off AFM force measurements using OH -SAM tips on cypris footprints of <i>B. amphitrite</i> (A) and <i>B. improvisus</i> (B). The means and standard deviations were calculated by fitting the histogram to a Gaussian distribu	86

Fig. 46 Screen grabs of barnacles that have been scanned and their basal areas measured using the automated methods' software.	96
Fig. 47 General structure of hydroxyl terminated poly(dimethylsiloxane).	97
Fig. 48 General structure of tetraethyl orthosilicate–crosslinker (TEOS).	98
Fig. 49 General structure of bis(2-ethylhexyl)hydrogen phosphate (BEHHP).	98
Fig. 50 Values of elastic modulus calculated using storage modulus at 20 degrees by dynamic mechanical analysis (DMA) with 95% confidence interval.	100
Fig. 51 Cyprid settlement (\pm standard error) after 48 h for <i>B. amphitrite</i> and <i>B. improvisus</i> . Data were obtained for 20 cyprids per surface and 15 replicates. Tukey pairwise comparisons are presented. Means that do not share a letter are significantly different.	102
Fig. 52 Percentages (\pm standard error) of juveniles of <i>B. amphitrite</i> and <i>B. improvisus</i> removed from the surfaces under shear. Tukey pairwise comparisons are presented. Means that do not share a letter are significantly different.	103
Fig. 53 Percentages (\pm standard error) of adults of <i>B. amphitrite</i> and <i>B. improvisus</i> removed from the surface by the push-off machine. Tukey pairwise comparisons are presented. Means that do not share a letter are significantly different.	104
Fig. 54 Percentages (\pm standard error) of base coverage of <i>B. amphitrite</i> and <i>B. improvisus</i> remained on the surfaces after removal by push off. Tukey pairwise comparisons are presented.	105
Fig. 55 Percentages (\pm standard error) of adhesive coverage of <i>B. amphitrite</i> and <i>B. improvisus</i> remained on the surfaces after removal by push off. Tukey pairwise comparisons are presented. Means that do not share a letter are significantly different.	107
Fig. 56 Bases tended to remain intact on the surface with an elastic modulus of 32 MPa. (A) <i>B. amphitrite</i> , (B) <i>B. improvisus</i> .	110
Fig. 57 Bases remaining on the surface with an elastic modulus 0.73 MPa (A) <i>B. amphitrite</i> , (B) <i>B. improvisus</i> .	110
Fig. 58 Adhesive stained with CBB on the surface with an elastic modulus of 0.36 MPa (A) <i>B. amphitrite</i> , (B) <i>B. improvisus</i> .	111

Chapter 1. Fouling and adhesion

1.1 Introduction

Marine organisms that colonise submerged substrata are commonly sessile and thus unable to move once permanently settled. Bacteria, algae, plants and animals, individually or in colonies grow on substrata from the littoral to the abyssal zone. These organisms are collectively referred to as biofouling, which is defined here as the colonisation and growth of organisms on submerged artificial substrata. Some of these fouling organisms may develop complex and diverse sessile assemblages, which can grow spatially depending on the environmental conditions such as currents, light and oxygenation. The biomass that these assemblages attain depends on a balance between the input of energy for growth and reproduction, for example by photosynthesis by algae in the photic zone, and controls to growth such as predation.

The planktonic-benthic transition is a crucial point in the life cycle of fouling species. They need to find a suitable place to settle that requires strong adhesion, an adequate flux of nutrients for growth and development, and for those that reproduce sexually, the presence of conspecifics.

Competition for the space by benthic organisms pertains to both natural and artificial, surfaces; the former including basibionts. Settlement is challenging and competition for space means that incumbents may modify the settlement behaviour of other potential colonisers by changing the surface character and perhaps the chemistry of the overlying water.

Given the importance of this phase of the life cycle and the challenges faced, it should not be surprising that sessile organisms have evolved strategies, under intense selection pressure, to increase their chance of finding a suitable location to settle. Thus organisms have developed different and complex systems for sensing and fixing onto substrata. Accompanying the great diversity, of fouling species worldwide are differences in their requirements in terms of the physical and chemical characteristics of the surface and the nature of the adhesives used, perhaps even for closely related species.

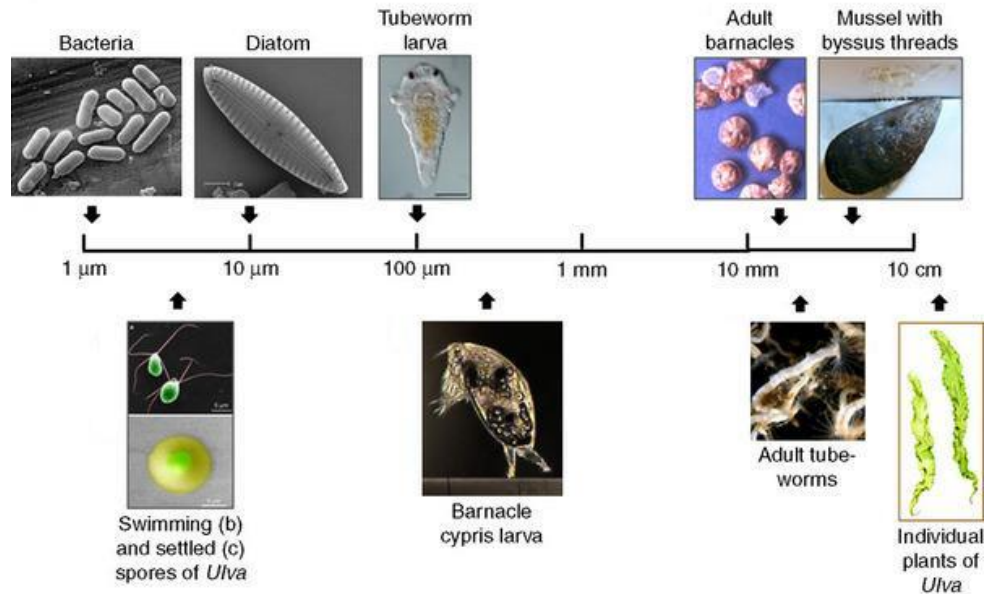


Fig. 1 Representative fouling organisms with their scale size (Callow, 2012).

Fouling organisms are typically divided into microfouling (unicellular organisms such as bacteria, fungi and algae), or macrofouling forms (e.g. hydrozoans, bryozoans, barnacles, polychaete tubeworms, molluscs and ascidians) (Fig. 1). Biofouling is commonly regarded as a successional process (Wahl, 1989) such that when a surface is newly immersed it is conditioned within seconds to minutes by adsorption of molecules to form a conditioning layer. Microfouling, including bacteria, diatoms, then follows during hours to days, and finally macrofouling over days to weeks. This successional hypothesis has been challenged as it suggests that macrofouling requires the presence of microfouling. Each of these groups of foulers have different lapses of time to approach and settle onto a surface, generally after few minutes/hours a surface is covered by molecules and micro-fouler generating a biofilm, after hours/days is possible to detect macro-foulers, but as Callow and Callow (2011) specify, it does not follow a linear successional model (“step by step”), different organisms are continually approaching and covering surfaces making layers on layers building real assemblages of organism or community of organisms.

While this holds for some species, such as *Hydroides elegans* (Hadfield, 2011), it does not for others, e.g *Balanus amphitrite* (Olivier, *et al.*, 2000) and an alternative dynamic model of fouling has been proposed (Clare *et al.*, 1992). It is, of course, inevitable that bacteria will rapidly colonise surfaces, but their presence does not constitute the presence of biofilm. Biofilm describes the development of a 3-dimensional structure

through secretion of extracellular polymeric substances (Dobretsov *et al.*, 2013) to create a gel matrix.

Marine biofouling is most commonly discussed in the context of ships' hulls, but affects all surfaces immersed in the marine environment including, aquaculture cages, heat exchangers and pipelines. Efforts are thus needed to avoid this unwanted accumulation of organisms. The accumulation of marine organisms on the surface not only weakens materials but also increases their roughness and frictional drag. The frictional drag on a heavily fouled hull can result in a power penalty of up to 86 % (Callow and Callow, 2011). The drag increment, with relative higher surface exposed to the water (Grigson, 1992), is reflected in higher consumption of fuel to maintain speed (Townsin, 2003), with a concomitant increase in greenhouses gas emissions. Schultz *et al.*, (2011), based on calculations for a mid-sized naval vessel, estimated that the total cost of hull fouling to the US Navy is \$56 million per annum. Kempf, (1937) revealed that the maximum drag penalty takes place when barnacles cover 75% of the hull and was only reduced by one third for 5% coverage. Schultz (2004), however, showed a peculiarity of barnacles with respect to their effect on the drag, namely low coverage resulted in higher drag than high coverage (Thompson *et al.*, 2008).

Attempts to mitigate fouling date back to early history (Callow, 1990; Anderson *et al.*, 2003), and presumably have challenged humans ever since they first put to sea. Initially, the issue was protection of wood against fouling but also wood borers. Since the advent of metal-hulled vessels other measures to control fouling have been introduced (Holm, 2012). The first patents in this field were issued in the 1600s in Great Britain and many studies were presented at the Institution of Naval Architects in the late 19th century (Townsin, 2003).

More advanced coatings were developed in the 20th century including the now infamous (by virtue of its damaging environmental effects) tri-butyl-tin (TBT) in a self-polishing copolymer (SPC) matrix. Abbott *et al.*, (2000) calculated that TBT formulations saved \$730 M during 1989 for the world's commercial fleet. TBT is the most toxic substance deliberately introduced into the marine environment (Goldberg, 1986). The controlled release of the biocide afforded long-term antifouling efficacy of at least 5 years. The environmental impact it caused, however, (Strand and Jacobsen, 2005, Chambers, 2006; Garaventa *et al.*, 2007; Kim *et al.*, 2011) led the International Marine Organization

(IMO) to introduce a total ban on TBT for marine antifouling in 2008. There followed a return to copper as the main biocide, which continues to the present day. The best SPC formulations containing copper are as good as the banned TBT copolymers but require addition of so-called booster biocides to control copper-tolerant species such as *Ulva* sp. (Lejars *et al.*, 2012). Copper and booster biocides have themselves attracted attention for potential adverse effects on the marine environment and there is increasing regulatory pressure (e.g. Biocides Product Regulation EU No 528/2012). As a result, there is intense interest in finding new, nontoxic, or environmentally benign solutions to control fouling (Bressy *et al.*, 2009).

Fouling-release (FR) coatings are one such approach. These coatings, which are based on mainly on silicone elastomer technology, operate by weakening the adhesion of fouling organisms, such that the surface self cleans under hydrodynamic shear (Buskens *et al.*, 2013). The characteristics important to their efficacy include low surface energy (Brady, 2001), low elastic modulus (Berglin and Gatenholm, 2003; Sun *et al.*, 2004), smoothness (Hoipkemeier-Wilson *et al.*, 2004; Petronis *et al.*, 2011) and coating thickness (Chaudhury *et al.*, 2005). These features decrease the thermodynamic work of adhesion of organisms facilitating release by peeling from the paint. Although, more environmental friendly and efficient against hard fouling, e.g. barnacles, FR coatings are less effective against microfouling; diatoms being a particular problem for coatings based on polydimethyl siloxane (PDMS_e) (Anderson *et al.*, 2003). One possible solution to overcome this problem is hydrophilic polymer brushes, which by entropic repulsion of proteins in the hydrated forms of polymer, can prevent the adhesion of macromolecules and avoid the formation of biofilm (Buskens *et al.*, 2013). Commercial coatings are also now available that claim to be as effective against slime formation, e.g. the fluoropolymer Intersleek 1100SR. Previous limitations of fluoropolymers include a surface energy out the range of Baier curve (see below) and being thinner compared with silicone-based coatings, requiring more energy to fracture the bonds between foulant and coating (Chambers *et al.*, 2006). Fracture is a phenomenon based on the separating of a solid body or joint into two or more parts (Meyers and Chawla, 1984). Their lower values of elastic modulus also led to a shorter effective life (Dobretsov and Thomason, 2011).

Vessels are affected by other limitations since the hull is not the only vulnerable part,. Fuel tanks, ballast tanks and others internal parts cannot be treated with the usual

antifouling coatings and are ‘weak points’ that are of particular concern with regard to translocation of invasive species and need special maintenance procedures. Ideally, therefore, a universal solution is required to control marine biofouling.

1.2 Adhesion

In nature adhering to rock, plants, or other natural substrata is fundamentally important to the life of numerous organisms. Examples are presents in all the groups of unicellular organisms, plants and animals, including the adhesins of bacteria, the proteinaceous material used by insects to attach their eggs to the waxy surface of plants (Voigt and Gorb, 2010; Viegas, 2009), hairy adhesive systems used by e.g. insects and geckos (Smith *et al.*, 2006; Varenberg *et al.*, 2010; Barnes *et al.*, 2011), spider web glue (Choresh *et al.*, 2009) and the underwater adhesives of sessile marine organisms such as algae, tubeworms, starfishes and barnacles that use adhesives to fix themselves either temporarily (during exploration) or permanently (e.g. Flammang and Walker 1997; Callow and Callow 2006; Stewart *et al.*, 2011; Kamino, 2013). All these examples involve one or more chemical and/or physical adaptations, including hooks, locks, clamps, spacers, suction cups, friction, and wet and dry adhesion (Fig. 2) (Gorb, 2008; del Campo *et al.*, 2013).

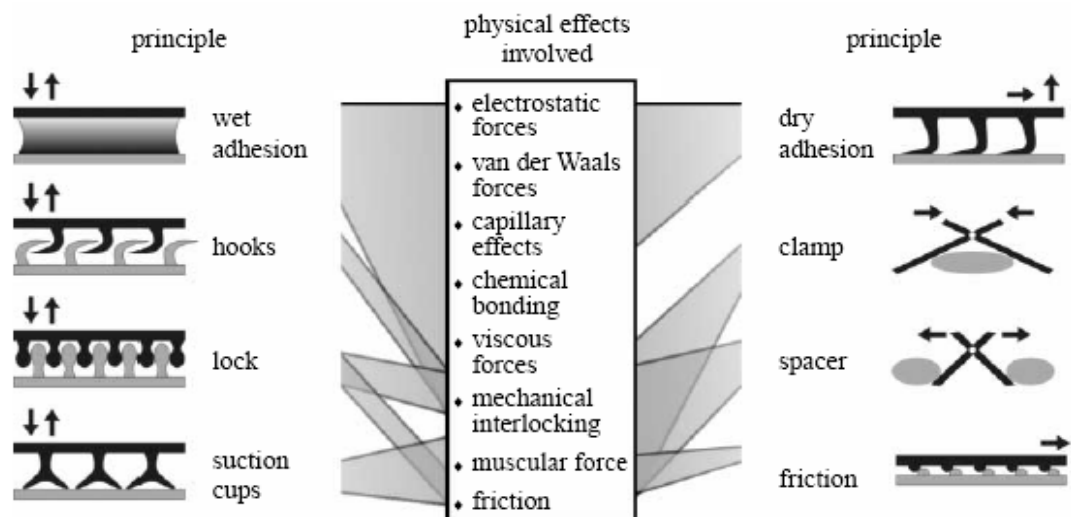


Fig. 2 Functional principles of biological attachment systems and physical effects involved. After Santos *et al.* (2013) from Gorb (2008).

These mechanisms rely on a combination of physical effects such as electrostatic forces, van der Waals forces, capillary effects, viscous forces, mechanical interlocking, muscular force and friction (Fig. 2).

The fundamental concepts of how materials interact when brought into close contact are crucial to understanding how adhesion works. In the context of underwater adhesion, such understanding is crucial to efforts to interfere with the process (fouling deterrence and fouling release) and biomimetic approaches to engineering adhesives that can function in an aqueous environment such as the human body. Only interference with adhesion is considered here.

Underwater adhesion involves 3 phases, a solid surface, a liquid adhesive and a liquid medium. In order to adhere, it is necessary that the adhesive comes into direct contact with the substratum. Therefore, the water needs to be displaced otherwise the interfacial interactions would be only a small fraction of the equivalent in air ($1/80^{\text{th}}$ at 25°C) due differences in the dielectric constant of air and water (Waite, 2002).

Nakano *et al.* (2007) listed some of the processes involved in underwater adhesion: displacement of the bound-water layer, spreading, coupling, curing, cleaning of biofilms, and protection from microbial degradation. Not all types of adhesion involve all these processes. For example, reversible adhesives, such as those of sea urchin tube feet, do not cure. The reactions are complex and need a precise sequence, which can fail if this order is interfered with by another factor or environmental condition such as temperature or pH. Others factors that can potentially interfere with adhesion include the presence of oil, slime and oxides. If close contact is prevented, the strength of the bond is dependent on the cohesive strength of the intervening water phase (Schonhorn, 1981; Waite, 2002).

In order to model adhesion underwater, differences in humidity, salinity, bacterial attack and protein concentration, that could affect adhesion, need to be taken into account. Stewart (2011) also highlighted the mechanism by which marine bioadhesives penetrate the ionic clouds above mineral surfaces, pointing to the important role played by the functional groups of the amino acid side chains and their effective concentrations in the adhesive proteins.

In nature different types of adhesive are involved in sticking to surfaces. This presents a major challenge when considering the design of a surface that is faced with the great diversity of marine fouling species. Few marine organisms have been studied in any detail (Ulva, diatoms, echinoderms, sandworms, limpets, octopods), and even fewer that comprise the typical biofouling community. Among macrofouling invertebrates, tubeworms, mussels and barnacles have received most attention (Kamino, 2010) (Fig. 3). The remainder of this chapter will be concerned with colonisation of surfaces by barnacles.

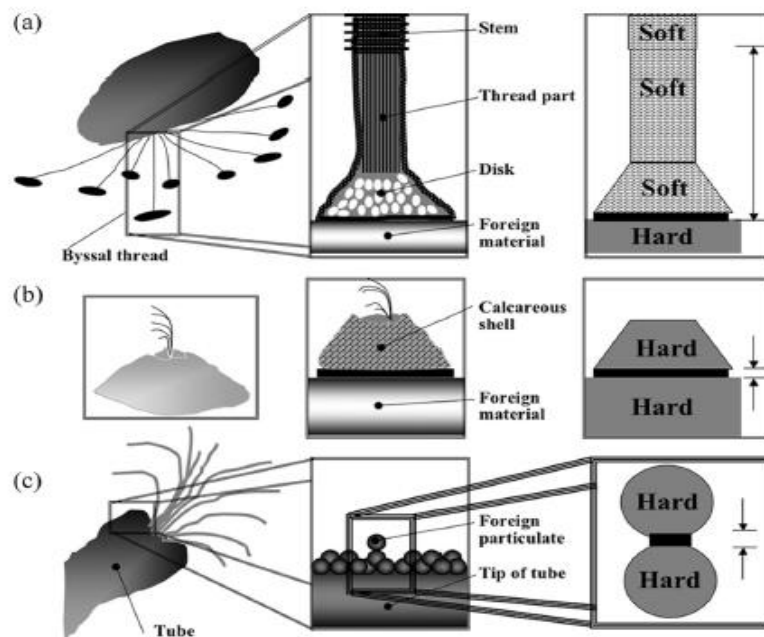


Fig. 3 Mode of attachment of most investigated bio-fouling organisms, (a) mussel, (b) barnacle and (c) tubeworm (Fig. from Kamino, 2010).

1.3 Barnacles

Barnacles of the superorder Thoracica can be found in all marine habitats from the intertidal to the deep sea and between tropical and sub-polar zones and are found colonising both inanimate and animate substrata; the latter including e.g. whales, sea snakes, turtles and decapod crustaceans (Anderson, 1994). The body of the barnacle is protected by hard calcareous shell plates that are fixed to the substratum either by a calcareous (e.g. *Balanus amphitrite*) or membranous basis (e.g. *Elminius modestus*). They are thus adapted to colonise a wide variety of habitats, most marine surfaces and a

wide range of environmental conditions. While some species are highly selective in their settlement requirements, e.g. *Chelinibia manati* (the manatee barnacle) (Mignucci-Giannoni, *et al.*, 1999), others are far less so and among these are some well-known representatives of the fouling community. The latter, can of course adhere to a wide range of surfaces, which, as mentioned above, represents a major challenge for fouling control. Barnacles are also particularly problematic fouling species as their relatively large form incurs a major drag penalty and growth of the shell plates can damage coatings.

The barnacle life cycle (Fig. 4) comprises 6 nauplius stages, all but the first of which are planktotrophic, and a highly specialised settlement stage – the cypris larva or cyprid. The latter is lecithotrophic and is often said to have a single role of finding a suitable place to settle. Some species are highly gregarious in their settlement behaviour requiring that the cyprid is able to recognise conspecifics. Gregariousness results in the hermaphroditic adults being sufficiently close for cross fertilisation via the highly extensible penis.

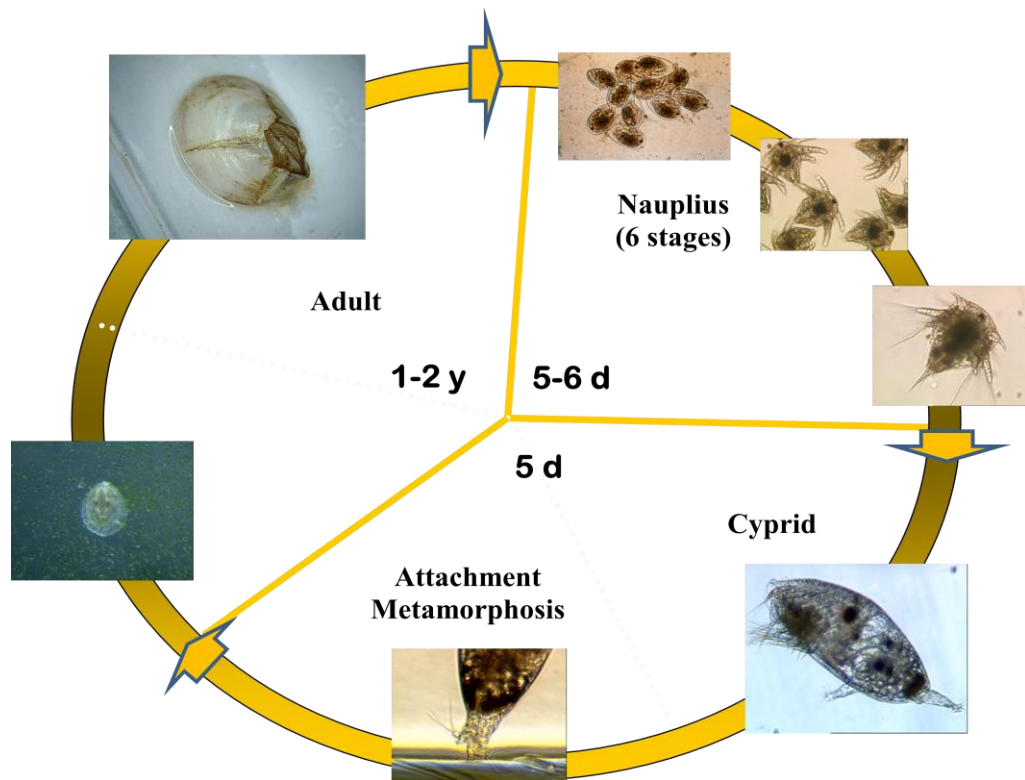


Fig. 4 Life cycle of a thoracican barnacle showing the planktonic, planktobenthic and benthic stages.

1.3.1 *The cyprid*

The cyprid is a planktobenthic stage, which is responsible for finding a place to settle and metamorphose to the adult form. This is not a simple task. Settlement (fixation) is irreversible, so the site 'chosen' must allow development and growth of the barnacle to maturity and be sufficiently close to potential mates. Settlement is thus likely to be under strong selection pressure. Furthermore, as the cypris larvae is lecithotrophic, it has finite energy reserves and thus a limited time to reach this goal (Tremblay *et al.*, 2007). Cypris larvae are well endowed with sensory appendages to sample the physical and chemical nature of the substratum (Maruzzo *et al.*, 2011) and to adhere to the substratum both temporarily (reversible adhesion) and permanently. Reversible adhesion, which allows surface exploration, combines a complex surface morphology on the adhesive disc (dry adhesion) with a wet adhesive. (Aldred and Clare, 2008).

The settlement stage cyprid is a highly specialised lecithotrophic larva (Walker *et al.*, 1987). The body of the cyprid is enclosed in a cuticular bivalve carapace, which is moderately smooth, without pronounced sculpturing. Lattice organs (similar for *Balanus amphitrite* and *B. improvisus*, Jensen unpublished, reported in Glenner and Høeg, 1995), which are reported to be proprioceptive mechanoreceptors (Ito and Grygier, 1990), occur in certain areas of the carapace in specific patterns. Three types of appendages emerge from the ventral side of the carapace: two frontal filaments, six pairs of thoracic appendages, or thoracopods and two antennules. In relation to settlement, the thoracopods can be used for fast movements, either toward the substratum, or to return to the plankton if the substratum is rejected.

The antennules are adorned with structures that enable cyprids to walk on the surface in a bipedal fashion (Crisp, 1976 and recent Maruzzo *et al.*, 2011) as well as mechano- and chemoreceptors, to detect and probe the nature of the substratum. The antennules comprise four segments, each of which has different functions:

Segment 1: proximal to the body, this segment does not have setae. It is composed of two sclerites, which serve as an important articulation in the antennular apparatus (Lagersson and Hoeg, 2002); these join the dorsal wall of the mantle to the second antennular segment.

Segment 2: composed of a single thick inflexible cuticle (Fig 5), is characterised by a single seta near to the third segment and contains the unicellular glands that secrete temporary adhesive. This segment has a major role in the antennular movements when the cyprid is exploring the substratum (Lagersson and Høeg, 2002).

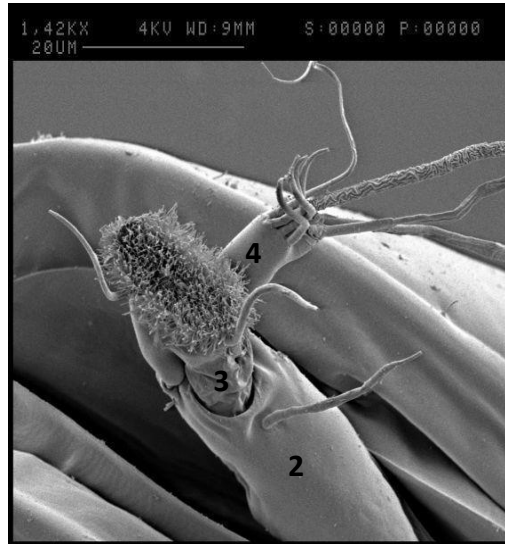


Fig. 5 Antennule of *Balanus amphitrite* cyprid showing the 2nd, 3rd and 4th segments (after Aldred and Clare 2008).

Segment 3: is a very specialised segment responsible for anchoring onto the substratum. This segment ends with the bell-shaped attachment disc (Nott and Foster, 1969) and measures 30 μm in length (for *B. amphitrite*, it is 25 μm for *B. improvisus*) (Fig. 6). The disc is covered by cuticular villi, encircled by a velum, and contacts the surface directly. The segment contains a single muscle that enables the movements of the 4th segment.

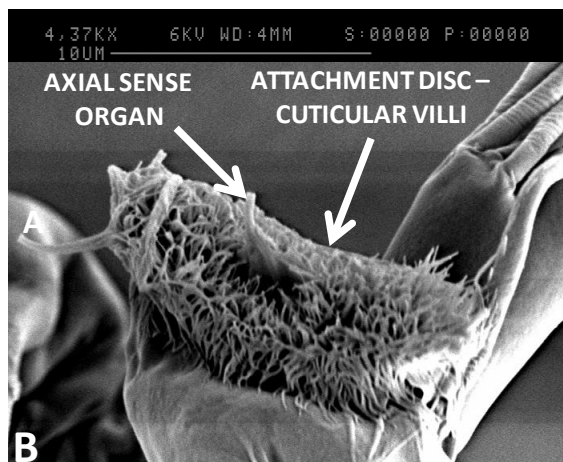


Fig. 6 *Balanus improvisus*: the 3rd segment of the cyprid antennules.

The axial sense organ is located in the middle of attachment disc. This organ is regarded as chemosensory (Nott and Foster, 1969). In between the cuticular villi of the disc are pores where the temporary adhesive and permanent cement are secreted to the surface. Saroyan (1969) and Lindner and Dooley (1969) proposed that the attachment disc has a suction function on the surface, but this has been rejected since antennular muscles do not allow this kind of movement (Barnes, 1970; LagerSSon and Høeg, 2002).

Segment 4: branches laterally from segment 3 at an angle of between 45 - 90° (Clare and Nott, 1994) (Fig. 7). The segment has a cylindrical shape. Two groups of setae are located distally: the four subterminal setae are open-ended and make intimate contact with the substratum during searching behaviour (LagerSSon *et al.*, 2003). They are believed to be chemosensory (Gibson and Nott, 1971; Hallberg *et al.*, 1992). The terminal setae are chemosensory and/or mechanosensory in function (Maruzzo *et al.*, 2011) and contain numerous dendrites (Barnes, 1970). Elbourne and Clare (2010) compared the flicking rate of this segment when exposed to seawater and adult-conditioned seawater but found no significant differences.

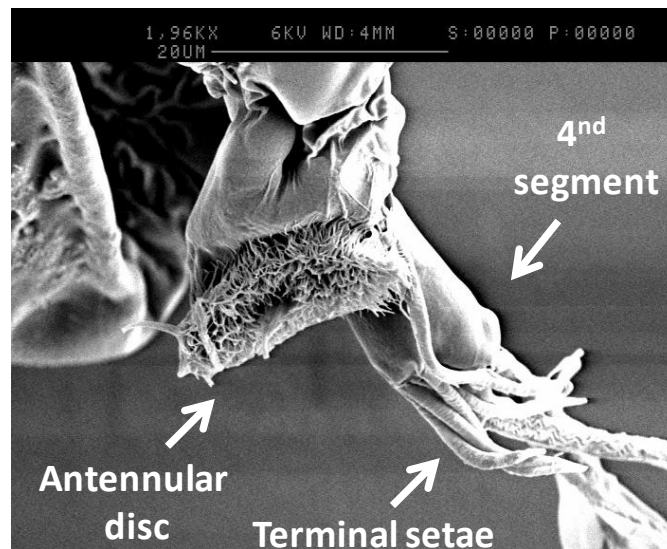


Fig. 7 Terminal and sub-terminal setae of the 4th antennular segment of *Balanus improvisus*.

Nevertheless, given that some of the setae are aesthetasc-like (crustacean chemoreceptors), it is suspected that flicking aids the access of odour molecules to the chemosensory setae (Clare, 2011).

The antennules are thus key to surface exploration and selection of settlement sites. The length of time that the cypris spends exploring is suggested to be dependent on the strength of stimuli perceived from the prevailing chemical and physical features (Kamino, 2010). Once on the surface, cyprids have different options depending of the nature of the surface; they can fix in place temporarily, continue exploring, or reject the surface and swim away and probe other places subsequently for a more suitable surface for settlement and metamorphosis.

1.3.2 Barnacle adhesives

1.3.2.1 Temporary adhesive

In addition to the complex morphological adaptations described for the antennules, the exploration phase is also characterized by the secretion of a proteinaceous material, often referred to as temporary adhesive (footprint) for its putative reversible adhesive properties between the antennular disc and the substratum. The temporary adhesive is produced by approximately twenty unicellular glands located in the second antennular segment (Nott, 1969; Nott and Foster, 1969; Walker, 1971; Okano *et al.*, 1996). The secretion passes through ducts and exits to the surface through pores in the third segment between cuticular villi.

The combination of the hairy attachment disc and the adhesive ensure that the cyprid can remain in contact with the substratum while searching (Aldred and Clare, 2008). It has been suggested that the strength of adhesion can be sensed by the cyprid in view of observations made of cyprids ‘pulling’ on the antennules (*S. balanoides*; Crisp and Meadows, 1963; Aldred *et al.*, 2013b). If the surface is considered ‘unsuitable’, the cyprid moves away toward another potential attachment surface leaving the footprints on the surface (Fig. 8). These footprints have been shown to render a surface more attractive to conspecific cyprids and thus also serve a pheromonal function (see below). Although now regarded as a true adhesive (Aldred *et al.*, 2013a) some uncertainty remains regarding the mechanism of adhesion, including whether the adhesive displaces water (Aldred and Clare 2009).

The temporary adhesive not only has the role of an adhesive but also as a chemical signal for others cyprids to settle (Yule and Walker, 1985; Clare *et al.*, 1994).

Gregariousness is essential for sessile organisms that engage in cross fertilisation (Andersson, 1994; Head *et al.*, 2004).

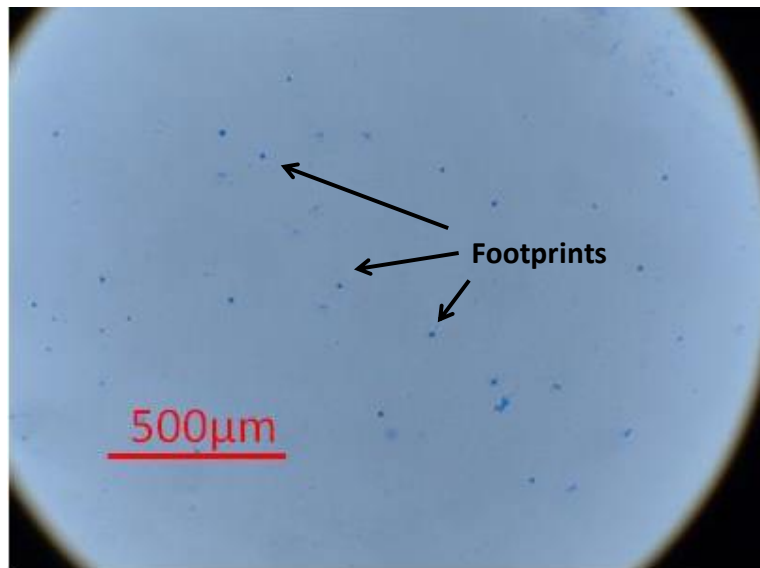


Fig. 8 Footprints of *B. amphitrite* stained by Coomassie Brilliant Blue-G-Colloidal Blue-silver (CBB-G).

Furthermore, the cyprid is particularly discriminating in its choice of settlement site (Knight-Jones, 1953; Crisp and Meadows, 1962, 1963). Settlement is mediated by specific environmental cues (Clare, 1995; Walker, 1995), including the presence of conspecifics. Conspecifics are recognised by a chemosensory mechanism (Knight-Jones and Crisp, 1953; Crisp and Meadows, 1962; 1963), which has been studied intensively (Gabbott and Larman, 1987; Clare, 2011) since gregariousness was first described by Knight-Jones and Stevenson (1950) and Knight-Jones (1953).

Crisp and Meadows (1962) isolated a water-soluble settlement inducer from adult barnacles (*S. balanoides*) which they termed “arthropodin”. The signal was identified as a protein with physicochemical properties similar to the arthropod cuticular protein of the same name (Fraenkel and Rudall, 1947). Arthropodin has also variously been referred to as “settlement factor” (Gabbott and Larman, 1971; Larman *et al.*, 1982; Rittschof *et al.*, 1984) and “settlement pheromone” (Clare *et al.*, 1994; Clare, 1995; Clare *et al.*, 1995; Clare, 2011). More recently Matsumura *et al.* (1998) purified an adult glycoprotein from *B. amphitrite* with settlement-inducing activity, which they termed the settlement-inducing protein complex (SIPC). The SIPC comprised three major subunits of 76, 88 and 98 kDa (Matsumura *et al.*, 1998c).

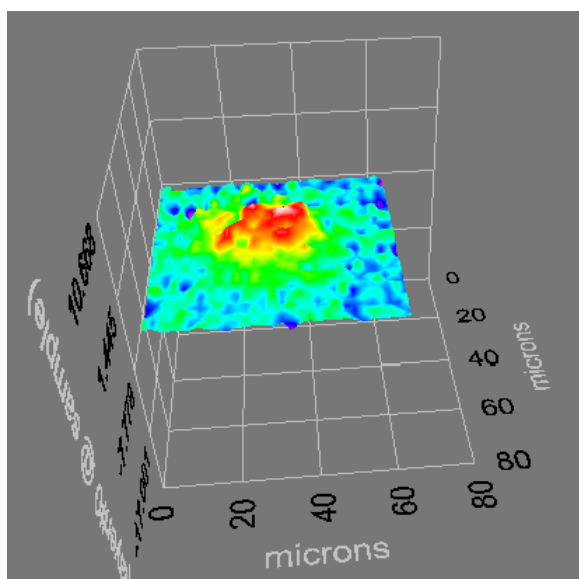


Fig. 9 Footprint of *B. amphitrite* cyprid visualised on a $-CH_3$ terminated SAM by imaging ellipsometry.

The SIPC has been located in cyprid footprints by immunocytochemistry (Dreanno *et al.*, 2006b), suggesting that it accounts for their settlement-inducing activity. Dreanno *et al.*, (2006a) showed that the SIPC is also a cuticular protein found in most of the barnacle tissues and at all the stages of development (Dreanno *et al.*, 2006b), highlighting that it is probably the same protein as ‘arthropodin’. It is reasonable to propose that the SIPC is responsible for stimulating gregarious settlement of cyprids in response to detection of adults and cyprid footprints. This relation between a chemical signal associated with the cuticle and the temporary adhesive was first proposed by Walker and Yule, (1984a), who also hypothesised that glands that secrete temporary adhesive are modified tegumental glands.

Walker and Yule (1984a) first described the deposition of footprints for *Semibalanus balanoides*. Clare *et al.* (1994) later showed the same for *B. amphitrite*, noting that footprints had a diameter of $\sim 30 \mu\text{m}$ (Fig. 9); smaller than those of *S. balanoides* ($\sim 50 \mu\text{m}$) but the same as the attachment disc. The footprints are optically transparent but can be visualised by staining with Coomassie Brilliant Blue (CBB; Walker and Yule, 1984 b; Clare *et al.*, 1994) (Fig. 8).

Imaging surface plasmon resonance (iSPR) is an imaging optical transducer technique able to determine the refractive index of very thin layers adsorbed on a surface

(Rothenhäusler and Knoll 1988). The technique was used to visualise footprints of *S. balanoides* deposited onto an oligo(ethyleneglycol)-coated surface and bare gold (Aldred *et al.*, 2011) and the frequency of deposition on various other surfaces. Not only were significant differences detected in the frequency of footprints deposited on surfaces but the thickness of the footprints also varied according to the surface explored by the cyprids. The thickest footprints (~13 nm) were deposited onto a –COOH self-assembled monolayer similar to estimates made by atomic force microscopy (Phang *et al.*, 2008).

Atomic force microscopy has been used to characterise footprints on surfaces (Phang *et al.*, 2007; 2009a). The fundamental basis of this instrument is related to a mechanical probe (a silicone nitride cantilever tip) that follows and reproduces the shape of the same surface or any objects present on the surface with very high resolution. The minute deflections of the cantilever are detected by a laser that transfers and reproduces the image. This technique has been used widely to measure nano and micro scale properties of molecules (Ikai *et al.*, 1997; Horber and Miles, 2003; Giannotti and Vansco, 2007; Shibata *et al.*, 2010), microorganisms (Janovjak *et al.*, 2003) diatoms (Higgins *et al.*, 2003; Pletikapić *et al.*, 2012) and algae (Callow *et al.*, 2000b), including quantification of the physical force of extracellular polymeric substance of diatoms (Svetličić *et al.*, 2013). Callow *et al.* (2000b) showed, using AFM, the secretion of *Ulva linza* spores attaching permanently to a surface

With AFM a combined study of footprint morphology and nanomechanical properties was possible. AFM images of footprints provided information on shape, size and thickness. Phang *et al.* (2008) described footprints of *S. balanoides* as fibrillar, with nanofibrils varying between 7 and 150 nm. Phang *et al.* (2010) observed a porous microstructure, with suggestions of single adhesive protein chains at high magnification. This kind of micro structure may result from either radial shear of the protein or failure of this material during the detachment phase combined with the cuticular villi, indeed the detachment of antennular disc from the surface creates micro bubbles at the adhesive interface (Aldred *et al.*, 2013) which may explain the characteristic appearance of the adhesive with AFM.

Footprints on a substrata, being a network of proteinaceous material and having two interfaces, protein-sea water and protein-surface, can be stretched in order to measure

the strength of adhesion with the surface. This operation may meet some obstacles during the measurements, indeed is difficult to know if the tip traps a single or a group of proteins (Mitsui *et al.*, 1996) and may give a wrong interpretation of the adhesive properties of the molecule. This is related to the protein domains, the grade of organization of the protein and the folding and unfolding behaviour. Based on these features it is possible to understand how the protein folds and the type of bonds, specifically the location and strength of the bonds. These aspects will undoubtedly influence the force required to unfold a domain (Fisher *et al.*, 1999).

In this context Phang *et al.* (2010) investigated footprints of *B. amphitrite* cyprids deposited onto silane-modified glass surfaces, observing stretching of groups of proteins, connected via sacrificial bonds, which gave a saw-tooth fingerprint during the stretching with a force peak of 250-1000 pN. The stretching phase was followed with the refolding phase, with the reforming of footprint domains and bond reformation. Protein behaviour during stretching (unfolding) and release (refolding) by the AFM tip may mimic what happens in nature when the cyprid probes the surface with temporary adhesive during the exploration phase until detachment from the surface.

An understanding of exploratory behaviour by cyprids is likely to be fundamental to new developments in antifouling technology that focus on deterrence rather than adult removal and chemical attack with toxic compounds.

1.3.2.2 Permanent adhesive

“Crustacea attached by the anterior end of the head, by cement proceeding from a modified portion of the ovaria;...”

This was how Darwin described attached larvae of cirripedes in 1854. Subsequently, many studies dedicated to cementation confirmed that cyprids secrete a permanent adhesive from the paired cement glands within the body when a substratum is suitable for settlement. This is a crucial step since it is also the last phase of the settlement process. Indeed, the process is permanent since it fixes the cyprid in place while it undergoes metamorphosis to the juvenile. As Darwin again highlights:

“Cirripedes are permanently attached, even before their final metamorphosis, by a tissue or cement, first debouching through the second pair of antennae, and, subsequently, in most cases, through special orifices, penetrating the anterior part of the head; this cement proceeds from glands, which certainly are modified portions of the ovarian system. This fact I consider of the highest classificatory importance, for it is absolutely the one single character common to all Cirripedes, besides such as show only that these animals belong to the articulated kingdom, and are Crustaceans.”

When Darwin made these observations he probably did not realise the practical applications of knowledge of the attachment phase to the development of technologies for antifouling and artificial adhesives.

The proteinaceous material secreted to fix the cyprid onto a surface prior to metamorphosis has been studied with respect to its composition (Walker, 1971), and the tissues involved in its production (Okano, 1996), storage and delivery to the substratum (Ödler *et al.*, 2006). The permanent adhesive is produced by cement glands located in the cyprid body, probably in different type of cells as suggested by Walker (1971) for *S. balanoides* and Okano *et al.* (1998) for *M. rosa*, and stored in vesicles. A muscular sac transfers the adhesive (Walley, 1969) from the cement collecting duct via the antennular duct (Ödler *et al.*, 2006 for *B. improvisus*) to the surface. Exocytosis of secretory granules is stimulated by the nervous system through release of dopamine and noradrenaline (Okano *et al.*, 1996). Once the adhesive is secreted onto the surface, it forms a plaque with a diameter of ~100 µm embedding completely the two antennules (Aldred and Clare, 2008). After it is externalized, the cement undergoes curing, and solidification (Aldred *et al.*, 2008). It has been suggested that cyprid permanent adhesive is similar to the adult cement (see Aldred and Clare, 2008). For example, on the basis of histological examination, the cyprid cement glands were observed to migrate during the metamorphosis and subsequently develop into the adult cement glands (Walker, 1971). In contrast, Aldred *et al.* (2008) using AFM reported a different structure for cyprid cement and Kamino and Shizuri (1998) concluded that the genes that encode for the adult cement are not expressed in the cyprid. However, only recently He *et al.* (2013) found the presence of two homologous 20kD cement proteins in both cyprid and adult cement, which lends support to Walker's (1971) study.

Walker (1971) proposed that adhesive hardening occurs *via* quinone tanning involving the enzyme polyphenol oxidase. Phang *et al.* (2006) suggested the presence of more components in the adhesive, estimating by AFM a curing time from deposition of 1-3 h. AFM only considers the outer part of the adhesive and excludes the inner core, indeed other studies suggested a longer curing time of up to 15 h (Aldred *et al.*, 2008). Recently, using confocal microscopy, Aldred *et al.* (2013) emphasised the complexity of the dual-phase system of the adhesive highlighting differences in spreading of the two phases dependent on surface chemistry.

Few studies have been attempted to investigate the chemical composition of permanent adhesive. Schmidt *et al.* (2009) using confocal Raman microscopy, confirmed the organic nature of the adhesive represented by the C – H stretching signal. A high concentration of -OH was also found, which may be important to cement curing since as it is for the mussel byssal adhesive (Wiegemann, 2005).

Subsequent to metamorphosis, the juvenile begins to produce the adult permanent cement, which at only a few micrometres thick joins the calcareous barnacle basis to the substratum. The adult cement, produced by giant cells (Kamino, 2010), is a proteinaceous material (Walker 72, Kamino *et al.*, 96). Studies have been carried out to investigate the cypris cement composition but relatively little information exists. Walker (1971) described a layered zoned mass rather than homogeneous plaque.

1.4 Surface influence on barnacle adhesion

1.4.1 Surface chemistry

The selection of substrata is essential for barnacle cyprids as mentioned above. Surface chemistry has long been known to influence surface selection with surface energy regarded, until recently, as the main parameter that affects the adhesion of marine organisms (Crisp, 1984; Rittschof and Costlow, 1989; Brady and Singer, 2000). Moreover, a determinate range of surface energy values, between 20 and 30 mJ m⁻² and called the “Baier minimum” (Baier and DePalma, 1971), is believed to influence microbial adhesion. This theory has since been confirmed by other studies (Dexter, 1979; Baier and Meyer, 1992; Zhao *et al.*, 2009) but during the last decade new doubts have emerged. Maki *et al.* (1994) noted the absence of a correlation between wettability

and temporary adhesion strength of *B. amphitrite* cyprids, since confirmed by Aldred *et al.* (2011) for *S. balanoides*, emphasising the importance of the positive charge of the temporary adhesive in view of the fact that natural surfaces tend to be negatively charged. New information supporting this theory has been obtained using self-assembled monolayers (SAM) in laboratory settlement assays. Using cyprids of *B. amphitrite*, Ederth *et al.* (2011) obtained similar low values of settlement on surfaces with surface energies of ca 46 and 29 mJ m⁻².

Recent investigations with 7 SAMs of different of surface energy and wettability showed that cyprid settlement of *B. amphitrite* and *B. improvisus* (Petronne *et al.*, 2011; Di Fino *et al.*, 2013) was more affected by surface charge than surface, in marked contrast to previous reports (O'Connor and Richardson, 1994; Dahlström *et al.*, 2004) that did not control for other variables.

1.4.2 Topography

The preference of sessile organisms for rough rather than smooth surfaces may depend on the size of the organism and/or the part of the body that is in contact with the surface. Generally, invertebrate larvae tend to reject very smooth surfaces (Crisp, 1974). Based also on the characteristics listed above (1.1), rough surfaces may allow better adhesion through mechanical interlocking of the adhesive and the surface.

Early investigations in this regard started when Barnes and Powell (1950) using cyprids of *S. crenatus* found that glass fibre cloth with filament projections of ~8 µm inhibited settlement. Crisp and Barnes (1954) using *S. balanoides* demonstrated lower settlement on surfaces with sharp ridges. More recent investigations by Lemire and Bourget (1996) found low settlement on surfaces with V-shaped grooves. Many of these studies have focused on scales below the size (or the same size) of the cyprid body, which would prevent direct contact of the body with the surface (Aldred and Clare, 2008). Le Tourneux and Bourget (1988) reported that cyprids of *S. balanoides* discriminated microheterogeneities below 35 µm; a size similar to the diameter of antennular disc (40 µm). Similarly, Berntsson *et al.* (2000b) using cypris of *B. improvisus* observed a settlement reduction of 92% on surfaces with a topographic range of 30 - 45 µm compared with smooth surfaces. Berntsson *et al.* (2000a) highlighted the importance of

a correlation between microtextured surfaces and their orientation to the flow of water in cypris surface selection. Moreover, Berntsson *et al.* (2004) considered topography to be more important than chemical cues to settlement of *B. improvisus*. Aldred *et al.* (2010b) tested PDMS and polycarbonate textured surfaces in range between 4 and 512 μm and reported lowest settlement of *B. amphitrite* on a feature size of 256 μm ; a size that may minimise contact with the surface. In this regard we can ask the question: is the size of attachment disc important to surface selection on microtextured surfaces? If the antennular disc cannot make direct contact with the surface, presumably temporary adhesion cannot be effective.

1.4.3 Biofilm

Biofilm is a sessile assemblage of microorganisms joined to each other and enclosed in an exopolymeric matrix (Lewandowski, 2000). Microorganisms may quickly colonise a surface immersed in the sea, within hours of protein adsorption, with biofilm developing over a period of days. Prior colonisation by microorganisms changes the chemical and physical nature of the surface (Becker *et al.*, 1997; Huggett *et al.*, 2009). In this context, macrofouling larvae do not approach a completely clean surface during the surface exploration and different biofilmed surface may influence settlement behaviour. A number of studies have been carried out in the effect of biofilm on settlement of barnacles. No clear picture has emerged from these studies, however, which may reflect to some extent differences in conditions of laboratory assays and field tests. The latter are also difficult to interpret because of an inability to control other variables. For example, Maki *et al.* (1988; 1990; 1992) carried out a series of tests with cyprids of *B. amphitrite* but with different results. Avelin Mary *et al.* (1993) using five selected groups of bacteria found an inhibitory effect on settlement of *B. amphitrite*. Faimali *et al.* (2004) also observed inhibition of settlement onto different materials with biofilm of different age. In contrast Zardus *et al.* (2008) found increased ‘attachment strength’ of barnacles on biofilmed surfaces but did not examine the mode of failure. These multiple effects (Dobretsov *et al.*, 2013) of mainly laboratory experiments complicate any attempt to extrapolate results to the field.

1.4.4 Larval age

As cyprids are lecithotrophic (section 1.2.1), they have limited time to explore, settle and undergo metamorphosis because depletion of their finite energy reserves (lipid and protein (Shimizu *et al.*, (1996)) can eventually compromise settlement (Rittschof *et al.*, 1984; Satuito *et al.*, 1996; Tremblay *et al.*, 2007). Consequently as cyprids age they become less discriminating in their settlement requirements (Rittschof *et al.*, 1984; Marechal *et al.*, 2012). No correlation was found between cyprid age and gregariousness, for 1- to 7-day-old larvae of *B. amphitrite* and *B. improvisus* (Head *et al.*, 2004); a result since contradicted by the study of Marechal *et al.* (2012) on *B. amphitrite*.

1.5 Adult barnacle adhesion

Cyprid settlement is followed by metamorphosis, which comprises a drastic change in the morphology and physiology of the organism. Changes also occur in the adhesive system, possibly involving development of an adult cement system (Lacombe, 1970; Saroyan *et al.*, 1970; Walker, 1970; Fyhn and Costlow, 1976; Jonker *et al.*, 2012) from the de-differentiated (Walker, 1973) or intact cyprid cement glands (Saroyan *et al.*, 1968; 1970).

The adult cement system comprises cement glands and circular ducts in the basis, which increase in size as the barnacle grows allowing the transport of cement to the outer part of the basis (Fig 10). This ensures that fresh cement is deposited as the barnacle grows incrementally (Burden *et al.*, 2012). This may leave ducts located in the central part of the basis occluded since they are only occasionally used. There is, however, scant information regarding the status of ducts in relation to a possible flushing fluid after the cement has passed (Saroyan *et al.*, 1970).

The relatively large amount of cement produced by adults compared to cyprids has facilitated sampling and biochemical characterisation (Walker, 1972). Raman and Kumar (2011) have calculated from cross sections that the thickness of the cement in *B. reticulatus* is 2–3 μm on titanium and stainless steel. Although the quantity of material is not limiting to characterisation, the composition remains to be fully established. Recent investigations in this field have revealed that it is a multi-protein complex

(Kamino *et al.*, 2000; Kamino, 2006), some of which have been characterised (Kamino *et al.*, 2000; 2012; Kamino, 2001; Mori *et al.*, 2007; Urushida *et al.*, 2007) namely, cement proteins 100, cp68, cp52, cp20, and cp19 kD.

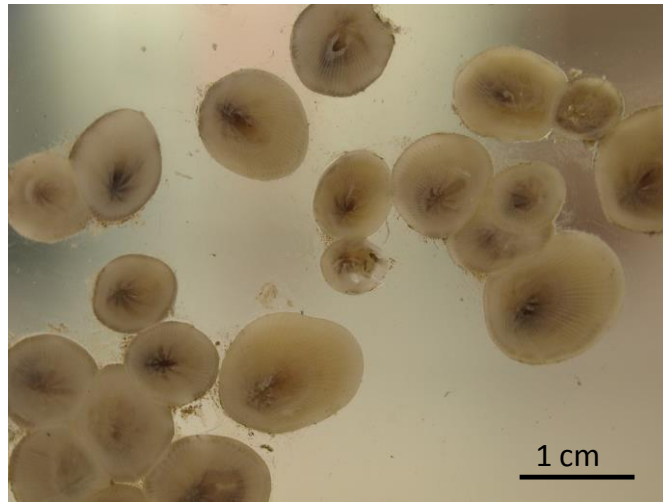


Fig. 10 Basal view of adult of *B. improvisus* attached to Plexiglas plate.

These proteins are unique among natural adhesive proteins and possess both hydrophobic and hydrophilic properties (specific for *Megabalanus rosa*; Kamino, 2013). A specific 36 kD protein, which in terms of amino acid composition shows some similarity to mussel adhesive proteins (Naldrett and Kaplan, 1997), was not found in *B. perforatus*. Indeed Naldrett and Kaplan (1997) showed the presence of a 38kD protein in the cement of this species. The 36kD Tyr-rich protein may be important to adhesion to the substratum through cross-links involving intermolecular disulfide bonds, but its role and that of other proteins found in the adhesive remain undetermined. DOPA (3,4-dihydroxyphenylalanine), an important amino acid in mussel byssus and tubeworms cement, is not present in barnacle cement, at least for *B. crenatus* (Naldrett, 1993) and for *M. rosa* (Kamino *et al.*, 1996).

Two ‘types’ of cement have been reported, ‘primary’ and ‘secondary’ (Kamino, 2006). The first is employed between the base of shell and the surface to ensure the attachment, while the second is secreted to fill possible damage to the shell or gaps through partial detachment from the substratum (Aldred and Clare, 2008). Secondary cement has also been referred to in the context of abnormal rubbery cement noted for a proportion of barnacles that grow on silicone elastomer coatings (Berglin and Gatenholm, 2003).

Under artificial conditions, adult barnacles can re-attach to the substratum with secondary cement. All early biochemical studies of adult cement used this secondary cement by virtue of its ease of collection (Walker, 1972). While it appears likely that the two ‘cements’ are the same, it is important to make the distinction when referring to barnacle cement (Kamino, 2006) until they have been fully characterised. Kamino (2010) has defined adult cement as the material secreted naturally for attaching to the substratum. Barlow *et al.* (2010), using ATR– FTIR spectroscopy characterised *in situ* the secondary cement of *B. amphitrite* finding up to the 50 % of the cement weight as water, and with protein secondary structure consisting primarily of β -sheet structures with hydrophilic natural state. While water is considered important to the molecular conformation of the cement, the method used to collect cement in the Barlow *et al.* (2010) and Dickinson *et al.* (2009) studies has been criticised by Kamino (2010). Indeed, Dickinson *et al.* (2009) report the presence of hyaline cells in their cement sample, strongly suggesting that they sampled haemolymph or cement contaminated with haemolymph from damage caused at the margin of the shell plates. Moreover, a claim that cement cured via the action of glutaminase (Dickinson *et al.*, 2009) was also questioned by Kamino (2010) as he was unable to find evidence of this enzyme in barnacle cement. The hypothesis proposed by Dickinson *et al.* (2009) that cement curing is analogous to haemolymph clotting may thus simply reflect the contamination of their sample by haemolymph.

Although curing of cement may occur (Kamino, 2006), the process is poorly understood and there is no information comparable to that obtained for mussels and tubeworms (Nicklisch and Waite, 2012). Indeed, Kavanagh *et al.* (2005) provided evidence of a viscous material at the interface of the barnacle, *B. eburneus*, observed during detachment from a silicone elastomer coating. While this observation may reflect the highly hydrated condition of cement deposited on silicone coatings (Wiegemann and Watermann, 2003), other observations on the mobility of barnacles (Crisp, 1960; Kugele and Yule, 1993) are consistent with a viscous interface and possibly an absence of curing.

In the context of fouling-release coating technology, there is considerable interest in the mode of removal of adult barnacles from silicone elastomeric coatings. Barnacles attach weakly on to these surfaces and it is questionable whether the mode of failure is comparable to the mechanism on natural surfaces, in view of the highly hydrated

adhesive mentioned above and the compliant nature of the elastomer. Kamino (2013) recently reviewed such modes of failure noting that the stress required to remove a barnacle from a silicone-based surface is inversely correlated with surface thickness. This is not accounted for in Kendall's model based on removal of a rigid cylindrical punch; so-called 'pseudobarnacle' (Kendall, 1971). Moreover, the model does not account for basal flexure noted for 'real' barnacles (Ramsay *et al.*, 2008). The model was improved by Hui *et al.* (2011), who took account of a crack-trapping mechanism operating during release of adult barnacles.

1.6 Scope of the thesis

This thesis compares two species of barnacle, *Balanus amphitrite* and *B. improvisus* (Fig. 11), in relation to settlement of cyprids and adhesion of juveniles and adults on a range of model surfaces for the first time in a controlled manner. To date there has arguably been an over-reliance on studies of *B. amphitrite*, the results of which may not be widely applicable to species. It was hoped that the knowledge gained would help to guide the development of novel environmentally-friendly antifouling coatings.

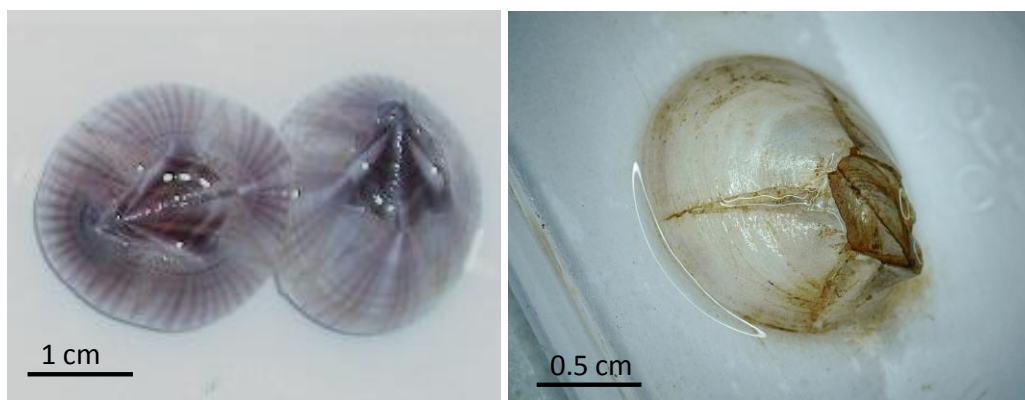


Fig. 11 Adult of (A) *B. amphitrite* and (B) *B. improvisus*.

The following 4 chapters comprise: the study of influence of surface charge and surface energy on the settlement behaviour of barnacles; footprint characterisation and the effect of elastic modulus on surface selection and barnacle adhesion.

Chapter 2. Influence of surface charge and surface energy on the settlement behaviour of barnacles

This chapter is based on the following publications:

Petrone L, Di Fino A, Aldred N, Sukkaew P, Ederth T, Clare AS, Liedberg B. 2011. Effects of surface charge and Gibbs surface energy on the settlement behaviour of barnacle cyprids (*Balanus amphitrite*). *Biofouling*. 27:1043-1055.

Di Fino A, Petrone L, Aldred N, Ederth T, Liedberg B, Clare AS. 2013. Correlation between surface chemistry and settlement behaviour in barnacle cyprids (*Balanus improvisus*). *Biofouling*. 30:143-152.

2.1 Introduction

Understanding the settling behaviour of fouling larvae during the initial stages of colonisation as well as the innate criteria they use to discriminate between surfaces (Matsumura *et al.*, 1998; Andersson *et al.*, 1999; Berntsson *et al.*, 2004; Murosaki *et al.*, 2009) will play an important role in the development of antifouling (AF) coatings. Different surface characteristics are important to the selection preferences of fouling species. For example, as mentioned in chapter 1.3.1, surface energy is considered an important modulator of settlement behaviour of many fouling species (Brady and Singer, 2000; Callow *et al.*, 2005; Hung *et al.*, 2008; Finlay *et al.*, 2010)

Gibbs surface energy is defined as the work done in a reversible, isothermal process to increase the surface of a substance by a unit area (Gibbs, 1928; Adamson, 1990). More broadly, it can be used to describe the 'reactivity' of a surface, which may be an important parameter in adhesion. Surface energy comprises two independent components, viz. dispersive (Lifshitz-Vander Waals (γ^{LW})) and polar (Lewis acid/base (γ^{AB})) forces (Good, 1993; van Oss, 1994). The former describes weak, long-range (100 Å) interactions caused by polarization and induced dipoles, and the latter (γ^{AB}) stronger

but short-range ($<3\text{\AA}$) electron donor–electron acceptor bonds, such as hydrogen bonds. In the context of marine biofouling, surface energy is deemed to be an important parameter for predicting the attachment and/or adhesion of marine organisms to surfaces (Crisp, 1984; Rittschof and Costlow, 1989; Brady and Singer, 2000). Numerous studies (eg Dexter, 1979; Baier and Meyer, 1992; Zhao *et al.*, 2009) have demonstrated a zone of minimal adhesion for surfaces with surface energy values between 20 and 30 mJ m⁻². This has become known as the ‘Baier minimum’; a reference to an empirical observation of the dependence of microbial adhesion on surface energy presented by Baier and DePalma (1971). Importantly, however, most studies that have attempted to correlate adhesion to surface energy have focused on experiments employing microorganisms for their conclusions (Ista *et al.*, 2004; Zhao *et al.*, 2004; Katsikogianni *et al.*, 2008; Li *et al.*, 2010) or involve complex systems, such as natural aqueous solutions (Dexter, 1979). There have also been attempts to explain observations in the context of theoretical models (Dexter, 1979; Brady, 1999). However, studies attempting to determine, in a controlled manner, the effects of surface energy on the settlement and adhesion of organisms at larger size scales (hundreds of μm) are limited (Tang *et al.*, 2005; Petrone *et al.*, 2009; Finlay *et al.*, 2010; Bennett *et al.*, 2010; Gunari *et al.*, 2011).

Hung *et al.* (2008) found that larvae of the barnacle, *Balanus amphitrite*, preferred to attach to glass (polar and high surface energy) compared to polystyrene (PS) (non-polar and low surface energy) surfaces. In contrast, O’Connor and Richardson (1994) found that settlement of *B. improvisus* cyprids was higher on PS compared to glass. The apparent preference of *B. amphitrite* for hydrophilic surfaces was reported in a number of studies (Rittschof and Costlow, 1989; Gerhart *et al.*, 1992; O’Connor and Richardson, 1994). However, similar experiments conducted using *B. improvisus* demonstrated an opposite tendency for settling on hydrophobic (low-SFE) surfaces (Dahlström *et al.*, 2004). The apparent difference in surface selectivity between these two species thus became a point of interest since the antifouling formulations have to be effective against a wider range of organisms.

Finlay *et al.* (2010) observed that *B. amphitrite* cyprids preferred to settle on high surface energy organosilica-based xerogel films. Importantly, however, two superhydrophilic zwitterionic polymer coatings, poly(sulfobetaine methacrylate) and poly(carboxybetaine methacrylate) possessing a strong electrostatically-induced

hydration layer, inhibited cyprid settlement, implying that high surface energy materials are not always inductive to settlement of cyprids of this species (Aldred *et al.*, 2010b). In the light of all of these data, it seems increasingly unlikely that surface selection by cyprids can be explained by a simple response to surface wettability. Indeed, experiments on sugar-terminated self-assembled monolayers (SAMs) have recently demonstrated that cyprid settlement was indistinguishable (and very low) for surfaces with advancing water contact angles ranging from <10 to 76° , and with surface energies of ca. 46 and 29 mJ m^{-2} respectively (Ederth *et al.*, 2011). Despite the varying conclusions and experimental approaches of studies aiming to clarify this issue, there remains a widely-held view that cyprids of *B. amphitrite* have a preference for 'high-energy' surfaces (Rittschof and Costlow, 1989; Gerhart *et al.*, 1992; Holm *et al.*, 1997; Qian *et al.*, 2000; Hung *et al.*, 2008).

The most well controlled experiments to date have used glass surfaces modified by silanisation as experimental substrata (Rittschof and Costlow, 1989; Robert *et al.*, 1991; Gerhart *et al.*, 1992; Phang *et al.*, 2009b). Gerhart *et al.* (1992) observed settlement of *B. amphitrite* cyprids on a range of surfaces differing in surface chemistry and surface energy. Their conclusion was that cyprids settle in higher numbers on high energy surfaces. However, the silanised surfaces tested varied in several facets, not least in terms of their surface functional groups, charges and chlorinated and fluorinated end-groups. Additionally, contrary to the initial prediction, no linear relationship was evident between surface energy and settlement for cyprids during experiments, casting some doubt upon the conclusion of that element of the study. Given the importance of *B. amphitrite* as a model organism and, indeed, surface energy in the design of minimally adhesive marine coatings, a controlled study with well-characterized surfaces is long overdue (Callow and Callow, 2011).

The chemisorption of alkylthiol molecules on gold surfaces results in the formation of a well-ordered and densely packed SAM (Bain and Whitesides, 1988) to which a multitude of chemical functionalities can be terminated. The relative ease of preparation and stability of these surfaces, combined with the ability to easily vary the thiol terminal groups make SAMs suitable for a wide range of applications (Bain *et al.*, 1988; Bain and Whitesides, 1989; Dubois and Nuzzo, 1992). SAMs can thus provide a uniform set of surfaces that differ primarily in the nature of the exposed terminal group, allowing clearer interpretation of the cyprid settlement preference on a range of well-characterised and

homogeneous surface chemistries. SAMs have been used previously in investigations of the attachment of organisms to surfaces, for instance algal spores, diatoms and marine bacteria (Callow *et al.*, 2000a; Finlay *et al.*, 2002; Ista *et al.*, 2004; Callow *et al.*, 2005; Ederth *et al.*, 2008). Aldred *et al.* (2006) investigated the attachment and adhesive spreading of mussel (*Mytilus edulis*) byssal threads on alkanethiol SAMs varying in wettability. Using this method, the adhesive plaques of adult mussels were shown to spread preferentially on high-energy surfaces. Using environmental scanning electron microscopy (ESEM), Petrone *et al.* (2009) demonstrated that larvae of the mussel *Perna canaliculus* did not adhere to Teflon, a highly hydrophobic and low-energy surface. Instead, the larvae were observed to stick to each other.

In this chapter the influence of surface energy on the surface preference of *B. amphitrite* and *B. improvisus* cyprids is investigated. The data demonstrate the necessity for well-controlled experimental procedures to quantify the effects. Initially, previous experiments were reproduced to observe the difference in settlement between laboratory-grade glass and PS substrata. The effect of cyprid age on the settlement behaviour of *B. improvisus* was evaluated using sealed PS Petri dishes to reduce the phenomenon of floating cyprids, as proposed by Qiu *et al.* (2008). A more controlled approach towards performing the experiments was then adopted using SAMs that differ in surface energy. Finally, the settlement of cyprids on SAMs with terminal functional groups that varied only in terms of charge and Lewis acid/base characteristics was studied to partition the observed effects on settlement between those arising from a response to Gibbs surface energy and those resulting from changes in surface charge.

2.2 Materials and methods

2.2.1 Culture of cyprids of *B. amphitrite*

Adult barnacle brood-stock (supplied from the Duke University Marine Laboratory, North Carolina, USA) was allowed to release nauplii naturally. Approximately 10,000 stage 1 nauplii were collected over a period of 2 to 3 h. The nauplii were attracted to a cold light source, according to the protocol of Elbourne *et al.* (2008), and transferred at intervals to a dilute solution of *Tetraselmis suecica* for temporary storage at 25°C. When sufficient numbers had been collected, all nauplii were transferred to a clean

plastic bucket containing 10 l of 0.7 μm filtered seawater with 36.5 mg L^{-1} of streptomycin sulphate and 21.9 mg L^{-1} of penicillin G. The larvae were fed an excess of 40% of *Skeletonema marinoi* and 60% of *T. suecica* for 5 days until metamorphosis to the cyprid stage. Cyprids were then filtered from the solution, transferred into 0.22 μm filtered natural seawater (FSW) and used for settlement assays after 3 days of storage at 6°C.

2.2.2 Culture of cyprids of *B.improvisus*

Polystyrene panels (15x15cm) with settled adults of *Balanus improvisus* were collected from Tjärnö Marine station laboratory, Gothenburg University, Sweden. The panels were transferred to the School of Marine Science & Technology at Newcastle University to start a new larger barnacle culture.

In order to improve the barnacle broodstock to guarantee a release of adequate numbers of larvae for future experiments, new panels were prepared to grow new adults. Panels were seeded with cyprids obtained from the original broodstock. The panels were held vertically during culture of the new broodstock. A box was built using five polystyrene panels 12x12 cm stuck together with silicone sealant. Considering the tendency of cyprids of this species to float on the water meniscus, FSW (with algae) was added in the box progressively every 24 hours in order to obtain settled juveniles at different levels on the walls of the box in order to obtain a homogenous distribution. When the basis of barnacles reached a diameter of 1-2 mm, all the panels were detached from the silicone and kept vertically in an aquarium containing 20 litres of artificial sea water.

The larvae released from the first stock of adults were cultured and used to obtain new broodstock on panels of Plexiglas. Barnacles were maintained in artificial seawater (ASW) (Tropic-Marin[®] 22) at 19 ± 2 °C. Adults were cleaned by brushing and the seawater was changed every 2 days. After three months adult broodstock were allowed to release nauplii naturally yielding ~10,000 stage-1 nauplii over a period of 3–4 h. The nauplii were attracted to a 'cold' light source and transferred at intervals to a dilute suspension of *Thalassiosira pseudonana* for temporary storage. When a sufficient number had been collected, the nauplii were transferred to a clean plastic bucket containing 10 l of filtered (0.7 μm) ASW with 36.5 mg l^{-1} of streptomycin sulphate and

21.9 mg l⁻¹ of penicillin G at 28 °C. The larvae were fed an excess of a mixture of 70% of *T. pseudonana* and 30% of *Tetraselmis suecica*. After 2 days, the suspension was filtered using a mesh of 120 µm and nauplii were stored in clean ASW with 50% of *T. pseudonana* and 50% of *T. suecica* for a further 2 days until metamorphosis to the cyprid stage. Cyprids were then filtered using a mesh of 200 µm from the solution and transferred into ASW. Following filtration, 0-day-old cyprids were used to identify a suitable container in which to carry out assays, free from experimental bias, and subsequently to investigate the effect of varying surface energy and charge on cyprid settlement. Additionally, other cyprids from the same batch were stored at 6 °C and aged for up to 5 days to study the effect of cyprid age on settlement.

2.2.3 Substrata for settlement assays

Settlement assays using cyprids of *B. amphitrite* were conducted on a range of substrata. Clean borosilicate glass shell vials, 19 × 65 mm, of 11.1 ml capacity (Fisher Scientific Co., USA) were prepared by heating to 500° C for 4 h (Gerhart *et al.*, 1992). Cleanroom-cleaned Nexterion® Glass B slides (Schott, Germany), 76 mm × 25 mm, 1 mm in thickness, and sterile flat-bottom 24-well PS plates for traditional tissue culture (TC Plate 24Well F) (Sarstedt, USA) (3.6 ml maximum volume per well) were used as received. Assays were performed using 20 cyprids per replicate with 2 ml of 0.22 µm filtered fresh sea water (FSW) with a salinity of 32.

Tests with *B. improvisus* were carried out in a number of borosilicate glass dishes (60 × 15 mm) prepared by heating both bottom and lid to 500° C for 4 h (Gerhart *et al.*, 1992). These dishes were filled to the brim with 15 ml of ASW, the lids were replaced and the two halves of each dish were held together with a rubber band.

Sterile PS Petri dishes (BD Falcon™ 1006, USA) were filled to the brim with filtered seawater (14 ml maximum volume per dish) and subsequently hermetically sealed with a PS lid, ensuring that no air bubbles remained inside. This configuration avoided the issue, previously reported, of cyprids being trapped at the air/water interface during assays. For comparison, cyprid settlement assays were also conducted in 24-well PS tissue culture plates (TC Plate 24-Well F, Sarstedt, USA), which presented the organisms with an air/water interface. Assays were performed using 30 cyprids per

replicate with 0.22 μm filtered ASW at a salinity of 22. Settled cyprids were counted on the base, sides and lid of 4 replicated dishes using for each chemistry. All the Petri dishes were immersed for the entire experiment in a container with ASW at a salinity of 22 pt to avoid any air seepage that would compromise the experimental design.

All assays were conducted in the dark at 28 °C with settlement of cyprids monitored at 24 and 48 h and expressed as percentage settlement.

2.2.4 Gold coating procedure

Glass slides, PS plates and silicon (Si) were gold (Au) coated prior to immersion in thiol solutions for SAM formation. Silicon (100) wafers (Topsil Semiconductor Material A/S, Denmark), used for ellipsometry-based SAM-stability measurements, were cut into pieces and subsequently cleaned with TL1 solution, which is a 1:1:5 solution of 25% NH_3 (Merck, Germany), 30% H_2O_2 (Merck, Germany), and 18.2 M Ω cm Milli-Q water (Millipore), for 10 min at 80°C. Subsequent metal deposition was carried out in a resistively-heated vacuum evaporation system with a base pressure of $< 4 \times 10^{-6}$ mbar. Glass slides and Si pieces were primed with 30 Å-thick layer of titanium (Ti) (Balzers, Liechtenstein, 99.9%) as an adhesion promoter and then coated with a 300 Å-thick Au layer (Nordic High Vacuum AB, Sweden, 99.9%) at a rate of 0.5 and 10 Å s^{-1} , respectively. PS plates and Petri dishes were placed on a rotating sample holder, which was gradually inclined by a moving arm at an angle up to 30° during metal evaporation, enabling metal deposition on both the side and the bottom of the dishes/wells. A schematic of the evaporation system for metal deposition on PS plates and a gold-coated plate and Petri dishes are shown in Figures 12 and 13 respectively.

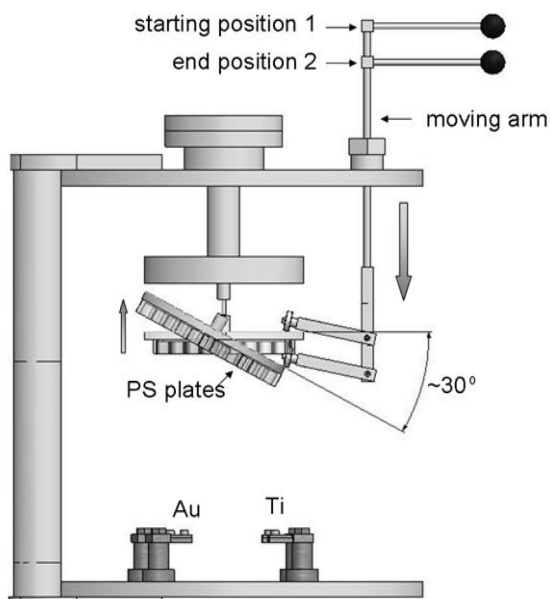


Fig.12 Schematic of the resistively-heated vacuum evaporation system for Ti and Au deposition, and the device for coating PS well plates. The initial and final positions are shown (horizontal and with the PS plates tilted at 30°, respectively). The plate rotates slowly around the vertical axis throughout the process.

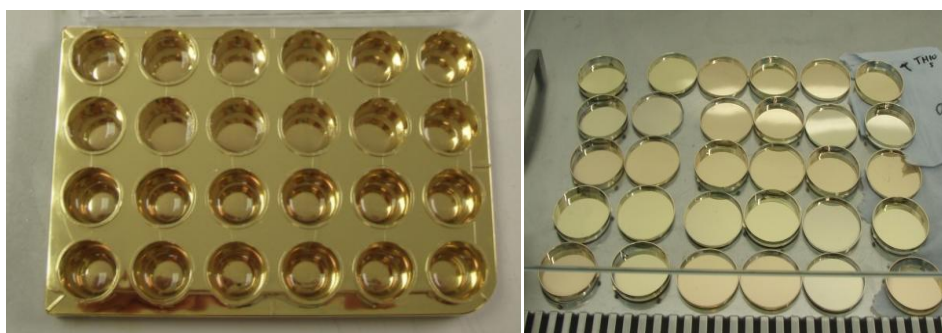


Fig. 13 A gold-coated PS 24-well plate and Falcon 1006 Petri dishes.

2.2.5 Self-assembled monolayer preparation

SAMs were prepared by immersing cleaned gold surfaces in thiol solutions for 24 hr in the dark. Subsequently, the formed SAMs were rinsed three times with 99.5% ethanol (Kemetyl, Sweden), and then dried with nitrogen. Figure 14 illustrates the chemical structure of the thiols used for the preparation of SAM surfaces, viz. $\text{HS}(\text{CH}_2)_{15}\text{CH}_3$ (1-hexadecanethiol) (Fluka Chemie, Switzerland), $\text{HS}(\text{CH}_2)_{16}\text{OH}$ (16-hydroxy-1-hexadecanethiol) (Sigma-Aldrich, Sweden), $\text{HS}(\text{CH}_2)_{16}\text{COOH}$ (16-mercaptohexadecanoic acid, MHA) (Sigma-Aldrich, Sweden), $\text{HS}(\text{CH}_2)_{11}\text{N}(\text{CH}_3)_3^+\text{Cl}^-$

(N,N,N-trimethyl-(11-mercaptoundecyl)ammonium chloride) (Prochimia, Poland), HS(CH₂)₁₆NH₂ (16-amino-1-hexadecanethiol) (Prochimia, Poland), HSCH₂COOH (thioglycolic acid) (Sigma-Aldrich, Sweden), and HSC₆H₄COOH (thiosalicylic acid, TSA) (Sigma-Aldrich, Sweden), HS(CH₂)₁₁PO(OH)₂ (11-mercapto-1-undecylphosphonic acid) (Prochimia, Poland), HS(CH₂)₁₁SO₃Na (sodium 11-mercaptoundecanesulfonate) (Prochimia, Poland).

After incubation, the surfaces were rinsed with ethanol, ultrasonicated in ethanol for 3 min and then dried under nitrogen flow. The Au-coated PS wells were filled by pipetting in 3 ml of 100 μM thiol solutions immediately after removal from the metal evaporation chamber.

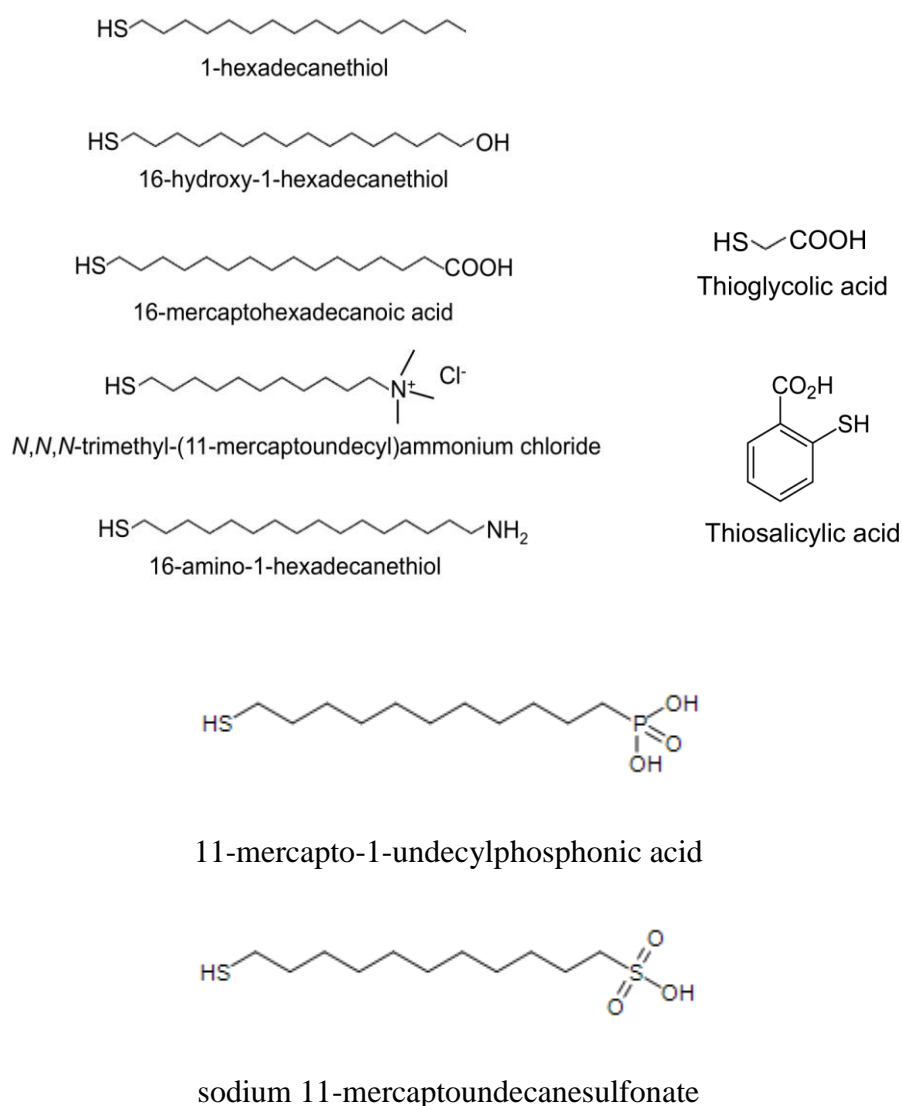


Fig. 14 Chemical structures of the thiols used for the preparation of the self-assembled monolayer surfaces.

2.2.6 Infrared reflection-absorption spectroscopy – IRAS

A Bruker IFS 66 FT-IR spectrometer, equipped with a liquid nitrogen-cooled mercury-cadmium-telluride (MCT) detector, was used to record IR spectra of the SAM surfaces on gold-coated Si substrata. IRAS spectra were acquired with *p*-polarized light aligned at a 85° angle of incidence, and with 2000 scans at 2 cm⁻¹ resolution. The background spectrum was obtained using a deuterated 1-hexadecanethiol [HS(CD₂)₁₅CD₃] SAM on gold. The optical bench was continuously purged with N₂ gas during the measurements.

2.2.7 Ellipsometry

Thickness measurements of SAMs on gold-coated Si substrata were carried out using an automatic null ellipsometer (Rudolph Research AutoEL III) equipped with a He–Ne laser ($\lambda=632.8$ nm), set at an incidence angle of 70°. SAM thicknesses were calculated from the measurement outputs (Δ and Ψ) using a three-layer parallel slab Au/SAM/air model. An isotropic refractive index, $n=1.50$ and $k=0$, was assumed for the SAM. The reported values were the averages of five measurements on each surface.

2.2.8 Contact angle goniometry

Advancing contact angles of SAMs prepared on gold-coated Si substrata were measured with a CAM 200 Optical Contact Angle Meter (KSV Instruments Ltd, Finland) equipped with a manual liquid dispenser. SAMs were withdrawn from ethanol solution, washed in ethanol and subsequently dried under a N₂ stream. The reported advancing contact angle values were the average of five measurements with each liquid (see next section for details) at different locations.

2.2.9 Surface energy calculation

Gibbs surface energy (γ_s) was estimated from contact angle data for each SAM using the Good–van Oss–Chaudhury (GvOC) model (Good, 1993). This is a relatively robust approach since it makes use of three different test liquids, rather than only one or two as required for other methods. Contact angles were measured with water (W), glycerol

(G) and diiodomethane(DIM), and their surface energy parameters are reported in Table 1. In the GvOC model, the surface energy is divided into a dispersive Lifshitz-Vander Waals (γ^{LW}) component and a polar Lewis acid/base (γ^{AB}) component. γ^{AB} is further divided into a Lewis base (electron donor) component γ^- and a Lewis acid (electron acceptor) component γ^+ , so that:

$$\gamma_S = \gamma^{LW} + \gamma^{AB} = \gamma^{LW} + 2\sqrt{\gamma^- \gamma^+} \quad (1)$$

The GvOC model provides a relation between contact angle and surface energy parameters

$$\gamma_{li} (\cos \theta_{li} + 1) = 2 \left(\sqrt{\gamma_S^{LW} \gamma_{li}^{LW}} + \sqrt{\gamma_S^+ \gamma_{li}^-} + \sqrt{\gamma_S^- \gamma_{li}^+} \right) \quad (2)$$

where the subscript S indicates the solid, and li denotes the liquid i . For an apolar liquid $\gamma^{AB} = \gamma^- = \gamma^+ = 0$, and thus γ_S^{LW} can be directly obtained from

$$\gamma_S^{LW} = \gamma_{li}^{LW} \frac{(\cos \theta_{li} + 1)^2}{4} \quad (3)$$

The so-obtained γ^{LW} and contact angles measured with two polar liquids can be substituted into Equation(2) to obtain γ^{AB} (a system of two equations with two unknown parameters, γ^- and γ^+).

LIQUID	γ	γ^{LW}	γ^{AB}	γ^+	γ^-
Water	72.8	21.8	51	25.5	25.5
Glycerol	64	34	30	3.92	57.4
Diiodomethane	50.8	50.8	0	0	0

Table 1. Surface energy components for water, glycerol and diiodomethane in mJ m⁻² (Good, 1993).

2.2.10 Stability tests

The stability of alkanethiol SAMs on gold has been tested in previous studies following 6 months immersion in NaCl at high concentration (1 M) (Ederth *et al.*, 1998) and also in biological media (Flynn *et al.*, 2003). These data suggest that SAMs in aqueous solutions can be reliably employed over a time scale of several weeks. However, prior to the biological assays, the stability of the SAMs was assessed by incubation for 4 days at 25°C in a simplified form of the artificial seawater specified by ASTM D1141-98 (2003). ASW was prepared by dissolving sodium chloride (420 mM), magnesium chloride hexahydrate (54.6 mM), sodium sulfate (28.8 mM), calcium chloride dihydrate (10.5 mM), and potassium chloride (9.3 mM) in Milli-Q water. The pH was adjusted to 8.2 with 0.1 M NaOH, and the ASW was subsequently filtered with a 0.2 µm filter (Nalgene, USA). After 4 days of immersion, SAMs were thoroughly rinsed with deionized water to remove salts, dried under a nitrogen stream, and their stability was subsequently investigated by contact angle goniometry, ellipsometry and IRAS. The ellipsometric thicknesses calculated for $-\text{CO}_2^-$ (MHA), $\text{N}(\text{CH}_3)_3^+$, CH_3- and $\text{OH}-$ terminated SAMs, along with the corresponding advancing water contact angles, remained unchanged after the period of immersion (Table 2). IRAS spectra showed CH_2 stretching vibrations to be about 2917 and 2850 cm^{-1} , which are indicative of crystalline-like assemblies of alkyl chains on the gold substratum. A comparison of the IRAS spectra before and after immersion in ASW showed negligible differences.

2.2.11 Data analysis

Settlement data are reported as means \pm standard error (SE). The effect of surface chemistry on settlement was examined by one-way analysis of variance (ANOVA) when the assumptions for parametric analysis were fulfilled. In addition Tukey pairwise comparisons using Minitab 15 and an α level of 0.05 were used.

When data were not normally distributed or showed dissimilar variances, Kruskal–Wallis analysis was used followed by Dunn’s test. All such analyses are displayed with 95% confidence intervals. The normality of the data was assessed using normal plots of residual values and homogeneity of variance was measured using plots of standardized residual values versus fitted values.

A general linear model (GLM) was designed to test the effects of charge and SFE independently on the settlement of the two species and to highlight any interactive effects. Under normal circumstances, data for unrelated assays would not be compared in this way, however, settlement on each surface was so similar between species (assays) that this approach was considered to be rigorous and highly illustrative.

To balance the model, two levels of SFE energy were assumed: 'low' including the CH₃ surface and 'high' including all other surfaces whose contact angles lay within a 10° range (only surfaces with data for both species could be included in the model). The model allowed investigation of the effects of surface charge, SFE, species and the interactions between SFE and species, and charge and species. The interaction between SFE and charge could not be investigated due to the absence of low-SFE charged surfaces. 'Species' was included as a covariate in the analysis.

2.3 Results

2.3.1 *Stability test in ASW*

Infrared Reflection-Absorption Spectroscopy (IRAS) was used to assess the stability of SAMs after 4 days immersion in ASW. IRAS spectra from the chemisorption of HS-(CH₂)₁₅-N(CH₃)₃⁺ on a gold surface, before and after immersion in ASW are shown in Figure 15. The absorption at 1081 cm⁻¹ associated with C-N vibrational mode splits to give a stronger additional band at 1099 cm⁻¹. The bands at 1489 and 1375 cm⁻¹ arise from CH₃ symmetric and asymmetric stretching vibrations, respectively. Lastly, the absorption at 1464 cm⁻¹ is due to the CH₂ scissoring deformation of the backbone chain.

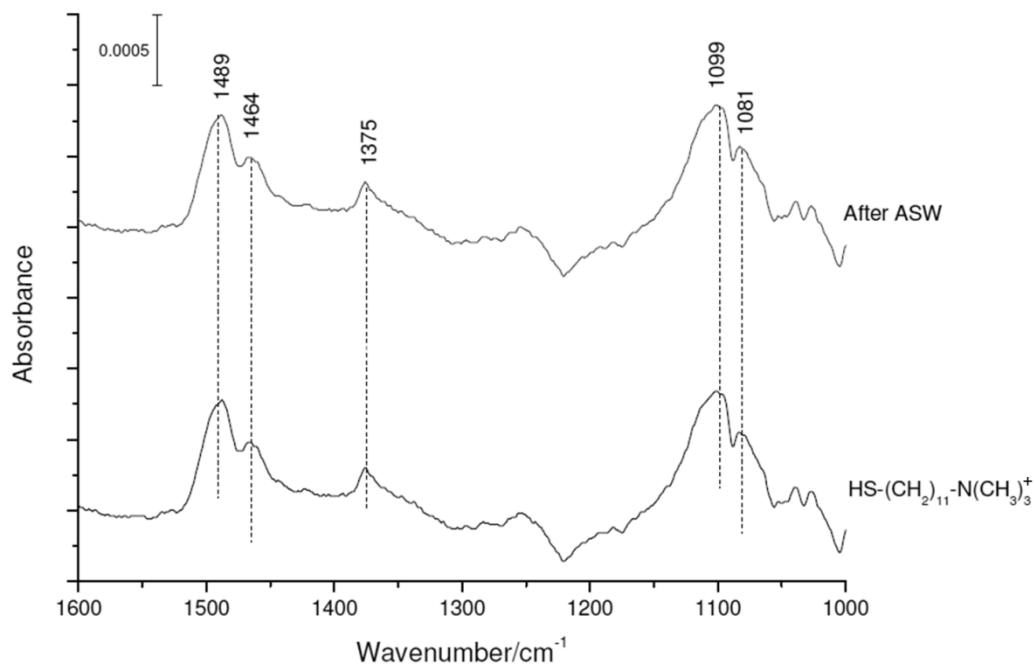


Fig. 15 IRAS spectra of $\text{N}(\text{CH}_3)_3^+$ -terminated SAM in the region between 1600-1000 cm^{-1} before and after 4 days immersion in ASW.

Figure 16 shows the IRAS spectra of SAM obtained from $\text{HS}(\text{CH}_2)_{15}\text{COOH}$ chemisorbed on gold. The peak at 1745 cm^{-1} associated with $\text{C}=\text{O}$ stretching mode of $-\text{COOH}$ groups slightly decreases after immersion in ASW due to the dissociation of the acid groups at the pH of seawater. The band peaking at 1717 cm^{-1} due to $\text{C}=\text{O}$ stretching mode of COOH dimers (hydrogen bonded acids) also appears less intense after immersion and shifts to 1700 cm^{-1} . Accordingly, the asymmetric and symmetric COO^- bands at 1562 and 1470 cm^{-1} , respectively, appear to increase after immersion. Contributions to the broad symmetric carboxylate stretching band are also present peaking at 1440 cm^{-1} , which are assigned to the bending mode of CH_2 groups. Finally, the band at 1314 cm^{-1} is assigned to $\text{C}-\text{O}$ stretch of COOH groups.

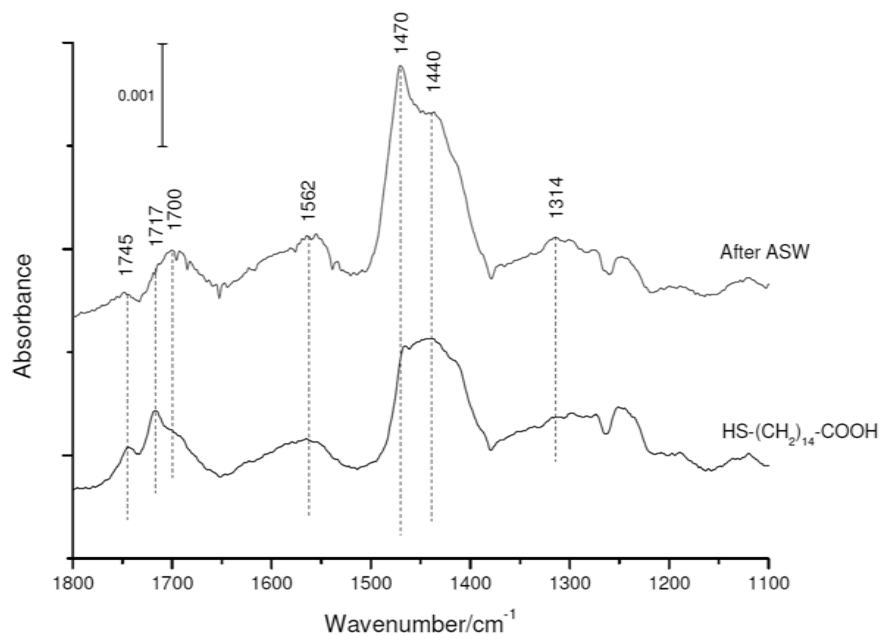


Fig. 16 IRAS spectra of HS-(CH₂)₁₅-COOH-terminated SAM in the region between 1800-1100 cm⁻¹ before and after 4 days immersion in ASW.

Figure 17 shows IRA spectra from the adsorption of HS-(CH₂)₁₅-CH₃ on gold, before and after immersion in ASW. The bands at 2964 and 2878 cm⁻¹ are assigned to the CH₃ asymmetric (ν_{as} CH₃) and (ν_s CH₃) symmetric stretching modes, respectively.

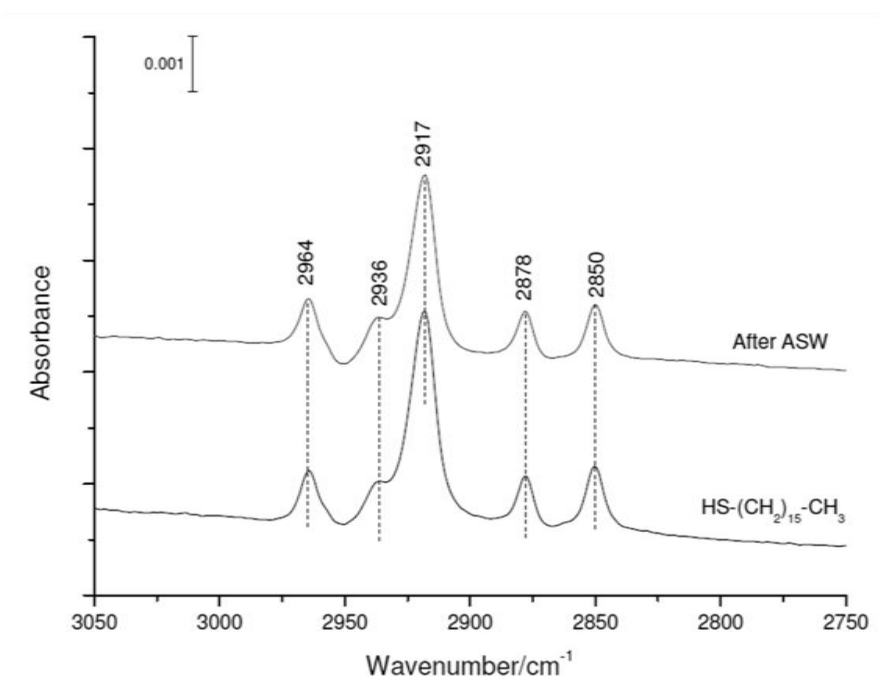


Fig. 17 IRAS spectra of CH₃-terminated SAM in the region between 3050-2750 cm⁻¹ before and after 4 days immersion in ASW.

The bands at 2917 and 2850 cm^{-1} are assigned to the $\nu_{as}\text{CH}_2$ and $\nu_s\text{CH}_2$ modes, respectively. The band observed at 2936 cm^{-1} arises from the splitting of the $\nu_{as}\text{CH}_3$ band, owing to Fermi resonance interactions with the lower frequency of the asymmetric CH_3 deformation mode. IRAS spectra associated with the chemisorption of $\text{HS}-(\text{CH}_2)_{15}\text{-OH}$ on a gold surface before and after immersion in ASW are shown in Figure 18.

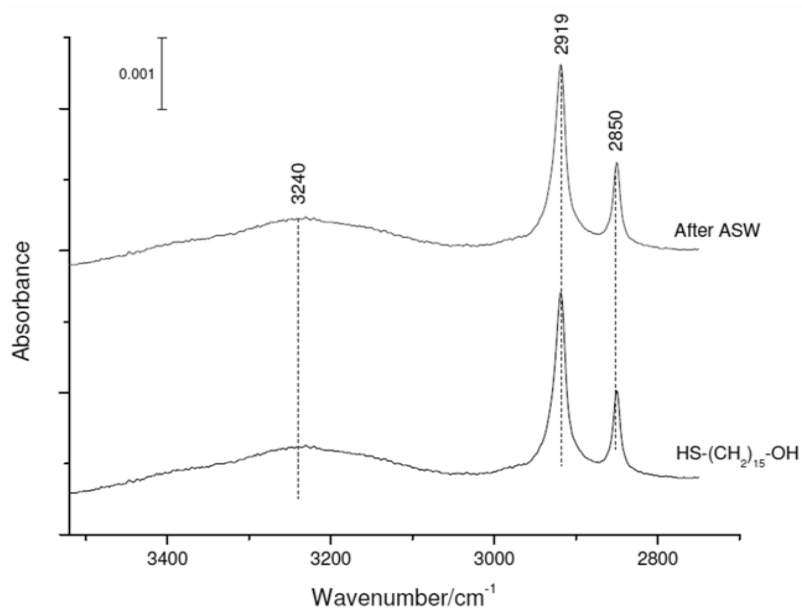


Fig. 18 IRAS spectra of $\text{HS}-(\text{CH}_2)_{16}\text{-H}$ -terminated SAM in the region between 3500-2700 cm^{-1} .

The bands at 2920 and 2850 cm^{-1} are assigned to the $\nu_{as}\text{CH}_2$ and $\nu_s\text{CH}_2$ modes, respectively. The broad adsorption peaking at 3050 cm^{-1} arises from the OH stretching vibration before and after 4 days immersion in ASW.

2.3.2 Effect of cyprid age

Three-day-old cyprids of *B. amphitrite* were used for all the bioassays presented in this thesis as is conventional for antifouling tests with this species (insert reference). Methodology for *B. improvisus* is less established and thus assays with a range of ages of cyprids have been used in order to understand how the settlement behaviour can be influenced.

Figure 19 shows the mean settlement percentage of different ages of cyprids, ranging from 0- to 5-days-old, after 24 and 48 h in PS Petri dishes. After 48 h, the mean settlement percentages (\pm standard error) for 0-, 1-, 2-, 3-, 4- and 5-day-old cyprids were $46 \pm 12\%$, $53 \pm 9\%$, $51 \pm 5\%$, $34 \pm 3\%$, $28 \pm 11\%$ and $60 \pm 3\%$, respectively. Settlement data differed significantly between different ages of cyprid ($p < 0.05$, $F = 4.46$) (ANOVA, Tukey test) and pairwise comparisons are presented in Figure 19. Cyprids of 0, 1, 2 and 5 days old settled in significantly higher numbers compared to 3- and 4-day-old cyprids at 48 h. Settlement after 24 h did not yield significant differences.

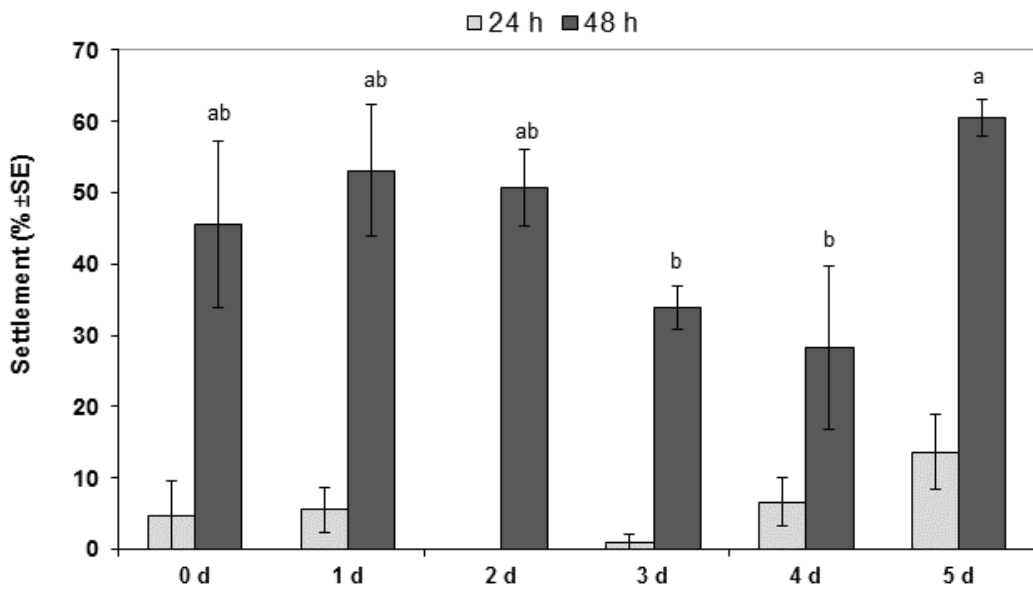


Fig. 19 Mean percentage settlement (\pm standard error) of cyprids of *B. improvisus* from 0- to 5-days-old in uncoated PS Petri dishes after 24 and 48 h in FSW (salinity = 20). Results of Tukey pairwise comparisons are presented. Means that do not share a letter are significantly different.

2.3.3 Determination of settlement assay method

Prior to assays of settlement of cyprids of *B. amphitrite* and *B. improvisus*, different designs were tested to determine which was the most consistent approach to assess the effect of a single surface variable. Initially, settlement assays were conducted in drops on glass microscope slides; a surface with high wettability and high surface energy (Zisman, 1972). Additionally, two SAMs, alkyl- (CH_3) and hydroxyl (OH)-terminated, were also prepared on Au-coated glass slides. The advancing water contact angles (θ_w) for CH_3 - and OH -terminated SAMs were 107° and 39° , respectively, and for the

microscope slide glass a value of 16° was recorded. A volume of ~ 2 ml filtered seawater containing 20 cyprids was placed on each substratum, resulting in a droplet height of ~ 0.5 cm for the CH_3 -terminated SAM at the highest point of the meniscus, and of < 0.3 cm for the OH-terminated SAM with the solution spreading to the edge of the slide. In three replicate assays performed on these three chemistries, cyprid settlement was consistently negligible after 48 h.

2.3.4 Effect of container

While *B. amphitrite* settlement assays in PS 24-well plates presented no particular issues, cyprids of *B. improvisus* were found floating on the water meniscus, as mentioned previously. An attempt was made to address this problem by removing the air-water interface in dishes (Qiu et al., 2008).

PS 24-well plates were used to determine the percentage of cyprid (0-day-old) settlement after 24, 48 and 72 h. Settlement (\pm standard error) was low at each observation, $5 \pm 2\%$, $9 \pm 3\%$ and $15 \pm 4\%$, respectively (Figure 20A). Low settlement values reflected the large number of cyprids 'floating' trapped in the liquid meniscus. Performing settlement assays in sealed FalconTM 1006 Petri dishes, containing no trapped air, negated this issue and the mean percentage of settled cyprids increased to $46 \pm 11\%$ after 48 h and $80 \pm 8\%$ after 72 h (Figure 20B).

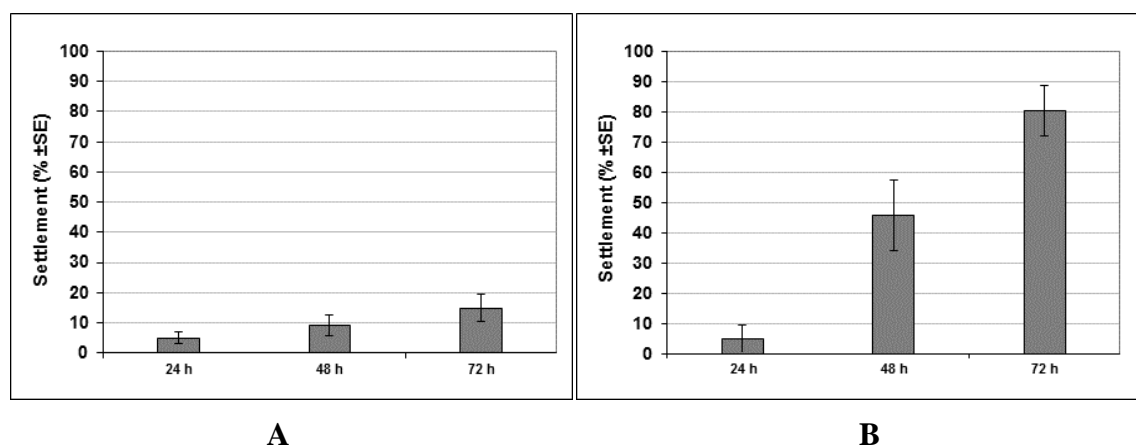


Fig.20 Mean percentage of cyprids (\pm standard error) (0-day-old) of *Balanus improvisus* in FSW (salinity = 20) settled after 24, 48 and 72 h in (A) uncoated PS 24-well plates and (B) uncoated sealed Petri dishes.

2.3.5 Settlement assays using glass and polystyrene

Settlement assays with cyprids of *B. amphitrite* were carried out in glass vials and in PS 24-well plates with the same number of cyprids in the same volume for each treatment, viz. 20 cyprids in 2 ml of FSW and 12 replicates for each surface. Surface energy values for glass and PS, estimated by the GvOC approach, were 48.0 and 47.3 mJ m⁻², respectively. Figure 21A shows the mean settlement percentage of cyprids after 24 and 48 h in glass vials and in PS well plates. The mean percentages of settlement for glass and PS were 43 ± 4% and 15 ± 4% at 24 h, and 57 ± 5% and 32 ± 5% at 48 h, respectively. Settlement differed significantly between these surfaces at both 24 h ($p < 0.05$, $F = 25.72$) and 48 h ($p < 0.05$, $F = 11.39$) at 95% confidence (ANOVA).

Figure 21B shows the mean percentage settlement of cyprids of *B. improvisus* tested in borosilicate glass dishes and PS Petri dishes. After 24 h the mean percentage settlement on glass was 1.9 ± 1.85 % and 4.8 ± 4.8 % on PS. After 48 h settlement on glass was 2 ± 2 % and on PS 45.6 ± 11 %. Settlement on the surfaces did not differ after 24 h ($p > 0.05$, $F = 0.65$) but did after 48 h ($p < 0.05$, $F = 27.59$) at 95% confidence (ANOVA).

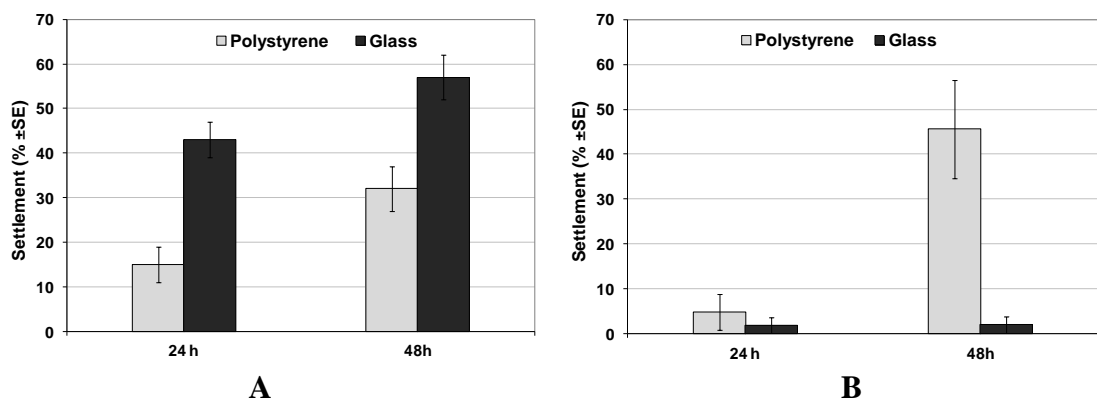


Fig. 21 Mean percentage settlement (\pm standard error) of (A) *B. amphitrite* in FSW (salinity = 32) and (B) *B. improvisus* cyprids in FSW (salinity = 20) on glass and polystyrene after 24 h and 48 h.

2.3.6 Settlement in relation to Gibbs surface energy

Tests were continued using plates with wells containing OH- and CH₃-terminated SAMs. These SAMs had surface energy values of ca 47.4 mJ m⁻² and 19.6 mJ m⁻², respectively. Figure 19 shows the percentage settlement of cyprids of both species on these two surfaces after 24 and 48 h.

Settlement was not significantly different on the two types of SAM for *B. amphitrite* at 24 h ($p > 0.05$, $F = 12.87$), but was after 48 h ($p < 0.05$, $F = 25.66$) at 95% confidence (ANOVA) (Fig 22A). Settlement of *B. improvisus* on these surfaces showed the same trend (Fig 22B) with no significant differences after 24 h ($p > 0.05$, $F = 2.34$) but significant differences after 48 h ($p < 0.05$, $F = 24.26$) at 95% confidence (ANOVA).

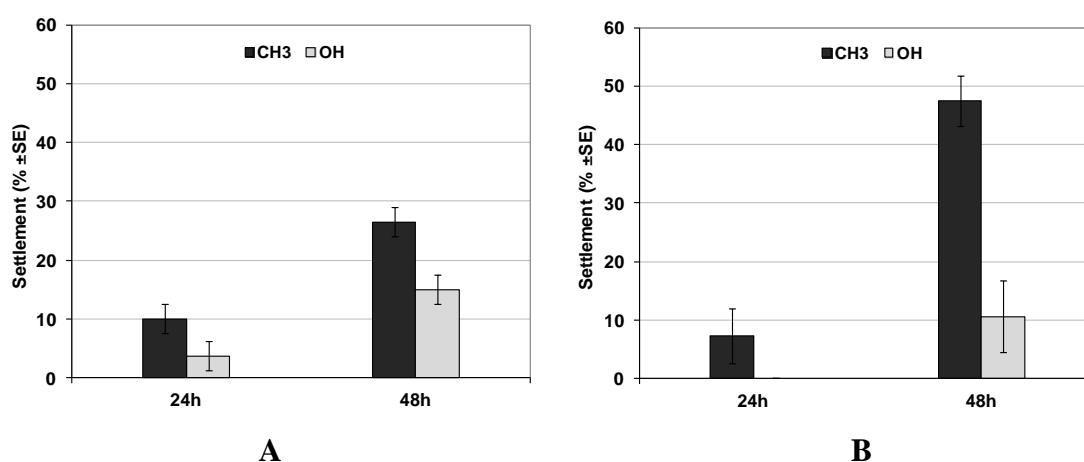


Fig.22 Mean percentage settlement of cyprids (\pm standard error) of (A) *B. amphitrite* in FSW (salinity = 32) and (B) *B. improvisus* cyprids in FSW (salinity = 32) settled on CH₃- and OH-terminated SAMs after 24 h and 48 h. Settlement on the control PS was $13 \pm 2\%$ and $29 \pm 3\%$ after 24 and 48 h, respectively.

2.3.7 Settlement in response to surface charge

2.3.7.1 *B. amphitrite*

In addition to the CH₃- and OH-terminated SAMs tested previously, two further alkanethiols (see Figure 14) were included in this experiment to determine the effects of surface charge on surface selection by cyprids. Both $-\text{CO}_2^-$ (MHA) and $\text{N}(\text{CH}_3)_3^+$ -terminated SAMs have low advancing water contact angles (45° and 60° , respectively) and relatively high overall γ_s (41.5 mJ m^{-2} and 50.9 mJ m^{-2} , respectively). For comparative purposes, the OH-terminated SAM used in the paragraph 2.3.6 was also included here (Table 3) as a neutrally-charged, high-energy ($\gamma_s = 47.4 \text{ mJ m}^{-2}$) control surface. Cyprid settlement data were plotted against the nominal surface charge after a 48 h exposure to surfaces (Figure 23). Three additional high energy, charged SAM surfaces, derived from $-\text{CO}_2^-$ (TSA – thiosalicylic acid) and $-\text{CO}_2^-$ (thioglycolic acids) (negatively-charged) and an $-\text{NH}_3^+$ -terminated SAM (positively-charged), were also included. Kruskal–Wallis analysis followed by Dunn's test suggested that settlement was

similar on all threenegatively-charged surfaces and on both positively-charged surfaces. Increased settlement was shown onthe negatively charged surfaces, however, compared tothe positive and neutrally-charged surfaces (see Table 2for results of pairwise comparisons; Kruskal–WallisW = 28.24, $p < 0.001$). Settlement on the secondpositively-charged NH_3^+ -SAM was also negligible,confirming previous results on the $\text{N}(\text{CH}_3)_3^+$ -SAM.

Differences	Significant level
$-\text{N}(\text{CH}_3)_3^+$ vs $-\text{CO}_2^-$ (MHA)	<0.01
$-\text{N}(\text{CH}_3)_3^+$ vs $-\text{CO}_2^-$ (TSA)	<0.01
$-\text{N}(\text{CH}_3)_3^+$ vs $-\text{CO}_2^-$ (thioglycolic acid)	<0.001
$-\text{NH}_3^+$ vs $-\text{CO}_2^-$ (thioglycolic acid)	<0.05

Table 2. Significant differences identified using Kruskal–Wallis/Dunn’s tests on data in Figure 20.

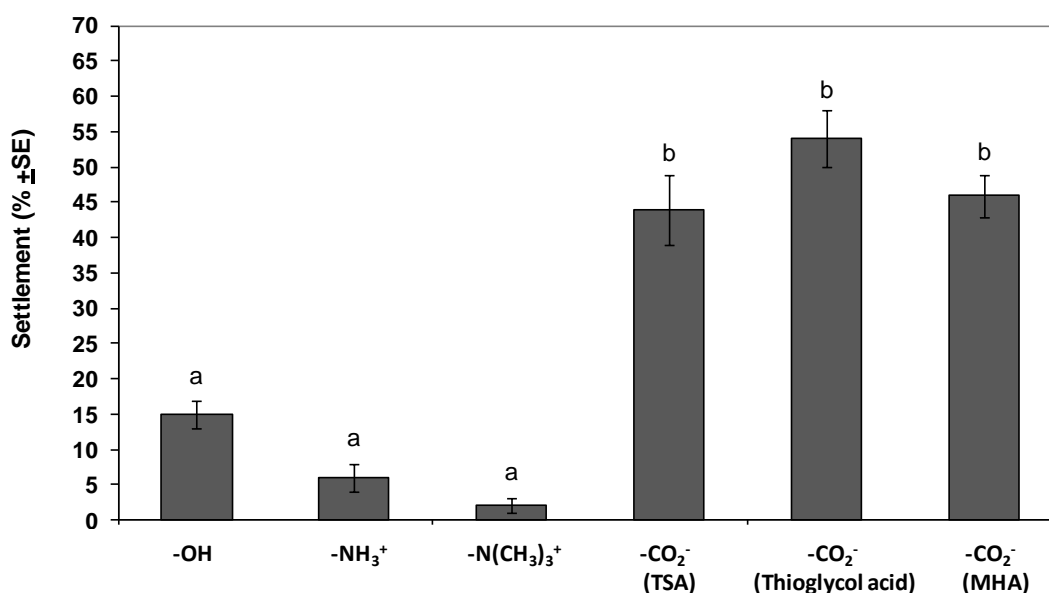


Fig. 23 Mean percentage settlement (\pm standard error) of *B. improvisus* on SAMs applied to 24 well plates with 2 mL FSW (salinity= 32) after 48 hr, where $-\text{CH}_3$ is an abbreviation of $\text{HS}(\text{CH}_2)_{15}\text{CH}_3$, $-\text{OH} = \text{HS}(\text{CH}_2)_{16}\text{OH}$, $-\text{NH}_3^+ = \text{HS}(\text{CH}_2)_{16}\text{NH}_2$, $-\text{N}(\text{CH}_3)_3^+ = \text{HS}(\text{CH}_2)_{11}\text{N}(\text{CH}_3)_3^+$, $-\text{CO}_2^-$ (TSA) = $\text{HSC}_6\text{H}_4\text{COOH}$, $-\text{CO}_2^-$ (thioglycolic acid) = HSCH_2COOH and $-\text{CO}_2^-$ (MHA) = $\text{HS}(\text{CH}_2)_{16}\text{COOH}$. Tukey pairwise comparisons are presented. Means that do not share a letter are significantly different.

Differences between the positively-charged SAMs and the OH-terminated SAMs were not significant (Dunn's test). Data for all surfaces were plotted against surface energy in Figure 20. Glass and oxygen plasma treated PS (Session 2.3.5) were not included as these surfaces differed in more than one parameter. Mean percentage settlement was also plotted against the dispersive (γ^{LW}) and polar (γ^{AB}) components of surface energy separately and additionally against γ^+ and γ^- , and still no trend emerged (data not presented). Contact angles measured with the three test liquids (θ_W , θ_{DIM} , θ_G) and surface energy parameters (γ_s , γ^{LW} , γ^{AB} , γ^+ , γ^-) for all surfaces are reported in Table 3, along with the settlement assays in which they were employed.

2.3.7.2B. *improvisus*

Tests were conducted with 0-day-old cyprids as described in the literature (O'Connor and Richardson, 1994; 1996; Berntsson, Jonsson, *et al.*, 2000; Dahlström *et al.*, 2000; Berglin *et al.*, 2001). SAMs were prepared from positively charged ($-\text{N}(\text{CH}_3)_3^+$ and $-\text{NH}_3^+$), negatively charged ($-\text{SO}_3^-$, $-\text{PO}_3^{2-}$ and $-\text{CO}_2^-$ (TSA)), and neutral hydrophilic and hydrophobic ($-\text{OH}$ and $-\text{CH}_3$) tail groups. Thickness, advancing water contact angle with three liquids (W, DIM and G) and Gibbs surface energy for SAMs used in this work are reported in Table 3.

Compared with the test carried out with *B. amphitrite*, here are reported settlement responses using different negatively charged surfaces ($-\text{SO}_3^-$, $-\text{PO}_3^{2-}$). The only negatively charged surface in common between the two species was $-\text{CO}_2^-$ (TSA).

$-\text{CO}_2^-$ (MHA) and $-\text{CO}_2^-$ (thioglycolic acids) were toxic. The reason for the toxicity may be correlated to their exclusion in combination with leachate, since tests with *B. improvisus*, compared to those with *B. amphitrite*, were carried out using closed and sealed supports. This was supported also by toxicity tests carried out using cyprids of *B. amphitrite* in the same conditions, in Falcon 1006 Petri dishes, in which the mortality was 100 % after 24 h (results not presented here).

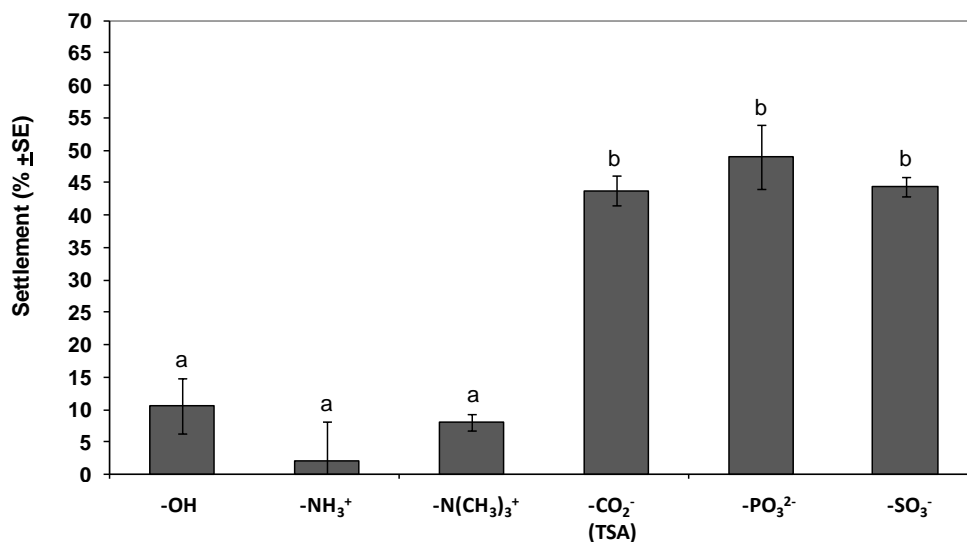


Fig. 24 Settlement of cypris larvae of *B. improvisus* on SAMs applied to sealed Petri dishes with 15 mL FSW (salinity=20) after 48 hr, where -CH₃ is an abbreviation of HS(CH₂)₁₅CH₃, -OH = HS(CH₂)₁₆OH, -NH₃⁺ = HS(CH₂)₁₆NH₂, -N(CH₃)₃⁺ = HS(CH₂)₁₁N(CH₃)₃⁺, -CO₂⁻ (TSA) = HSC₆H₄COOH, -PO₃²⁻ = HS(CH₂)₁₁PO(OH)₂ and -SO₃⁻ = HS(CH₂)₁₁SO₃Na. Tukey pairwise comparisons are presented. Means that do not share a letter are significantly different.

Settlement was enumerated at 48 h to allow comparison with previous studies. Cyprid mean parentage settlement was $11 \pm 6\%$ on the neutral and hydrophilic OH-SAM, and $47 \pm 4\%$ on the neutral and hydrophobic CH₃-SAM (Figure 24). Settlement was $8 \pm 2\%$ and $2 \pm 1\%$ on the positively charged N(CH₃)₃⁺- and NH₃⁺-SAMs, respectively. Cyprid settlement was highest on the negatively charged surfaces with average percentages of $44 \pm 4\%$ on SO₃⁻, $49 \pm 2\%$ on PO₃²⁻ and $43 \pm 5\%$ on CO₂⁻(TSA) SAM. Settlement differed significantly between surfaces ($p < 0.05$, $F = 30.42$) at 95% confidence (ANOVA, Tukey method). On comparison of the present data with those presented by Petrone *et al.* (2011), a close similarity was noted between the settlement response of cyprids of *B. amphitrite* and *B. improvisus* to the range of surfaces under investigation. A GLM was used to illustrate these similarities. Taken together, the data satisfied the assumptions of normality and homogeneity of variance required for this test.

The results of the GLM indicated a significant effect of species ($F = 6.15$ $p = 0.021$), with generally higher settlement of *B. improvisus* across the range of surfaces. Given the differences in assay method and period of time between conducting the two assays, however, this result is not considered to be particularly informative. What was of special interest was the relative response of the two species to the physico-chemical properties

of the surfaces. SFE did not influence settlement significantly ($F = 1.48$ $p = 0.235$). On the contrary, charge exerted a significant effect ($F = 4.08$ $p = 0.03$) with both species settling in greater numbers on negatively charged surfaces. The interaction between SFE and species produced a significant result ($F = 10.41$ $p = 0.004$), suggesting a difference in the way that the two species respond to SFE. This result may be explained by the far higher settlement of *B. improvisus* on the CH₃ SAM compared to the OH SAM; a difference that was much reduced, although nevertheless significant (Petrone *et al.*, 2011) for *B. amphitrite*.

Surface	Thickness (Å)	Contact angle (°)			Surface energy parameter (mJ m ⁻²)				
		θ_W	θ_{DIM}	θ_G	γ^{LW}	γ^{AB}	γ^+	γ^-	γ_s
Glass	-	16 ± 2	34 ± 3	31 ± 2	42.5	5.5	0.1	71.1	48.0
PS	-	79 ± 3	26 ± 3	54 ± 2	45.8	1.5	0.1	6.8	47.3
-CH₃	18.4 ± 0.2	107 ± 1	77 ± 1	83 ± 2	19.1	0.5	0.1	0.5	19.6
-OH	21.3 ± 0.2	39 ± 2	38 ± 3	18 ± 2	40.6	6.8	0.3	40.7	47.4
-CO₂⁻ (TSA)	3.8 ± 0.4	56 ± 3	19 ± 2	21 ± 2	48.1	3.8	0.2	19.3	51.9
-CO₂⁻ Thioglycolic acid)	3.5 ± 0.3	27 ± 2	61 ± 2	52 ± 5	45.4	7.7	0.5	27.2	53.1
-CO₂⁻ (MHA)	21.3 ± 0.2	45 ± 3	40 ± 2	41 ± 2	39.6	1.9	0.0	43.9	41.5
-NH₃⁺	20.8 ± 0.5	47 ± 2	32 ± 3	49 ± 2	43.4	10.1	0.6	46.0	53.5
-N(CH₃)₃⁺	14.3 ± 0.5	60 ± 2	28 ± 3	50 ± 3	45.0	5.9	0.3	26.8	50.9
-SO₃⁻	20.6 ± 0.3	63 ± 1	37 ± 2	50 ± 1	25.2	14.8	1.8	30.5	40
-PO₃²⁻	25.1 ± 0.4	41 ± 3	41 ± 3	37 ± 1	29.3	7.7	1.2	11.9	37

Table 3. The subset of samples used in each comparative experiment is indicated, as well as SAM thicknesses, contact angles measured with the three test liquids (γ_W , γ_{DIM} , γ_G), and surface energy parameters (γ^{LW} , γ^{AB} , γ^+ , γ^- , γ_s) calculated with the GvOC model, for all surfaces.

The interaction between charge and species was not significant ($F = 0.13$ $p = 0.876$); both species responded similarly to surface charge. The clustering suggested by these results can be seen clearly in an overlay of the two datasets (Figure 25).

2.4 Discussion

The central aim of this investigation was to determine specific effects of surface wettability and Gibbs surface energy on the settlement of cyprids of *B. amphitrite* and *B. improvisus*, and to this end, experiments were carried out initially on the substratum that has been used most often in the literature, i.e. glass microscope slides. The expectation was that settlement would be higher on high surface energy materials (Rittschof and Costlow, 1989; Gerhart *et al.*, 1992; Hung *et al.*, 2008) and lower on those surfaces with lower surface energy, as previously reported. However, despite repeated attempts, cyprid settlement was consistently low or negligible when tested in drop-assay format (Aldred *et al.*, 2010b; Petrone *et al.*, 2011; 2013) on SAM-coated microscope slides. It was concluded that the low contact angle of water on the more hydrophilic surfaces restricted cyprid movement and these data were thus considered to be unreliable. SAMs on gold-coated glass slides have been used to conduct settlement assays with microorganisms smaller than cyprids, for instance algal spores, diatoms and marine bacteria (Callow *et al.*, 2000a; Finlay *et al.*, 2002; Ista *et al.*, 2004; Callow *et al.*, 2005; Ederth *et al.*, 2008). Glass slides are used regularly for various standard biofouling assays and, while this is unproblematic when the whole slide is immersed in a solution containing the organisms under investigation, the method presents difficulties for assays such as those with cyprids. To date, experiments using cyprids confined to droplets on flat surfaces have often exhibited low settlement. However, for many novel antifouling materials, particularly those involving texture modulation that cannot be applied in wells, tubes or dishes, there remains no other viable option.

Further settlement assays of *B. amphitrite* cyprids were thus performed in glass vials and PS well plates that offered similar environments for the cyprids. Likewise, assays with *B. improvisus* used borosilicate glass dishes and PS Petri dishes. These formats had the advantage that a large volume of water could be used and a constant, large surface area was available to the cyprids for settlement, while also minimizing evaporation. In this

way, cyprids were not restricted for swimming space by the low contact angle of sessile water drops on high-energy surfaces, nor was space for settlement limited on low-energy surfaces where the contact angle was high, thus creating a smaller droplet 'footprint'. Using this method the assays conducted by previous researchers were reproduced (e.g. Rittschof and Costlow, 1989; Gerhart *et al.*, 1992; O'Connor and Richardson, 1998); these authors concluded that high-energy surfaces were preferable on the basis of cyprid settlement on glass and PS.

Initially *B. improvisus* cyprid settlement assays were carried out following the same method used for *B. amphitrite*. However, settlement assays carried out in 24 PS well plates resulted in negligible settlement after 48 h (see Fig. 20) due to cyprids becoming trapped at the air/seawater interface. The phenomenon of 'floating cyprids' in conventional 24-well plate settlement assays (Qiu *et al.*, 2008) is particularly problematic for *B. improvisus*. Observations in initial assays suggested that very few cyprids (< 10%) were able to actively explore the bottom of the wells, with most remaining trapped in the meniscus. The causes of this effect, and the reasons for differences observed among species of barnacle cyprids, are unknown. However, it is likely a combination of factors, such as the nature and efficiency of the culture filtration procedure and the natural hydrophobicity of the cyprid cuticle. Pye and Mott (1948), first observed this phenomenon with cyprids of *B. crenatus*. The issue was resolved by filling assay bottles to the brim and closing the lid to exclude air. Since the problem was found only with this species and not with the larger cyprids of *B. balanoides* (= *Semibalanus balanoides*) that became the model barnacle species of the 1970s and '80s (Holm, 2012), little further research on this technical issue was conducted. As *B. amphitrite* became established as a laboratory test species, however, methods to address 'floating' were developed since this species is affected, albeit to a lesser degree. Qiu *et al.* (2008) suggested that the size and relative strength of cyprids from the different species may explain why smaller cyprids of *B. crenatus* and *B. amphitrite* may be more prone to floating than those of *S. balanoides* or *Megabalanus* spp., having a proportionally larger surface area in contact with the air-water interface and reduced strength to break free. Although plausible, this explanation does not completely explain why there are such stark differences in the frequency of floating between species with similar-sized cyprids, such as *Elminius modestus* where floating is highly problematic and *B. amphitrite* where it is relatively less common. Variation in

the behaviour of cyprids (encountering the meniscus more frequently, for example) or differences in the composition/physical nature of the cuticle may further explain the phenomenon. Similar findings were described by Petrone *et al.* (2013), comparing settlement results from a sessile drop assay, glass vials and opposed glass surfaces.

In recognition of the effect of physical entrapment at the meniscus on the results of cyprid assays, particularly those using species highly prone to floating, Qiu *et al.* (2008) designed an assay format that used filled and hermetically sealed Petri dishes; essentially a modification of the method used by Pyefinch and Mott (1948). This method was adopted in this work with *B. improvisus* and demonstrated a marked improvement in the reliability of the assay compared to more conventional approaches (Fig 17B). Settlement assays were conducted in PS Falcon™ 1006 Petri dishes, which provide a hermetic seal when closed and thus a suitable environment for swimming and surface exploration by cyprids. In so doing, floating was entirely avoided and all cyprids were actively involved in the assay. Borosilicate Petri dishes were also used for assays for comparison.

Before assaying larvae of *B. improvisus*, it was necessary to address uncertainty regarding the effects of short-term cold storage of cyprids (Rittschof *et al.*, 1984; O'Connor and Richardson, 1994; Head *et al.*, 2004). Using Falcon Petri dishes, cyprids of 0-, 1-, 2-, 3-, 4- and 5-days-old were tested to clarify this point. Fig. 19 shows that there were significant differences between the settlement recorded using cyprids 0-, 1-, 2- and 5-days-old compared to 3- and 4-days-old. Dahlström *et al.* (2000) observed that storage (no details provided by authors) of cyprids of *B. improvisus* for more than 24 h decreased settlement by more than 50%. Although this dramatic effect was not observed, younger cyprids (0-day-old) were nevertheless preferred for use in assays, which enabled comparison with previous studies. The higher settlement of 5-day-old cyprids is consistent with reduced discrimination with age (Rittschof *et al.*, 1984) and depletion of energy reserves (Tremblay *et al.*, 2007); the cyprids become more 'desperate' to settle, consistent with the 'desperate larva hypothesis' (Toonen and Pawlik, 1994).

Settlement assays carried out in these more controlled conditions, PS well plates and glass vials for *B. amphitrite* and PS Falcon and glass Petri dishes for *B. improvisus*, confirmed that settlement was higher on glass than on PS for *B. amphitrite* and vice

versa for *B. improvisus*, for which settlement on glass was negligible. However, from these data alone it was impossible to draw conclusions on the basis of differences in surface energy.

Surface energy values for the glass and PS used in experiments, estimated by the GvOC approach, were 48.0 and 47.3 mJ m⁻², respectively. Thus, the total surface energies of the two materials were estimated to be very similar, despite the clear difference in advancing water contact angle (Table 3). High-energy PS for cell culture was selected specifically to demonstrate that differences in settlement between glass and PS were due to factors other than surface energy. Had surface energy been estimated only from the water contact angles (following e.g. Kwok and Neumann, 1999), the surface energy estimate for glass would have been far higher than for PS, thus leading towards the erroneous conclusion that differences in surface energy may be responsible for promoting cyprid settlement.

There is considerable variability in the reported surface energy value for glass surfaces, not only due to the inherent variability of the material, but also because of the numerous different approaches employed to determine surface energy (see e.g. Cerneet *al.* (2008) for a discussion on the choice of probe liquids). The surface energy value for glass presented here is not considered to be unreasonable. It should also be noted that the glass γ_s value reported in Table 3 does not refer to the vials or glass Petri dishes used for the cyprid settlement assays (Session 2.3.5), but to the microscope slides used initially, due to the difficulties associated with precisely measuring contact angles inside a glass tube. It is not only glass that shows considerable variability in reported surface energy however. PS has also been reported to possess surface energy ranging from 33 mJ m⁻², as tabulated by Zisman and Fowkes (1964), up to 40 (Brady, 1999) and 42.5 mJ m⁻² (Dann, 1965). The surface energies of both glass and engineered polymers also depend very much on the history of the surfaces and the fabrication and cleaning procedures used. For instance, oxygen plasma-treatment of PS well plates for cell culture studies (as used here) and acid-washing of glass increases wettability and surface energy of the materials.

One factor that varies between these surfaces, and which may explain the difference in cyprid settlement between the two materials, is surface charge. Glass surfaces acquire a negative charge density in water due to the deprotonation of terminal silanol groups (–

SiO⁻) (Behrens and Grier, 2001). At the pH of seawater, the surface charge of PS is not neutral, as its chemical structure would suggest, rather it possesses net negative surface charge (Norde and Lyklema, 1978; Ohsawa *et al.*, 1986; Schmitt *et al.*, 1999). Importantly though, this charge is significantly weaker than that of glass and it seems likely that charge, not surface energy, was the determining factor in settlement on these surfaces. The results from glass and PS suggest that a net negative surface charge may be inductive to settlement of cyprids of *B. amphitrite*, all other things being equal. Dahlström *et al.* (2004) also conducted assays on hydrophilic (glass) and hydrophobic (PS) surfaces revealing a preference of cyprids of *B. improvisus* for settling on non-polar, hydrophobic surfaces. The present results for *B. improvisus* support this conclusion and suggest that the preferences of these two species in response to SFE and charge are actually similar.

To determine the effects of surface energy in a more robust way, in the absence of charge effects, a settlement assay was conducted in PS well plates and PS Petri dishes coated with either OH- or CH₃-terminated SAMs. Prior to SAM formation, gold-coating by evaporation in vacuum is usually performed on substrata on a rotating sample holder to ensure homogenous deposition on the flat substratum surface, and is usually restricted to microscope slides and other 'two-dimensional' surfaces. With the modified system used here, however, the interior walls of the PS plates and Petri dishes received a uniform covering of gold, thus ensuring complete SAM coverage in each well (Figure 9). In all performed tests, cyprids of *B. amphitrite* were observed to settle not only on the horizontal bottom of the wells, but also vertically on the side walls of the wells. Cyprids of *B. improvisus* instead were mainly observed on the margin between base and wall of the Petri dish. OH- and CH₃-terminated SAMs differ significantly in surface energy, with values of 47.4 mJ m⁻² and 19.6 mJ m⁻² respectively, and neither carries a charge at the pH of seawater (the pK_a of organic alcohols lies in the range between 15.5–19 (Allinger *et al.*, 1980)). Again, contrary to the predictions of previous literature and the initial experiment (Section 2.3.5), for *B. amphitrite* the settlement assay did not indicate any preference of cyprids for the surface with higher surface energy at 24 h (Figure 21). After 48 h it is noteworthy that settlement was statistically higher on the low-energy CH₃ surface than on the high-energy OH- SAM for both species. The inconsistency between these findings, results of section 2.3.5 and the historical assays with glass and PS can probably be assigned therefore to either inappropriate estimation of surface energy for

the surfaces, as explained above, or the unquantified influence of other surface factors, such as surface charge. Either way, these data would seem to refute the prevailing view that cyprids of *B. amphitrite* and *B. improvisus* 'prefer' high-energy surfaces *per se*.

To further investigate the influence of surface charge, settlement assays were carried out on a series of SAMs differing primarily in charge, with relatively constant surface energy (Session 2.3.7, Table 3). Cyprid settlement was clearly dependent upon surface charge (Figure 23 - 24), with significantly higher settlement for both species on the negatively-charged CO_2^- (TSA) SAM, intermediate settlement on the neutral $-\text{OH}$ SAM, and lowest settlement on the positively-charged ($-\text{N}(\text{CH}_3)_3^+$) monolayer. To further validate the preference of cyprids for negatively-charged surfaces, SAMs of two other acidic thiols, $-\text{CO}_2^-$ (MHA) and $-\text{CO}_2^-$ (thioglycolic acids), were subsequently tested for *B. amphitrite* and $-\text{SO}_3^-$ $-\text{PO}_3^{2-}$ for *B. improvisus*. The results of these further tests supported the findings obtained comparing CO_2^- (TSA), $-\text{OH}$ and $-\text{N}(\text{CH}_3)_3^+$ SAMs (Figures 23 - 24, Table 3). Another positively charged SAM with NH_2 -termination, was also tested and once more cyprid settlement was negligible on this positively charged surface. When all settlement results for SAM surfaces were plotted against Gibbs surface energy, calculated using the GvOC model, no trend was evident for the relation between settlement and surface energy.

The GLM and data presented in Figure 25 support the conclusion that the two species studied to date in fact share very similar preferences with regard to charge and SFE. However, the magnitude of the difference in settlement between high and low SFE neutrally charged surfaces was far higher for *B. improvisus*. This observation, in conjunction with ambiguous results from *B. amphitrite* in previous studies, is probably the source of the widely held belief that these two species have opposite responses to SFE. In summary, it seems that charge is the overwhelming physicochemical stimulus and only when the surface charge is neutral do the organisms respond directly to SFE.

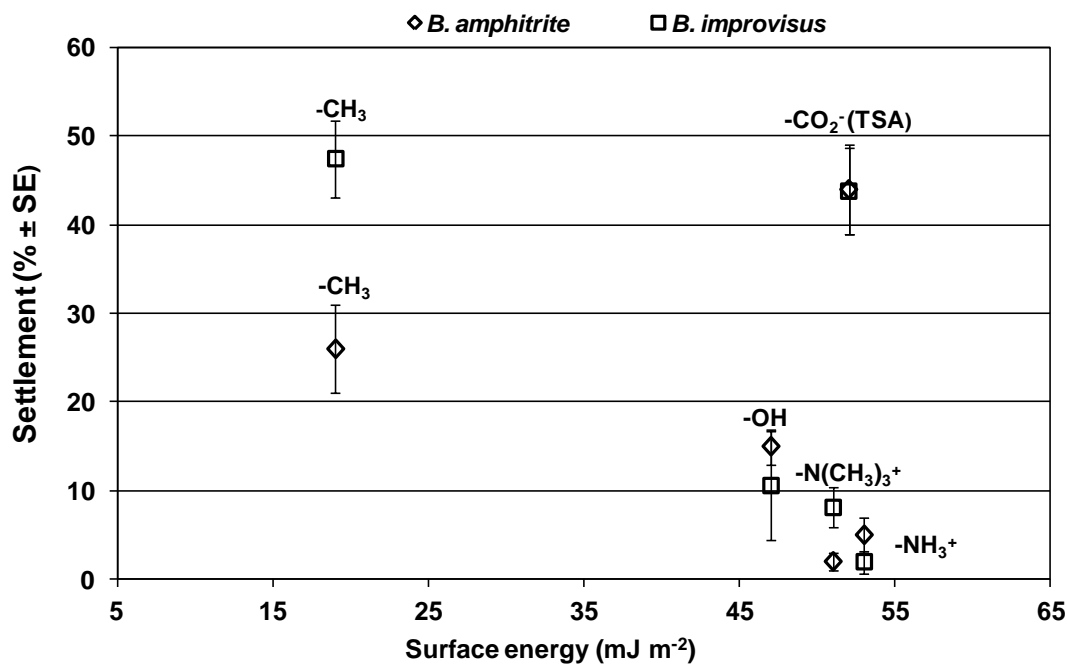


Fig. 25 Settlement percentage of cypris larvae of *B. improvisus* used in this work and *B. amphitrite* from a previous experiment (Petroni et al. 2011) where -CH₃ is an abbreviation of HS(CH₂)₁₅CH₃, -OH = HS(CH₂)₁₆OH, -NH₃⁺ = HS(CH₂)₁₆NH₂, -N(CH₃)₃⁺ = HS(CH₂)₁₁N(CH₃)₃⁺, -CO₂⁻ (TSA) = HSC₆H₄COOH.

To fully understand the ecological implications of this result, the question must be asked, how many naturally occurring surfaces carry a neutral charge? If the answer is very few, then perhaps the role of SFE in the decision-making process of cyprids at settlement has been overestimated.

The reduced settlement on positively-charged surfaces for both *B. amphitrite* and *B. improvisus* remains unexplained, but may be a consequence of reduced tenacity during temporary adhesion/surface exploration (Aldred et al., 2011). The effect is demonstrated clearly however by settlement onto the N(CH₃)₃⁺- and CO₂⁻ (TSA) terminated SAMs, which have similar surface free energy of 45 and 48 mJ m⁻² respectively (see Table 3), but opposite charges. The pKa of the CO₂⁻ (TSA) terminated thiols range between 4-5. Therefore, all SAMs were negatively charged in seawater. Furthermore, the pKa of the NH₃⁺-terminated SAM is about 9.5 and it is thus positively charged in seawater. It is however difficult to determine the effective pKa once the thiol molecules chemisorb on the gold surface. Thiols in solution possess a different pKa than molecules self-assembled on a surface. The pKa value can be higher in SAMs due to the proximity of like charges. The seawater pH ~8 is however sufficiently high to deprotonate carboxylic

acids from a SAM surface. Settlement on these surfaces was significantly different with over four times as many cyprids settling on the latter.

The data presented here run contrary to most previous findings, including those of Roberts *et al.* (1991) who used silanised glass surfaces to demonstrate higher settlement of cyprids of *B. amphitrite* on surfaces with higher surface energy, as well as those of Phanget *et al.* (2009b), who concluded that cyprids of the same species settled in higher number on aminosilane functionalised glass (NH₂)- than on alkyl (CH₃)- terminated glass. It should be considered, however, that in addition to the complexities of surface energy calculation and the presence of confounding chemical functionalities there are other problems associated with using silane chemistry on surfaces that are difficult to avoid. A significant number of silanol groups may be left ungrafted during a silanisation reaction; Vansant *et al.* (1995) reported that only 30 to 50% of silanol groups were actually grafted and, additionally, although NH₂ groups are positively charged at the pH of seawater (~8.2), at pH values above 7.0, aminosilane functionalised glass surfaces may exhibit a net negative charge, due to the presence of free silanol groups (SiO⁻) from the underlying glass surface or hydrolysed alkoxy groups of the silane molecules (Carre' *et al.*, 2003). On the other hand, one of the main advantages of using SAMs resides in the fact that this procedure ensures good coverage of the substratum surface. Additionally, IRAS spectra in the CH stretching region are indicative of the SAM structure. The bands arising from CH₂ asymmetric and symmetric stretching modes are found at ~2917 and 2850 cm⁻¹, respectively, which are indicative of well ordered, crystalline-like assemblies of the alkyl chains (see section 2.3.1) (Nuzzo *et al.*, 1987, 1989). In conjunction with the ellipsometric thicknesses (Table 3), this further demonstrates that the gold surface is completely covered by the SAM. As demonstrated in previous theoretical and experimental work (Marinova *et al.*, 1996; Dicke and Hähner, 2002; Chan *et al.*, 2003; Kreuzer *et al.*, 2003), SAMs and hydrophobic surfaces without dissociable sites will acquire a negative charge in water at pH >4 due to the ubiquitous phenomenon of preferential adsorption of hydroxyl ions (OH⁻). The top water layer of hydrophobic substrata is oriented, generating a dipole moment and thus a potential drop which induces the OH⁻ adsorption (Netz, 2004). Surface charge is screened beyond the double layer and at high ionic strength, such as in seawater, the potential drop occurs over a very short distance (only a few Å; the Debye screening length). Measurements of surface charge in seawater are particularly challenging, due to its high ionic strength

(~0.7 M). The Debye length at such an ionic concentration is below 1 nm. Nonetheless, cyprids showed that they were able to discern between positive and negative surface charges by intimate contact of their antennular pads. Zeta potential measurements, as well as AFM force measurements with a charged probe, can be used to accurately measure surface charge of materials, and are undoubtedly useful tools for future experiments. The effect of the measured surface charge on cyprids' settlement behavior is an interesting experiments to be pursued in future research. However, surface charge is likely to play a critical role in the cyprid attachment process since cyprids explore and sense the substrate by making physical contact via the antennular discs (Aldred and Clare, 2009; Clare and Aldred, 2009; Maruzzo *et al.*, 2011).

Hence, the preference of cyprids for negatively-charged surfaces may have arisen from a natural adaptation, due to the fact that most surfaces are negatively-charged in natural aquatic environments (Schmitt *et al.*, 1999; Behrens and Grier, 2001; Stewart *et al.*, 2011). Additionally, pristine metal oxide surfaces become hydroxylated in water as a consequence of the dissociative coordination of water molecules (Lewis bases) to surface metal ions (Lewis acids), thus acquiring a negative charge at the pH of seawater (Stewart *et al.*, 2011). Another aspect that must be considered is surface contamination and conditioning, which is caused by adsorbed ions, biopolymers and microbial biofilms. Nowhere is this process more acute than in natural aquatic environments. Thus, high-energy solid/liquid interfaces are conditioned rapidly by organic layers lowering the interfacial energy (Wahl, 1989), which may go some way towards explaining the preferential settlement of cyprids also on low-energy surfaces.

To summarise, the present data suggest that total surface energy does not directly influence cyprid settlement in the manner predicted by previous studies and the substrata used for previous studies such as PS and silanized glass differ in too many respects to be appropriate for drawing such conclusions. Furthermore, the method of estimating surface energy may significantly affect the conclusions of any such study and should be considered carefully. Surface charge would seem to be a more important parameter for controlling settlement of cyprids in the design of barnacle-resistant marine coatings. It is worth bearing in mind when considering the low surface energy theory of minimally adhesive surfaces that most successful commercial products tend to also be soft and lubricious and, indeed, several contemporary products are amphiphilic in nature rather than super-low energy. It is also important to note that, as previously explained,

quantitative measurements of SAM surface charge are both difficult and uncertain in seawater due to the Debye length being in the order of a few Å. Thus, the use of ‘surface charge’ in this article should be considered as ‘nominal surface charge’, and the accurate quantification of surface charge at high ionic strength, such as in seawater, is the focus of on-going research.

Chapter 3. Footprint characterisation

3.1 Introduction

Underwater adhesion of fouling organisms has been considered for more than a century as one of the most challenging processes to understand. Interest is driven especially by the need to deter unwanted organisms from colonising ship's hulls and other man-made structures. On the other hand, there is a desire to emulate and synthetically reproduce such adhesives, due to the ineffectiveness of most synthetic glues in wet conditions (Brubaker and Messersmith, 2012; Brubaker *et al.*, 2010; Matos-Pérez *et al.*, 2012).

Marine sessile organisms are never certain of the substrate they will encounter for settlement. Those that do not have stringent, specific requirements for settlement sites tend to be able to colonise a broad range of substrata. They have evolved complex adhesives to cope with substrata of different nature, in a wide range of environmental conditions, such as temperature, salinity, pH and solar radiation. Generally the values of pH and ionic strength in sea water are 8.2 and 0.7, respectively (Yebra *et al.*, 2004; Kunz, 2010), but such values can change in different regions of the ocean and with the vertical distance from the water surface, as well as in brackish waters.

In antifouling research, there is a need to consider the adhesive composition and the mechanisms of adhesion during the early life stages of fouling organisms, rather than focussing on engineering new coatings targeting adult stages (Petrone, 2013; Lu *et al.*, 2013; Wang and Stewart, 2012). An aspect of particular interest is how the bioadhesives displace surface-bound water molecules at a solid/liquid interface. This initial step constitutes a major obstacle in adhesion, and a comprehensive explanation on the adhesion strategy of fouling organisms might reveal critical clues for developing novel underwater adhesives for human purposes (for instance as a sealant in surgery) (Lee *et al.*, 2011).

Barnacle cyprids use two different antennular secretions to select the most suitable place to settle on (Schmidt *et al.*, 2009; Kamino *et al.*, 2012). Different adhesives are employed in well-defined settlement phases by cyprids, and a series of glands are involved in the production of the adhesive components. Prior to permanent attachment, cyprids probe different substrata 'walking' in a bipedal fashion. In so doing, they

secrete a temporary adhesive (footprint) (Clare *et al.*, 1994) that, in combination with others sensory structures, provides information regarding the features of the substrata. The combined effect of temporary adhesive and sensory appendages helps the cyprid discriminate and, eventually, select the most appropriate surface for settlement. This initial secretion or 'first kiss' adhesive allows the cyprids to remain anchored to the surface during exploration, so that they are not washed away by shear forces (Clare and Matsumura, 2000). It has been empirically calculated that the strength of adhesion of cyprids of *Semibalanus balanoides* on the order of 0.068 - 0.076 MNm⁻² on clean glass (Crisp *et al.*, 1985; Walker and Yule, 1984b; Yule and Walker, 1985).

The major mechanical and chemical sensory structures involved in exploratory behaviour are concentrated in the terminal section of the 3rd and 4th antennules (Nott and Foster, 1969; Blomsterberg *et al.*, 2004), as previously described in section 1.2.1. Barnes (1970) described the fourth segment as filled with neurone dendrites, thus proving the high potential sensorial level of this organ. This segment combines with the 3rd segment, which bears the attachment disc, and with the axial sensory organ, located in the centre of the attachment disc (see Fig. 6) to provide chemical and physical information of potential settlement sites.

The temporary adhesive is secreted via pores on the attachment disc and by a process which is poorly understood, makes contact with the substratum. At this stage, the substratum and attachment disc are separated by a layer of adhesive. As cyprids explore surfaces they may leave behind, depending on the nature of the surface, deposits of adhesive, which are referred to as footprints (references).

Cyprid footprints have been considered as a voluntary secretion (Aldred *et al.*, 2013b), and are essentially used by cyprids to make contact with substrata. These temporary secretions cover the antennular disc area and, upon detachment, part of this material may remain on the substratum (Crisp, 1984). The adhesive secretion allows a temporary anchoring point and, during this phase, that may last few seconds or minutes, cyprids probe the substratum. The information from the adhesive contact and mechano-chemical receptors is then processed. Other receptors, such as those located on the shield (lattice organs), do not contribute to this exploratory phase in which an appropriate surface to settle on is selected (Bielecki *et al.*, 2009).

It has been demonstrated that one of the most important components of footprints of cyprids is the settlement-inducing protein complex (SIPC) (Matsumura *et al.*, 1998). The SIPC is a large glycoprotein with a pheromonal role, which induces cyprid settlement and is also contained in the footprint secretion (Clare, 2011), as previously described in section 1.2.2. Further roles of footprints are still unclear, and its adhesive role in temporary attachment of cyprids onto surfaces has been considered for a long time as the principle mechanism of adhesion for cyprids (see 1.2.2) perhaps in addition to dry adhesion by the cuticular villi. Structurally this material, once deposited onto a surface, has sticky and visco-elastic properties which resist detachment, maintaining the adhesion between the two surfaces even in a fluid medium (Aldred and Clare, 2009).

Nott and Foster (1969) first suggested the existence of a secretion involved in surface exploration by *Semibalanus balanoides*. Working on the same species, Walker and Yule (1984b) pointed to the role of settlement preference for cyprids. Yule and Walker (1985) supported the hypothesis that the secretion is a modified integumentary protein (Knight-Jones, 1953; Crisp and Meadows, 1962; 1963; Larman *et al.*, 1982) and also suggested that it acts as a powerful stimulus to conspecific cyprid settlement. As described in the section 1.2.2, this pheromonal function has since been confirmed. Cyprids are induced to explore and settle on surfaces that have previously been explored by conspecific cyprids and in so doing deposit more footprints. There is strong evidence that the footprints are proteinaceous (references). The cypris larvae of barnacles recognise proteins on surfaces as also observed for larvae of other organisms, such as oysters (Crisp, 1967; Bayne, 1969; Ritz, 1974), *Spirorbis* spp. (Williams, 1964; Gee, 1965), *Sabellaria* (Wilson, 1968, 1970a; b), *Protodrilus* (Gray, 1966; 1967a; b) and *Clava* (Williams, 1965).

3.1.1 Adsorption

In the process of underwater adsorption, atoms, ions or molecules (adsorbate) bind via a variety of physicochemical interactions onto a solid surface (adsorbent) (McQuillan, 2002), depending upon the nature of adsorbate and adsorbent. Adhesion, instead, is a phenomenon contextualised in a macroscopic view, and follows from the adsorption process at an atomic and molecular level (Petroni, 2013). The interactions between two materials brought into close contact depend also upon the presence of a medium, which

would be water in case of an aqueous environment. Since water contains various dissolved ions, inorganic and organic, it is not possible to explain the interfacial equilibrium only in terms of the electric double layer, but other more specific adsorption interactions are often involved (Stewart *et al.*, 2011). In order to adsorb and subsequently adhere underwater, adhesive proteins from fouling organisms need to initially displace surface-bound water molecules (Hanein *et al.*, 1993) and ions. Ligand exchange reactions, such as those occurring at a liquid/solid interface, are governed by a decrease in total free energy, which can be described as follows:

$$\Delta G_{\text{ex}} = RT \ln K_{\text{ex}} = \Delta H_{\text{ex}} - T\Delta S_{\text{ex}} \quad (4)$$

where ΔH_{ex} and ΔS_{ex} are, respectively, the enthalpy and entropy associated with the exchange process, and K_{ex} is the equilibrium constant of the exchange reaction.

Adsorption is therefore determined by the net change in the system free energy, which depends on the chemical nature of both adsorbate and surface-binding site, and also on the water hydration shell surrounding them (Stewart *et al.*, 2011). Upon adsorption, rearrangements of the water hydration layer(s) occur both around the adsorbate and substrate surface, with the interfacial energetics of adsorption dictated by the interplay of direct solute-surface and solvation forces. In this context the specific nature of dissolved ions becomes predominant, particularly with respect to their size, with small ions interacting more strongly with water (dipolar) molecules as compared to ions of larger diameters (bearing the same charge). A strong water affinity thus generates a more oriented hydration shell surrounding smaller ions (hydration entropy > 0).

In the case of proteins comprising the adhesives secreted by marine organisms, adsorption in wet conditions is regulated by net and local charges, hydrophobic and hydrophilic domains, as well as functional groups present in the amino acid side chains. Mussels and sandcastle worms have evolved amino acid residues with post-translational modification, such as hydroxylated tyrosine and phosphorylated serine; on the contrary, thus far no post-translational modification has been found in barnacle cement (Kamino *et al.*, 2000; Kamino, 2010). Many proteins upon adsorption undergoes conformation change, fibrinogen, for example, is used to study and compare the sticky properties of

others proteins because its tendency to adsorb to a wide range of substratum, the adsorbed amount, orientation, and conformational change (Berglin *et al.*, 2009).

3.1.2 Approach to the study

While significant progress has been made towards characterising adult barnacle cement (Kamino, 2013) knowledge of cyprid adhesives and barnacle adhesion in general is poor. Difficulties generally encountered in protein extraction and isolation from marine biofouling organisms are exemplified by the fact that about 10000 adult mussels are needed to extract 1 g of mixed adhesive protein (Strausberg and Link, 1990). In addition, bioadhesives are usually highly insoluble, which makes their extraction and purification even more challenging, thus meeting the limits of techniques currently used.

Recently, *in situ* analyses of adhesives secreted by marine organisms have been carried out using non-invasive spectroscopic techniques (Barlow and Wahl, 2012; Petrone, 2013). In particular, the use of electromagnetic radiation has become an important tool to analyse compounds at a liquid/solid interface, which is obviously not possible with techniques that require a vacuum or low-pressure gas phase (Zaera, 2012). Environmental scanning electronic microscopy (ESEM) has some more advantages compared with conventional SEM, including the fact that ESEM does not require coating procedures (with water vapour being the imaging gas in the chamber) (Callow *et al.*, 2005). ESEM is, however, still destructive for some biological structures.

X-ray photoelectron spectroscopy (XPS) is considered to be one of the most sensitive techniques to investigate the elemental composition of surfaces. The technique has a sampling depth that depends on the ray's angle of incidence on the surface (Berglin *et al.*, 2005). XPS has been used to understand the strength of the interactions between the *Mytilus edulis* foot protein (Mefp-1) onto different surfaces (Baty *et al.*, 1997), showing its feasibility in analyses of dehydrated biological samples in high-vacuum conditions.

Mefp-1 adhesion has also been investigated using the quartz-crystal microbalance with dissipation (QCM-D), which provides information on the total adsorbed mass and the mechanical properties of the resulting thin film by detecting changes in frequency and

dissipation of a vibrating crystal upon adsorption/adhesion of molecules on its surfaces (Rodahlet *et al.*, 1995). However, an important issue is water uptake from the samples during adsorption, which is included in the calculated total adsorbed mass, thus overestimating the amount of protein adsorbed (Höök *et al.*, 2001).

Investigations via non-destructive surface-sensitive techniques have been carried out only recently, for instance by Andersson *et al.* (2009) and Aldred *et al.* (2011), who have observed and quantified temporary adhesives of *S. balanoides* cyprids through a combination of conventional and imaging surface plasmon resonance (iSPR). Furthermore, attenuated total reflection infrared (ATR-IR) spectroscopy has been used to investigate the adhesion of *Perna canaliculus* mussel larvae showing its glycoproteinaceous nature with sulphated and carboxylated moieties (Petrone *et al.*, 2008). The vertical resolution of i-SPR is in the sub-nm range, but its lateral resolution is conventionally ~10 µm. Imaging ellipsometry has an improved lateral resolution compared to iSPR, of ~1-2 µm with a vertical resolution is in the sub-nm range. Both techniques are surface-sensitive and label-free. However, the depth sensitivity of i-SPR is ~200 nm, and will thus not be sufficient to image the thick footprints from cyprids. Additionally, confocal Raman microscopy has been used by Schmidt *et al.*, (2009) to image the cyprid cement, demonstrating its chemical composition and hydration state.

Raman scattering spectroscopy is widely used to study biomaterials or living tissues in water due to its relative insensitivity to absorption by water molecules at visible wavelengths (Barlow *et al.*, 2012). Moreover, this technique has been fundamental to identify high cysteine content in barnacle adhesive proteins (Naldrett, 1993; Naldrett and Kaplan, 1997; Kamino, 2001; Kamino *et al.*, 2000). Likewise, Raman spectroscopy was used by Wiegemann *et al.* (2006) to investigate S-S bonding in *B. crenatus* cyprid baseplate adhesive.

During the last decade, the instrument that probably gained most attention for its versatility in larvae adhesive investigations is atomic force microscopy (AFM). This instrument has been used for the characterization of both temporary and permanent adhesives of barnacle cyprids. Phan *et al.* (2006) calculated force-distance curves for the cement of *B. amphitrite*, and subsequently characterised the temporary adhesive of *S. balanoides* measuring differences in adhesion force on a series of functionalised surfaces (Phan *et al.*, 2008).

An improved understanding of properties and dynamic behaviour of macromolecules deposited onto a solid surface can be gained by using wavelength ellipsometry; a type of approach with high opto-electronic precision achievable even with macromolecular adsorption, such as footprints of cyprids. Ellipsometry (see Fig. 26) is a technique that is sensitive to intensity and phase changes of the probing polarized light (Azzam and Bashara, 1977), which makes it a powerful optical tool for studies of adsorbed organic layers with a resolution of 0.01 nm (Debe, 1987).

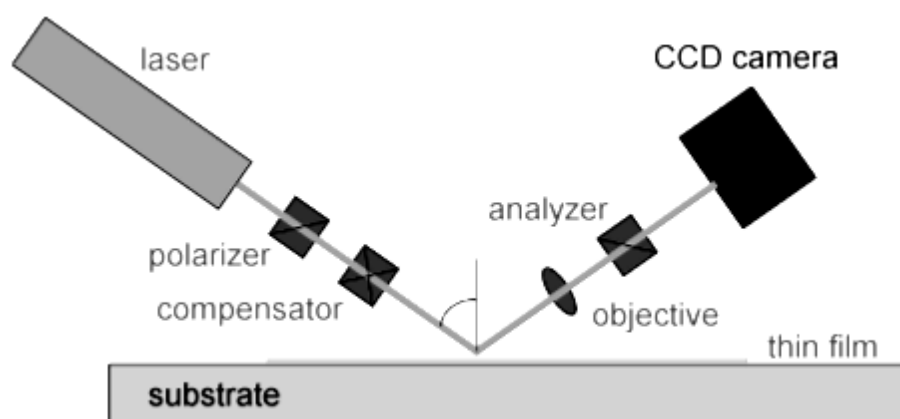


Fig. 26 Schematic of imaging ellipsometry with a sensitive CCD camera (from Nanofilm EP3 ellipsometry Nanofilm Technologie GmbH, Göttingen, Germany).

The data analysis is based on the changes in the elliptical polarization (phase) and intensity of an incident laser light upon reflection from a thin film (deposited/adsorbed onto a reflective substrate) (Jin *et al.*, 1996) (Fig. 27). The detected changes depend on the thickness and the morphology of the thin layer. A CCD camera detects and collects variations in polarization and intensity of the reflected light quantitatively pixel by pixel. Following mathematical modelling, thickness and morphology of the adsorbed thin organic layers can be obtained and visualized as 3-D maps.

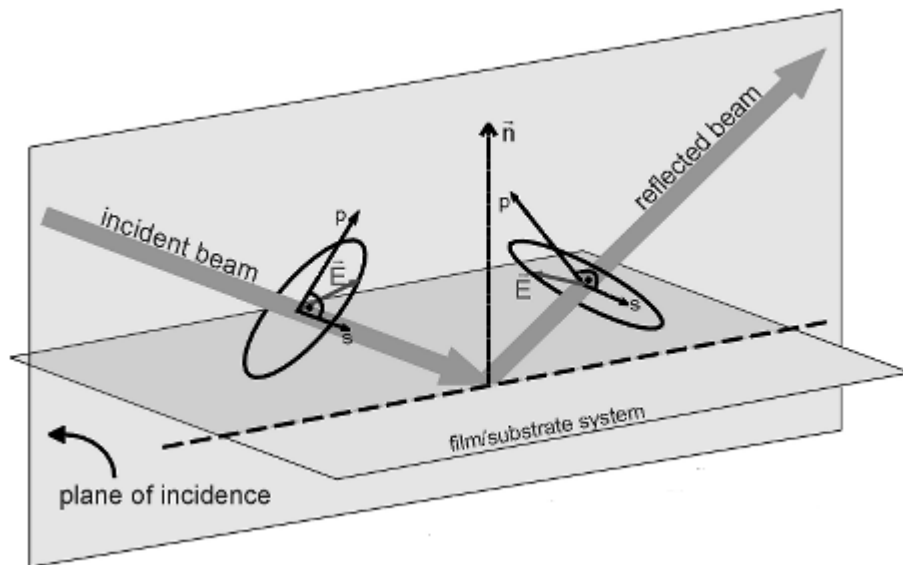


Fig. 27 Reflection of incident laser light from the sample (thin film on a reflecting substrate). Changes of the incident elliptical polarization are caused by intrinsic properties of the probed coating. (from Nanofilm EP3 ellipsometry Nanofilm Technologie GmbH, Göttingen, Germany).

As mentioned previously, the reactions on a surface depend on the nature of the surface itself. In many biological interfaces, reactions are mediated by proteins/enzymes (Arwin, 1998), which can have a dynamic interaction with the surface and can respond actively to different substrata or environmental conditions. An example of the use of ellipsometry in biological fields is given by Ducret *et al.* (2012), in which the extracellular matrix (ECM) of *Myxococcus xanthus* was imaged in 3D topographic reconstructions and its dynamic interactions observed between cells and surface. Additionally, Höök *et al.* (2001) for the first time used ellipsometry in combination with QCM-D and SPR, showing the adsorption kinetics of the mussel adhesive protein *Mytilus edulis* foot protein (Mefp-1).

In this chapter, both AFM and imaging ellipsometry have been used for footprint characterisation of *B. amphitrite* and *B. improvisus* cyprids. Morphological observations have been conducted on a variety of surfaces in order to investigate the effect of surface chemical cues on the footprint mode of adsorption. Also nano-mechanical properties of footprints were examined by AFM with functionalised tips.

3.2 Materials and methods

3.2.1 Culture of cyprids

Cyprids were obtained from the brood stock at Newcastle University following the same procedure explained in sections 2.2.1 for *B. amphitrite* and 2.2.2 for *B. improvisus*. After collection, cyprids were kept at 4°C in 0.22 µm filtered ASW and transferred to Linköping University, Sweden, and ETH-Zurich University, Switzerland, for footprint characterisations. Cyprids were allowed to explore surfaces for 4 hours, after which they were rinsed with MilliQ water in order to remove salt, which can interfere with the subsequent analyses.

3.2.2 Footprints observation

The deposition of adhesive footprints by two species of cyprids, namely *B. amphitrite* and *B. improvisus*, was investigated in this work. Prior to experiments on functionalised surfaces, the timescale of the cyprid's exploratory phase as well as the number of footprints secreted by both species were estimated in polystyrene Petri dishes (5 cm in diameter). Fifteen cyprids were introduced into the dishes and allowed to explore the surface for 1, 2 and 3 hr in artificial seawater (salinity of 33 for *B. amphitrite* and 22 for *B. improvisus*). Subsequently, cyprids were removed and the surfaces were rinsed with MilliQ water. Coomassie Brilliant Blue-G-Colloidal Blue-silver, prepared using 25% MeOH, 7% glacial acetic acid and 68% H₂O for 5 min, was then added on the surfaces to stain the footprints and destained for five hours, or until footprints were visible. Once background staining had reduced sufficiently, the substrata were again rinsed with MilliQ water and allowed to dry to increase contrast. Being essentially proteinaceous, cyprid's footprints bind to the neutral ionic species of Coomassie Brilliant Blue, thus making them visible. Footprints were observed at 20x magnification using an Olympus BH-1 compound light microscope.

3.2.3 Self assembled monolayer preparation

Footprints were investigated on 1 cm x 1 cm gold-coated silicon (100) wafers (Topsil Semiconductor Material A/S, Denmark), following the protocol described in section

2.2.4. Gold-coated silicon wafers were immersed in thiol solutions as described in section 2.2.5. Thiols used for imaging ellipsometry investigations were: HS(CH₂)₁₅CH₃ (1-hexadecanethiol); HS(CH₂)₁₆OH (16-hydroxy-1-hexadecanethiol); HSC₆H₄COOH (thiosalicylic acid, TSA) (Sigma-Aldrich, Sweden); and HS(CH₂)₁₁N(CH₃)₃⁺Cl⁻ (N,N,N-trimethyl-(11-mercaptoundecyl)ammonium chloride). Atomic force microscopy investigation was carried out on HS(CH₂)₁₅CH₃ (1-hexadecanethiol).

Table 4 reports contact angle and surface energy values for the SAMs used in this chapter.

SAM surface	Contact angle (°)			Surface energy (mJ/m ²)		
	θ _W	θ _{DIM}	θ _G	γ _{LW}	γ _{AB}	γ _S
CH ₃	107	77	83	19.1	0.5	19.6
OH	39	38	18	40.6	6.8	47.4
COOH	45	40	41	39.6	1.9	41.5
N(CH ₃) ₃ ⁺	60	28	50	45	5.9	50.9

Table 4. Values of contact angles and surface energy for each SAM.

3.2.4 Imaging ellipsometry

The imaging ellipsometer used in this section was an auto-nulling imaging ellipsometer EP3 –Nanofilm. The polarisation change is quantified by the amplitude ratio, Ψ , and the phase difference, Δ with a resolution of 0.001°. The light source consisted of an internal solid-state laser with a maximum laser power of 50 mW and a wavelength of 532 nm. The imaging system was equipped with a highly sensitive 1380 pixels x 1024 pixels CCD camera. The instrument calculates Δ or Ψ (ellipsometric parameters) and generates 2-D maps for the variations of such parameters in the investigated sample location. Optical modelling software (EP4 Model 1.0.0) allows fitting the measured data with the chosen model in order to obtain a thickness map of the investigated thin films. The electronic control unit controls all movements and signal processings in the opto-mechanical unit as well as the video streaming. It connects the opto-mechanical unit with the PC and builds the link between the measuring instrument and the control and evaluation software.

The thickness of cyprid footprints was evaluated using profile lines tracked on a number of footprints ($n = 30$), as depicted in the profile diagram in Fig. 31. Each footprint was

assessed by six profile sections (red line crossing the footprint, fig. 31) and the average was calculated to determine the thickness mean per each substratum and each species. The area of footprints was calculated using the map elaborated by the windows map displayed in fig. 32 using ImageJ.

The volume of proteinaceous material secreted during the surface exploration was calculated using the values obtained from the previous measurements, namely thickness and profile sections.

All footprint maps for the investigated surfaces are reported in Appendix 1.

3.2.5 Atomic force microscope

Atomic force microscopy (AFM) (MFP3D, Asylum Research, Santa Barbara, USA) was employed to calculate the strength of adhesion of cyprid temporary adhesive on a CH₃-terminated SAM using functionalised tips.

Functionalisation was performed on silicon nitride (DNP-SVeeco) tips by metal deposition (Baltec MED 020) in a high vacuum metal evaporation coater. AFM tips were primed with a 10 Å-thick layer of chrome as an adhesion promoter and then coated with a 100 Å-thick gold layer. Au-coated tips were immersed in 100 μM thiol solutions immediately after removal from the metal evaporation chamber and incubated for 24 hr in the dark. The following thiols were used to functionalise the AFM tips in this work: HS(CH₂)₁₅CH₃ (1-hexadecanethiol); HS(CH₂)₁₆OH (16-hydroxy-1-hexadecanethiol), HSC₆H₄COOH (thiosalicylic acid, TSA) (Sigma-Aldrich, Sweden); and HS(CH₂)₁₁N(CH₃)₃⁺Cl⁻ (N,N,N-trimethyl-(11-mercaptoundecyl)ammonium chloride). Functionalised AFM tips were rinsed with 99.5% ethanol prior to the measurements. The values of spring constant of cantilever were in the range of 500 – 700 pN/m and calibrated using the thermal noise method.

Imaging contact mode using feedback on deflection was used to scan the surface in order to locate footprints and, upon detection, footprints were imaged and force measurements were recorded. Each force measurement was recorded in different location of the footprint, this because is important to avoid unfolded zones (with stretched protein chains), from the previous measurement, which could give different values. Data are presented as means ± standard deviation of force curves obtained by pull-

off of different functionalised tips. Force curves were plotted together in histograms and shown in Gaussian distribution.

3.2.6 Scanning electronic microscope

Cyprids were prepared for scanning electron microscopy investigation by fixation in glutaraldehyde prepared at 4%. Following fixation, extraction of water from the sample is operated using a graded series of ethanol. The concentrations of ethanol used were at 25% and proceeded at 25% steps up to 75% followed by 10% changes to 100% ethanol. Subsequently, acetone has been used to replace the ethanol before to reach the critical point drier supplying liquid carbon dioxide under pressure. The samples were then coated with gold by metal evaporation.

3.2.7 Data analysis

Data of footprints obtained with imaging ellipsometry are reported as mean \pm standard error (SE). The effect of surface chemistry on cyprid footprints was examined by one-way analysis of variance (ANOVA) when the assumptions for parametric analysis were fulfilled. In addition, Tukey pairwise comparisons using Minitab 15 and an α level of 0.05 were used.

3.3 Results and Discussion

3.3.1 Cyprid antennular, morphological observations

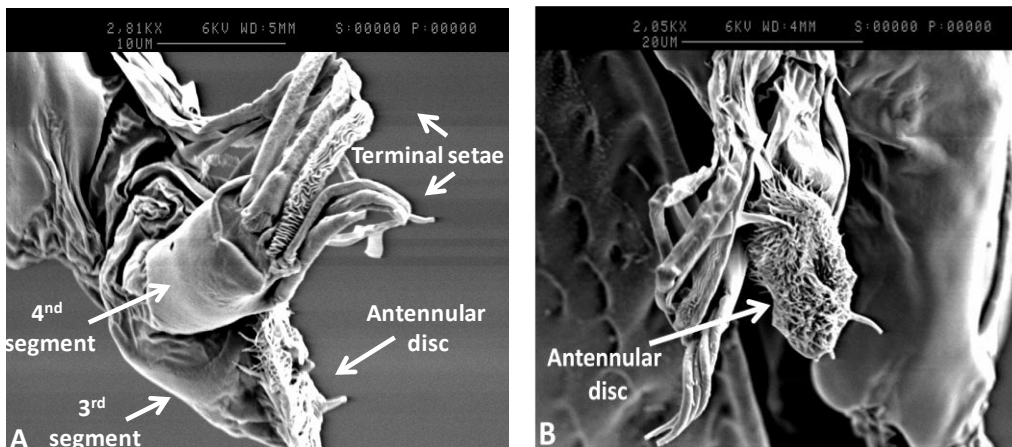


Fig. 28 Lateral (A) and bottom (B) views of SEM micrographs of an antennule of a cyprid of *B. improvisus* showing the attachment disc.

The antennular discs, present on 3rd segment (Fig. 28- 29), of *B. amphitrite* and *B. improvisus* measure about 25 and 20 μm in length respectively, and are characterised by a high density of sub-micron terminations, termed cuticular villi (Nott, 1969). Aldred *et al.*, (2013) calculated 10.2 villi μm^{-2} on a total area of 477 μm^2 for *B. amphitrite*. These structures are probably involved in adhesion to the surface, as already described by Phanget *al.* (2008) for cyprids of *S. balanoides* and Aldred *et al.* (2013) for *B. amphitrite*.

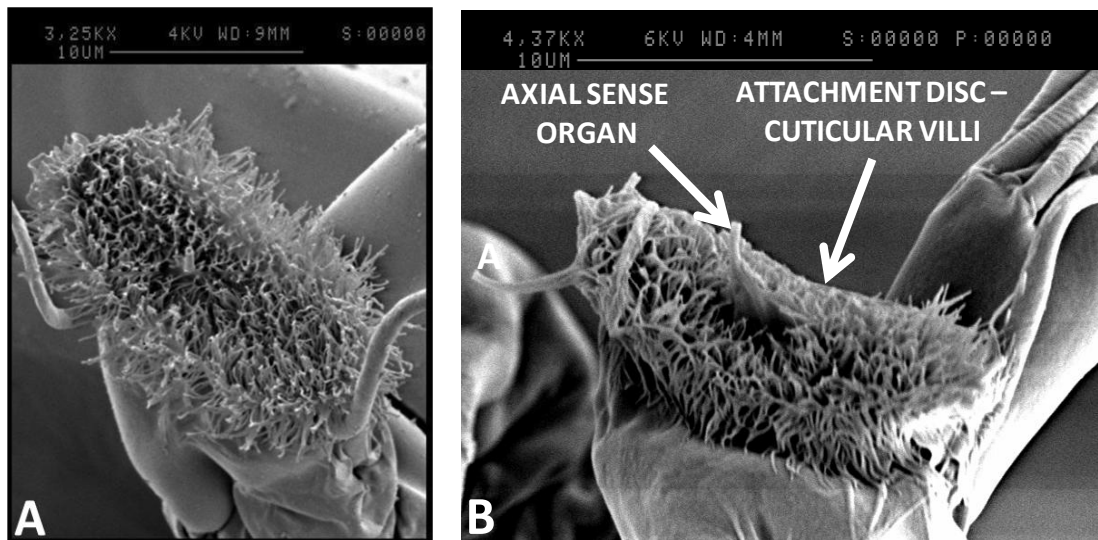


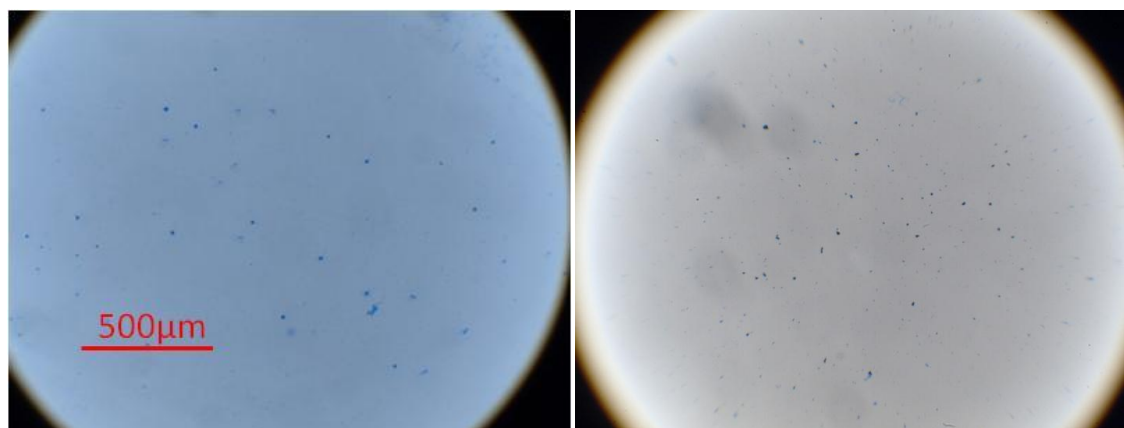
Fig. 29 SEM micrographs of cypris antennules of (A) *B. amphitrite* (Aldred and Clare, 2008) and (B) *B. improvisus* (this work).

Additionally, it has been proposed that the high cuticular villi density in cyprids (Fig. 29) is correlated to the tenacity reduction caused by water (Bielecky *et al.*, 2009) and the need to compensate for the high forces present in an aqueous system, if compared with terrestrial environment (Aldred and Clare, 2009).

The nature of underwater surfaces can modify the spreading of the temporary adhesive, and, as a result, the morphology of the deposited proteinaceous material can vary, as already demonstrated with cyprids of different species (Phanget *al.*, 2008; 2009b). Differences in adhesive spreading may provide a signal output to the cyprids during surface exploration, and it may further influence the type and number of ‘touch-downs’ of the antennules with the surface. The correlation between touchdowns and temporary adhesive secretion was investigated by Aldred *et al.* (2011) using iSPR, and no difference in the number of contacts of the antennules was observed for different surfaces; however, significant variations were found for the actual footprint deposition, revealing an effect of surface chemistry on deposited adhesive materials.

3.3.2 Microscopic observation of cyprid footprints

Cyprids of both species were allowed to explore the surfaces of PS Petri dishes for 1 hour. Subsequently the number of footprints was counted. Number was comparable for both species (80 – 90 footprints) and was deemed sufficiently high for the subsequent experiments of functionalised surfaces (Fig. 30).



A **B**
Fig. 30 Optical images of footprints stained by CBB-G for (A) *B.improvisus* and (B) *B.amphitrite* cyprids.

Microscopic observations of cyprids during the exploratory phase showed similar behaviours for both species, with greater exploration mostly centred in the middle of the Petri dish. No fast movements were observed and cyprids were seen to mainly walk in a ‘bipedal’ fashion (Phanget *al.*, 2010), in direct contact with the surface (Aldredet *al.*, 2010).

Due to the low resolution of this optical method (limited by the diffraction of light), it was not possible to compare the size and morphology of footprints between species. Nonetheless, it was helpful to quantify the number of footprints deposited onto a PS surface by both species and to assess the timescale of the footprint deposition. This information was relevant to simplify the operations with the other analytical instruments with higher resolution capabilities but slower detection, such as imaging ellipsometry and AFM.

3.3.3 Imaging ellipsometry

Imaging ellipsometry, as previously explained, has been used primarily because it requires the investigated thin film to be deposited on reflective substrata (i.e. Au or Si).

SAMs were used to investigate the effect of surface physico-chemical parameters on cyprid footprint deposition and characteristics. SAMs were applied on gold-coated surfaces, making ellipsometry suitable for footprint examination.

Cyprids were allowed to explore the surface for one hour, as the time scale required for footprint deposition was determined using the staining method (see previous paragraph), and subsequently imaging ellipsometry has been employed for the morphological characterisation of the temporary adhesive material. Cyprids were allowed to explore surfaces with CH_3 , OH , CO_2^- (TSA) and $\text{N}(\text{CH}_3)_3^+$ -terminal SAMs for 3 hours, thus exposing cyprids to a range of surface wettability, charge and free energy.

Footprints were detected by imaging ellipsometry on all SAMs, although the number, morphology and size varied among the different surfaces. Trails of cyprid footprints were imaged along the paths that cyprids followed during the exploratory behaviour on surfaces (see Fig. 31). The distance between consecutive footprints ($120\ \mu\text{m}$) was shorter than the usual length of a cypris step ($\sim 250\ \mu\text{m}$). This distance appears consistent with the “close search” described by Lagersson and Høeg (2002) for cypris exploration (inspection).

Yule and Walker (1987) estimated an exploring velocity of ~ 2 cypris body-lengths per second, with a tenacity of $< 0.3\ \text{MPa}$. During the inspection phase of the exploration, only $\sim 50\%$ of the adhesive disc is in full contact with the surface (Aldred *et al.*, 2013). In this initial phase, the adhesive is not fully released and, thus, spread on the surface. The subsequent close searching phase results usually in a complete contact between antennular disc and surface. Cyprids then probe the surface with both antennules (Crisp 1974), and this exploratory behaviour can explain the close proximity of consecutive pairs of footprints in the trail shown in Figure 31.

The time dedicated by cyprids to the exploratory phase is significantly influenced by the nature of the surface. Maleschlijski *et al.* (2012) investigated the exploratory phase of cyprids of *S. balanoides* with a three-dimensional tracking system, and observed differences in swimming behaviour in particular on a PEG-containing SAM. Cyprids swimming at high velocities ($10\text{--}25\ \text{mm/s}$) were in no or low contact with the surface, while low swimming velocities ($< 5\ \text{mm/s}$) were associated with a close contact with the surface.

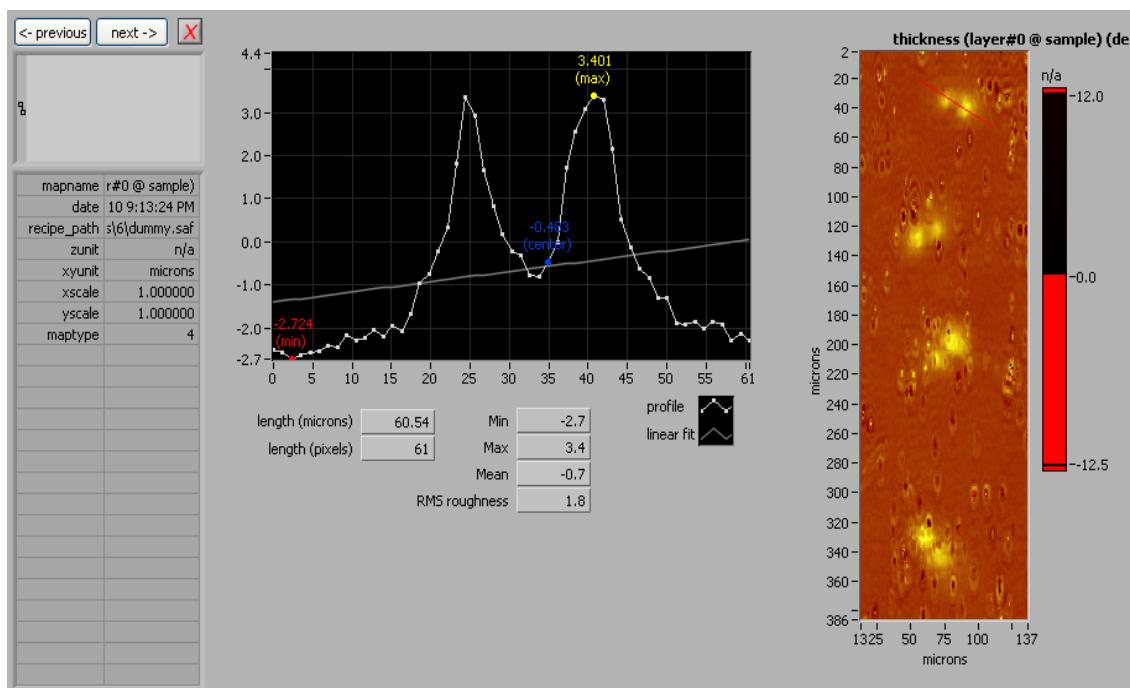


Fig. 31 Footprint trail (left) of *B. improvisus* cyprid and cross-section profile of a single footprint visualized by imaging ellipsometry on a CH₃-terminated SAM surface.

Here, footprints of two barnacle species (*B. amphitrite* and *B. improvisus*) were studied by imaging ellipsometry in order to compare shape, volume of adhesive material, thickness and coverage area on SAMs. Terminal groups of SAMs used for this study were selected from the surfaces used in cyprid settlement assays described in Chapter 2.

A map of a cyprid's footprint on CH₃-terminated SAM obtained by ellipsometry is shown in Fig. 32. The map window shows a heat map for the distribution of the footprint, and a cross section (profile diagram) showing the thickness profile obtained by drawing a line (red line in the map window) across a footprint. The *x* and *y* axes in the figure are in microns, thus the imaged footprint measures 30 μm in diameter with a maximum thickness of 2.5 nm.

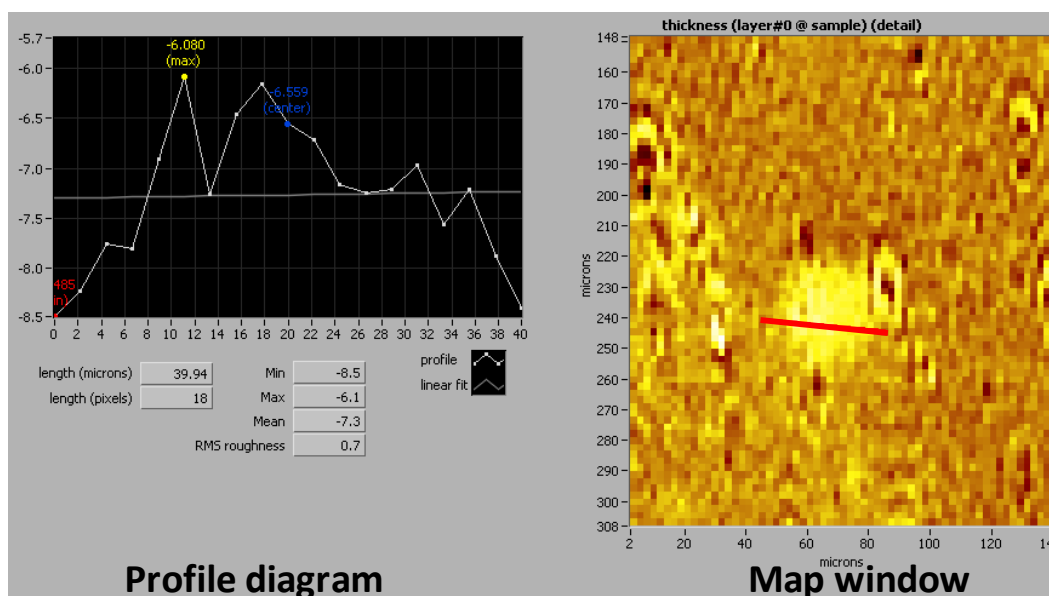


Fig. 32 Footprint of cyprid of *B. amphitrite* on a CH₃-terminated SAM, with cross section (profile diagram) and overall 2-D distribution on the surface (map window) with the red bar indicating the cross section.

From the images, it is clear that footprints are not homogeneous as a result of the uneven detachment of the viscoelastic antennular disc from the surface as well as the mechanism of the detachment (Andersson *et al.*, 2009; Aldred *et al.*, 2013). Appendix I contains the profile diagrams and map windows of footprints of both species deposited onto the four SAM surfaces used for this investigation.

In order to better visualise the topography of footprints, a 3-D map was calculated (see Fig. 33) via modelling of the ellipsometric parameters.

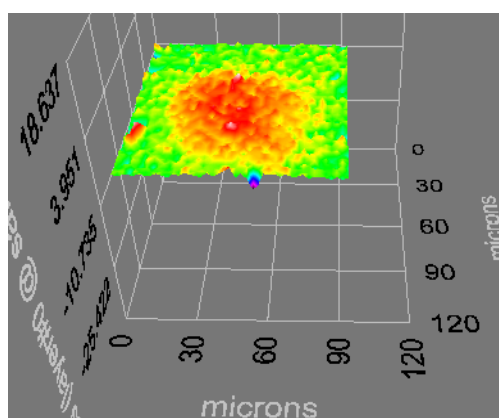


Fig. 33 3-D elaboration of cyprid footprint (*B. amphitrite*) on CH₃-terminated SAM.

Thickness, area and volume of footprints were calculated for CH₃, OH, CO₂⁻(TSA) and N(CH₃)₃⁺-terminated SAMs in order to gain information regarding the influence

of surface physicochemical properties on the adhesive spreading. Each of these footprint calculations are reported in the following sections.

3.3.3.1 Thickness

Cypris footprint thickness values were plotted against the nominal surface charge and surface free energy, as shown in Figure 34. Footprint thickness for *B. amphitrite* measured 1.8 ± 0.1 nm on CH₃-SAM, 4.7 ± 0.3 nm on N(CH₃)₃⁺-SAM, 3.7 ± 0.4 nm on CO₂⁻(MHA)-SAM and 1.8 ± 0.1 nm on OH-SAM. There were significant differences between coatings ($p < 0.05$, $F = 45.99$) at 95 % confidence (ANOVA, Tukey test).

For *B. improvisus* footprints measured, respectively 1.0 ± 0.04 nm on CH₃-SAM, 2.6 ± 0.4 nm on N(CH₃)₃⁺-SAM, 3 ± 0.3 nm on CO₂⁻(MHA)-SAM and 1.5 ± 0.1 nm on OH-SAM. There were significant differences between coatings ($p < 0.05$, $F = 31.53$) at 95 % confidence (ANOVA, Tukey test).

Data differed significantly with respect to the two species ($p < 0.05$, $F = 42.40$) at 95 % confidence (ANOVA, Tukey test).

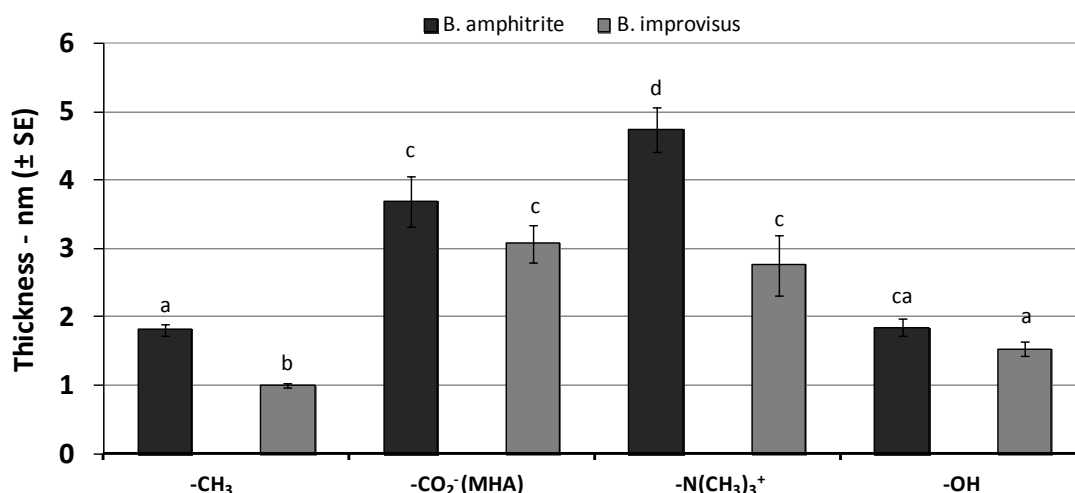


Fig. 34 Thickness (\pm standard error) of footprints from *B. amphitrite* and *B. improvisus* deposited onto different SAMs obtained by imaging ellipsometry. Results of Tukey pairwise comparisons are presented. Means that do not share a letter are significantly different.

High values of thickness were found on positively charged surfaces, on which the lowest percentage of cyprid settlement was also observed for both species (see section 2.3.7). These results suggest that the positively charged surfaces have low affinity for cyprid adhesive (lowest spreading) as compared to other surfaces (Petrone, 2013). In fact, Figure 35 shows 3-D footprint maps of both species deposited on $N(CH_3)_3^+$ -terminated SAM presenting regions with high peaks as well as regions of bare substratum (lack of adhesive material). It can be inferred that some proteinaceous material remained attached to the antennular disc during its detachment from the surface.

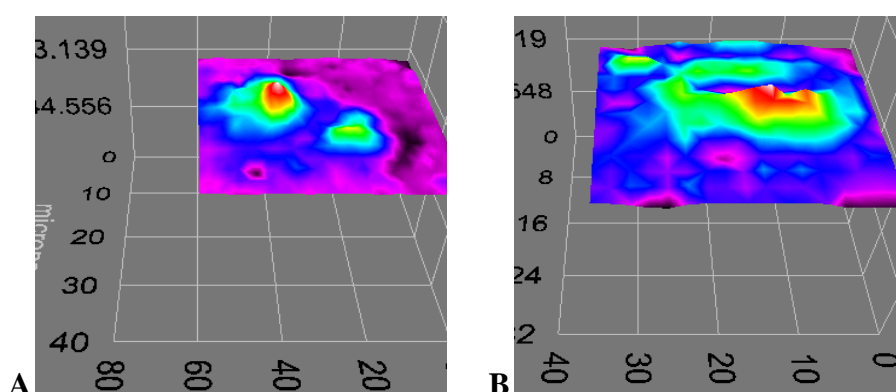


Fig. 35 3-D maps of cypris footprints of *B. amphitrite* (A) and *B. improvisus* (B) on $N(CH_3)_3^+$ -terminated SAM.

In addition, on the CH_3 -terminated SAM the thickness values were the lowest indicating higher affinity, and thus spreading of the footprint adhesive components on a hydrophobic surface (see Fig. 37).

3.3.3.2 Area

The area was calculated using ImageJ software. Footprints for *B. amphitrite* covered an area of $1637 \pm 295 \mu m^2$ on the CH_3 -terminated hydrophobic surface, $701 \pm 102 \mu m^2$ on CO_2^- (MHA)-SAM, $477 \pm 47 \mu m^2$ on $N(CH_3)_3^+$ -SAM and $484 \pm 79 \mu m^2$ on OH-SAM. Data on different surfaces differed significantly ($p < 0.05$, $F = 9.78$) at 95 % confidence (ANOVA, Tukey test).

For *B. improvisus* the area coverage was $1259 \pm 201 \mu m^2$ on the CH_3 -SAM, $361 \pm 32 \mu m^2$ on CO_2^- (MHA)-SAM, $367 \pm 55 \mu m^2$ on $N(CH_3)_3^+$ -SAM and $273 \pm 28 \mu m^2$ on OH-SAM. Results were significantly different ($p < 0.05$, $F = 10.66$) at 95 % confidence (ANOVA, Tukey test).

The bar plot of the area covered by footprints of the two species is shown in Figure 36. Data differed significantly with respect to the two species ($p < 0.05$, $F = 9.06$) at 95 % confidence (ANOVA, Tukey test).

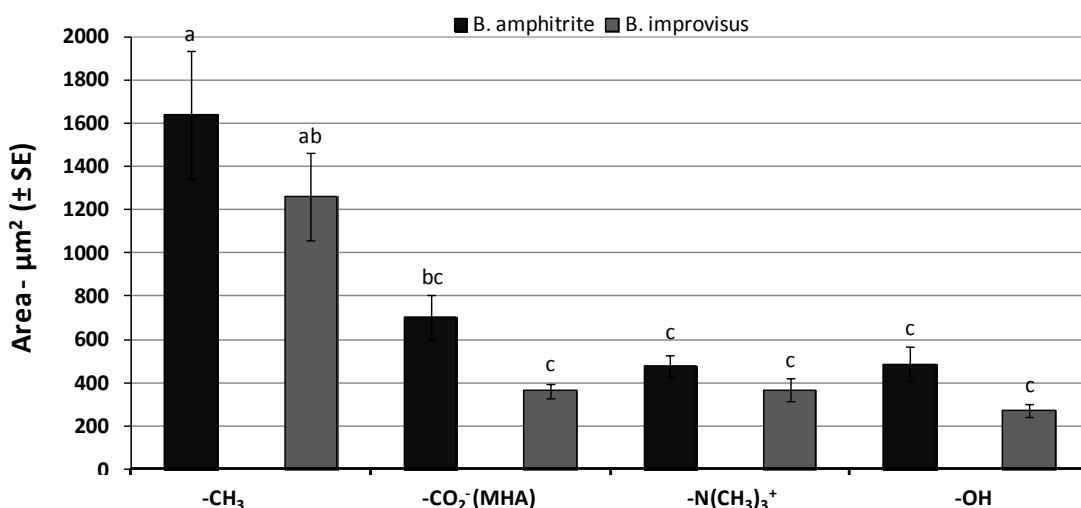


Fig. 36 Bar plot of footprints area (\pm standard error) of *B. amphitrite* (black) and *B. improvisus* (grey) deposited onto a series of SAMs. Data were obtained by imaging ellipsometry. Results of Tukey pairwise comparisons are presented. Means that do not share a letter are significantly different.

Spreading of footprint material was clearly higher on the CH₃ (hydrophobic) surface for both species, which corresponded to the low thickness values for this surface. This result demonstrates that on this hydrophobic surface the footprint material spreads more homogeneously (see Fig. 36 - 37), therefore showing higher affinity than on other SAMs used in this work.

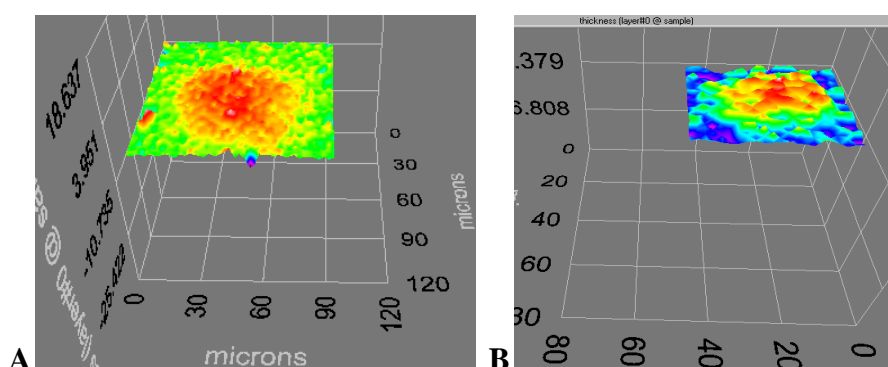


Fig. 37 Cypris footprints of *B. amphitrite* (A) and *B. improvisus* (B) on CH₃-terminated SAM.

Hydrophilic OH-SAM (see Fig. 38), negatively charged CO_2^- (MHA)-SAM (see Fig.39) and positively charged $\text{N}(\text{CH}_3)_3^+$ -SAM surfaces showed smaller surface coverage and irregular distribution.

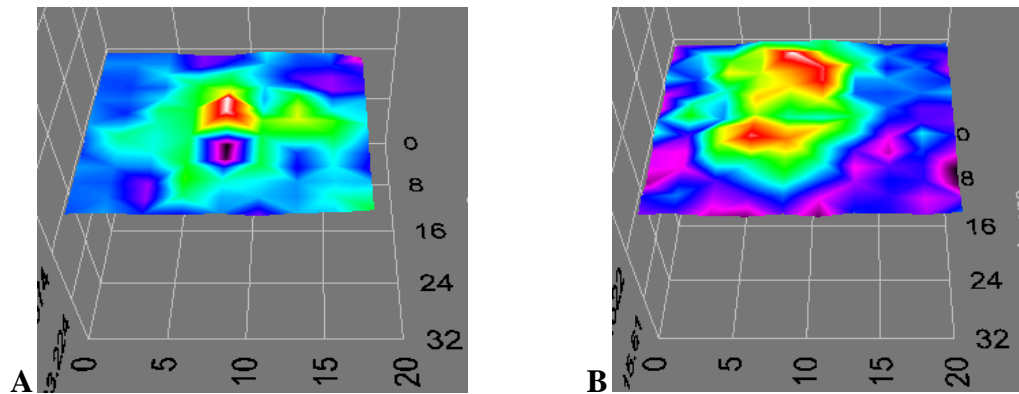


Fig. 38 Cyprid footprints of *B. amphitrite* (A) and *B. improvvisus* (B) detected on OH-terminated SAM. Note that in B the footprint has two distinct height profiles.

These data revealed that the only surface with high affinity for the footprint adhesive material is the hydrophobic one, on which highest spreading was observed.

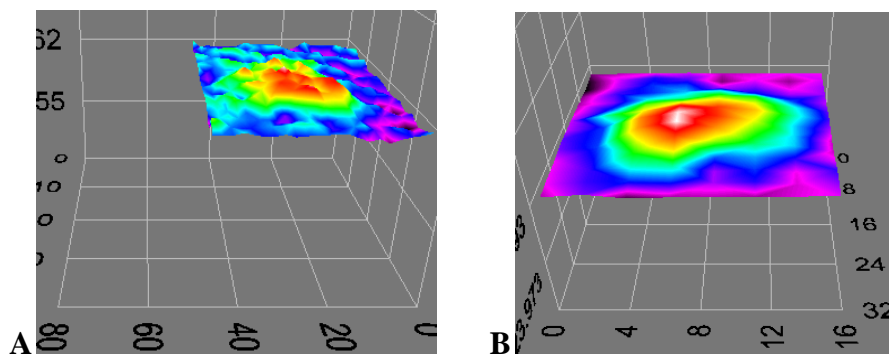


Fig. 39 Cypris footprints of *B. amphitrite* (A) and *B. improvvisus* (B) detected on CO_2^- (MHA) -terminated SAM.

3.3.3.3 Volume

This analysis revealed differences in footprint volume between the two species (see Fig. 40). Cyprids of *B. amphitrite* secreted a larger volume of footprint material than *B. improvvisus* on all SAMs, that is $3.3 \pm 0.7 \mu\text{m}^3$ vs. $1.2 \pm 0.2 \mu\text{m}^3$ on CH_3 -SAM, $2.7 \pm 0.5 \mu\text{m}^3$ vs. $1 \pm 0.1 \mu\text{m}^3$ on CO_2^- (MHA)-SAM, $2.3 \pm 0.3 \mu\text{m}^3$ vs. $1.6 \pm 0.8 \mu\text{m}^3$ on $\text{N}(\text{CH}_3)_3^+$ -SAM, and $0.8 \pm 0.1 \mu\text{m}^3$ vs. $0.4 \pm 0.1 \mu\text{m}^3$ on OH-SAM.

Data for *B. amphitrite* were significantly different ($p < 0.05$, $F = 5.55$) at 95 % confidence (ANOVA, Tukey test), while data for *B. improvisus* were slightly homogenous ($p = 0.043$, $F = 2.95$). Significant differences were observed when the two species were compared ($p < 0.05$, $F = 7$) at 95 % confidence (ANOVA, Tukey test).

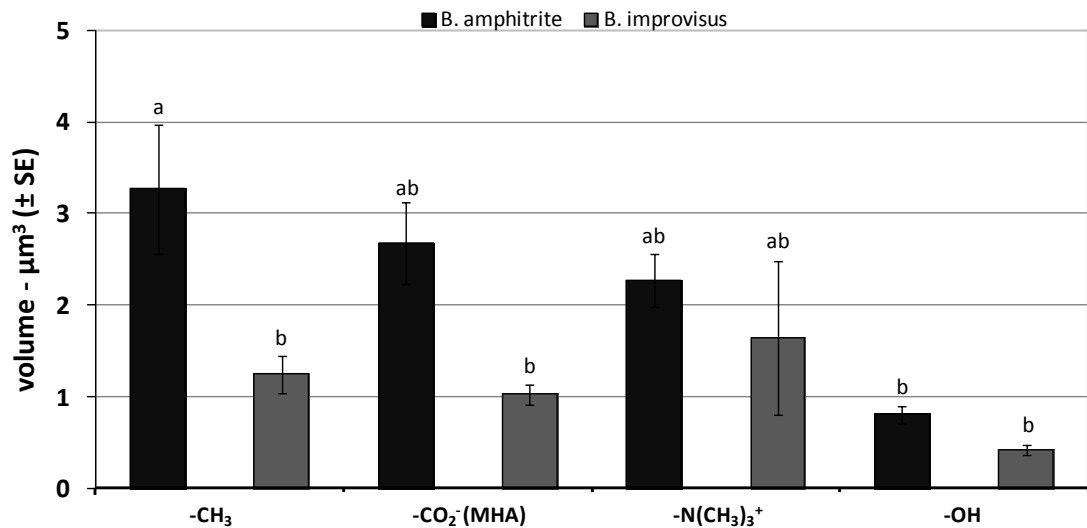


Fig. 40 Bar plot of the volume (\pm standard error) of footprints deposited onto different SAMs obtained by imaging ellipsometry elaboration. Results of Tukey pairwise comparisons are presented. Means that do not share a letter are significantly different.

3.3.4 Atomic force microscopy

Atomic force microscopy, as described in the section 3.1, is a powerful technique to reveal properties at the nano- and micro-scale. Characterization of footprint proteinaceous materials via staining methods may give rise to artefacts modifying the chemical structure of the proteins. The localisation of the footprint without staining procedures can be very time-consuming, as the only way to locate footprints is by scanning the entire surface with the AFM tip until a signal is detected.

Allowing the cyprids to explore small sample areas with a low quantity of seawater may be thought of as a strategy to reduce time for the location of footprints with an AFM. However, at room temperature the water evaporation of such small volumes causes a correspondingly large increase in the concentration of salts, which may be deleterious for the cyprids, for the structure of footprints. Moreover, salt crystal formation on surfaces interferes with the AFM investigation by covering the footprints with

extraneous material. These issues highlight the difficulties encountered in the location of cyprid footprints during AFM analyses.

The SAM surface chosen for this investigation was CH₃-terminated, because the ellipsometric investigation revealed that footprints covered the largest area on this surface among all SAMs, thus rendering the calculation of the adhesion strength more satisfactory with different functionalised AFM tips.

As described by Giannotti and Vansco (2007), the proteinaceous material behaviour can be measured via different kinetics aspects, such as single-chain viscoelasticity and plasticity (energy dissipation), whose effects in ideal conditions are reversible and measurable quantitatively by force-extension curves. This quantification is useful to determine the energy dissipation associated with bond rupturing in proteins, revealing important information regarding the protein-surface interaction (Lee *et al.*, 1994; Hinterdorfer *et al.*, 1996; Janshoff *et al.*, 1996; Carrion-Vazquez *et al.*, 2000).

The spreading of the footprint plays an important role in surface/footprint interactions. As described in the previous sections, the nature of the surface has a great influence on the spreading and the thickness of the secreted footprint (see Fig. 34-36). A homogenous footprint distribution on a surface allows its adhesion strength to be probed at different parts of the footprint with an AFM tip. In so doing, each analysis can be then assumed to be effectively a replicate measurement on the same footprint. The AFM analysis can alter protein structure, so a homogeneously spread footprint allows for replication of analysis in several points that are still naturally folded.

The AFM image in Fig. 41 of a footprint of *B. amphitrite* deposited onto a CH₃-terminated SAM presents a homogenous surface, as previously described with imaging ellipsometry (see Fig. 33). The footprint topography has a degree of roughness, which gives it an uneven appearance. Phan *et al.* (2008) also described the fibrillar appearance of footprints of *S. balanoides*.

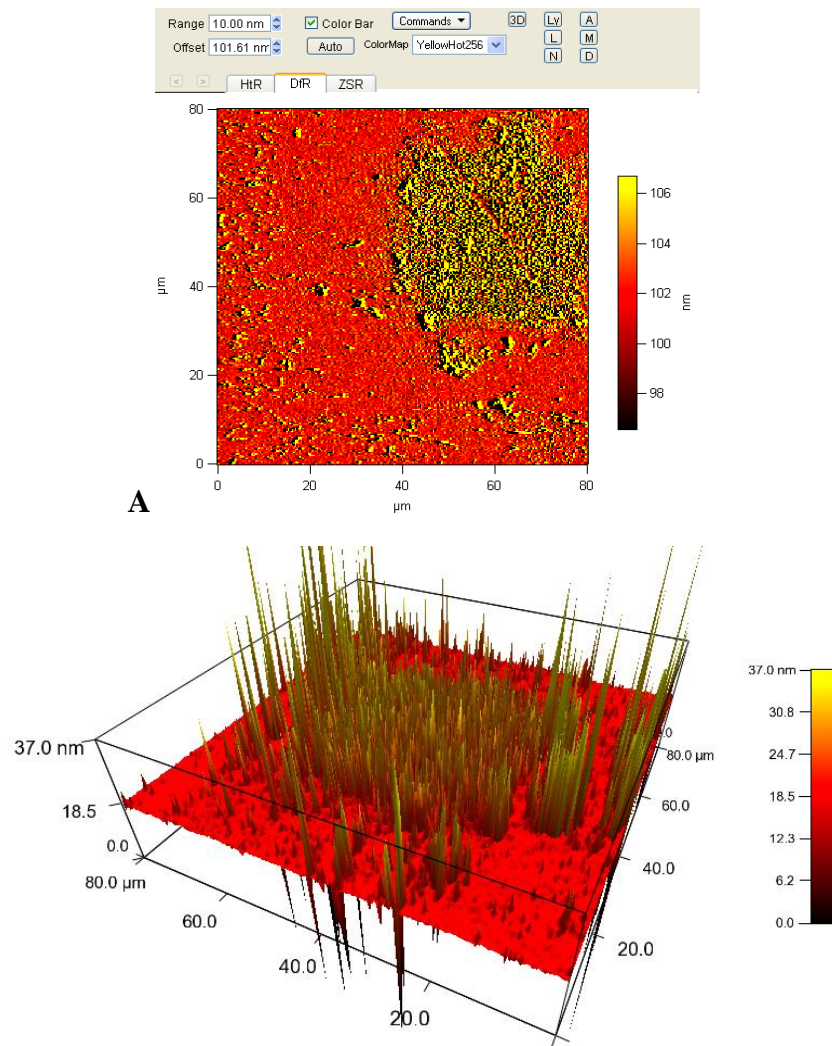


Fig. 41 Footprint of (A) *B. amphitrite* imaged by AFM on CH₃-terminated SAM surface and (B) its 3-D representation.

Force measurements have been carried out in order to calculate the adhesion strength of the footprints using different functionalised tips. The microscope tip was allowed to make contact with the proteinaceous material, which was then withdrawn until the tip detached from the footprint. Measurements were performed with functionalised AFM tips and force-extension curves were recorded, which are reported as means with the corresponding standard deviations. Each curve recorded is the result of the ruptures occurred to the sacrificial bonds of proteins up to the tip is completely detached from the footprint. Ruptures are presumably involved in the maintaining of tertiary structures of these proteins (Phanget *et al.*, 2009a) and are indicative of unfolding behaviour as observed by Li *et al.* (2002). Such behaviour has been observed by Brown *et al.* (2007) on fibrinogen oligomers finding sawtooth patterns similar to the unfolding behaviour found by Phanget *et al.* (2009a). In their study, Brown *et al.* (2007), found a peak force of 94 pN.

During the stretching operated by the tip the tension into the protein structure drops to a minimum generating, subsequently, the “pull off” event (Phanget *al.*, 2006), at this point, when the last link is ruptured, the contact between footprint and tip is lost. Figure 42 shows pull-off events recorded in the withdrawal cycle for measurements of footprint adhesion strength performed with a CH₃-SAM functionalised tip. The highest values of adhesion strength, 37.5 ± 0.9 nN for *B. amphitrite* and 71.9 ± 4.5 nN for *B. improvisus*, were recorded using this functionalised tip (which has the highest value of hydrophobicity).

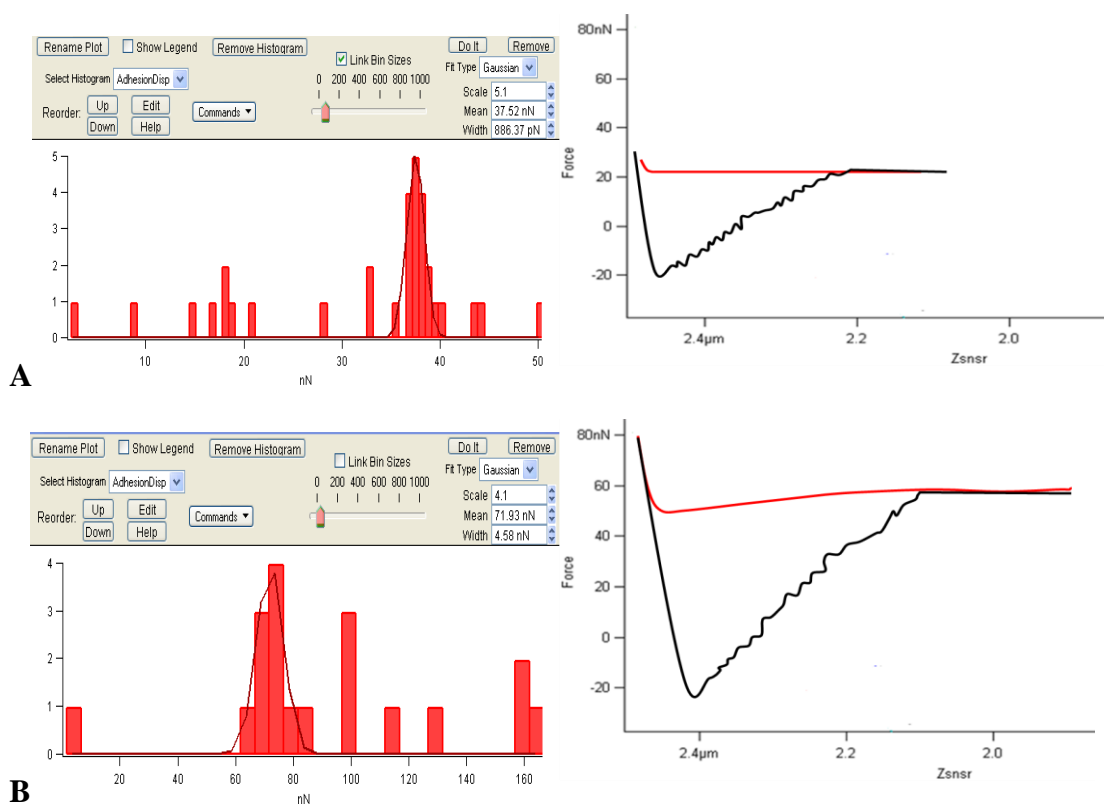


Fig. 42 Graphics show pull-off AFM force measurements using a CH₃-SAM tip on cypris footprints of *B. amphitrite* (A) and *B. improvisus* (B) with relative force curves, the red represent the approach and the black is the retraction curve. The means and standard deviations were calculated by fitting the histogram to a Gaussian distribution.

Force measurement carried out using tips with CO₂⁻(TSA)-terminated tip (Fig. 43) was 10.5 ± 0.1 nN for *B. amphitrite* and 6.2 ± 1.0 nN for *B. improvisus*. This values are lower compared with the values obtained using the CH₃-SAM tip, this may be explained by the stronger interaction existing with the hydrophobic material as already observed by Phang *et al.* (2009b).

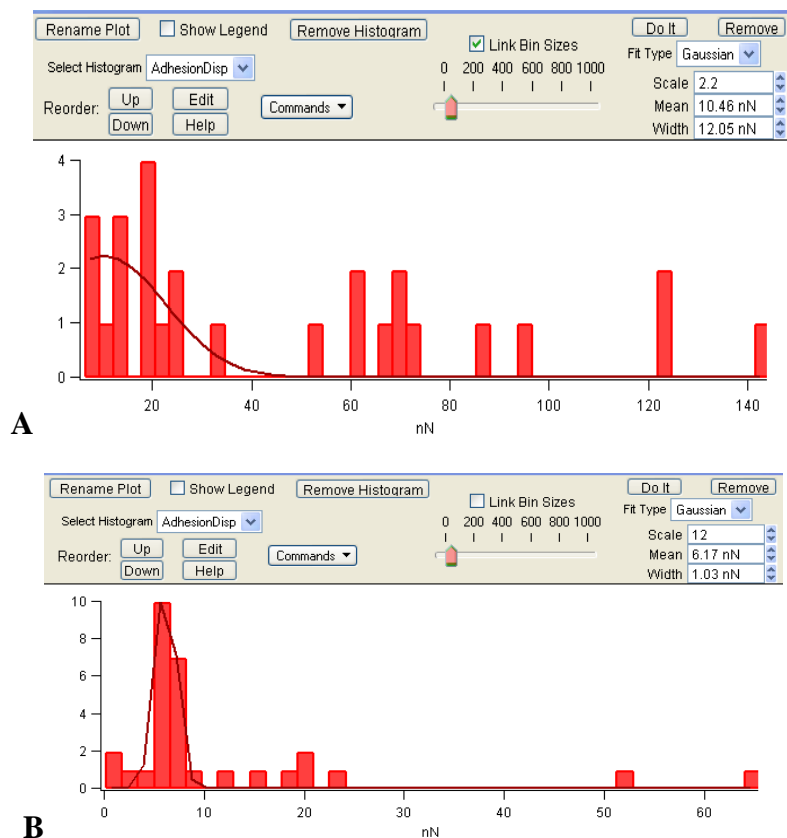


Fig. 43 Graphics show pull-off AFM force measurements using CO_2^- (TSA)-terminated SAM tip on cypris footprints of *B. amphitrite* (A) and *B. improvisus* (B). The means and standard deviations were calculated by fitting the histogram to a Gaussian distribution.

Lower adhesion resulted with tips coated with $\text{N}(\text{CH}_3)_3^+$ -SAM (Fig. 44), with an average of 6.2 ± 0.3 and 23.8 ± 0.2 nN for *B. amphitrite* and *B. improvisus*, respectively. The force required to detach the tip from the footprint was again lower if compared with the CH_3 -SAM tip. The lower force employed during the withdrawer may be explained by the lower number of sacrificial bonds ruptured during the stretching, highlighting the inferior interaction with the $\text{N}(\text{CH}_3)_3^+$ -SAM tip.

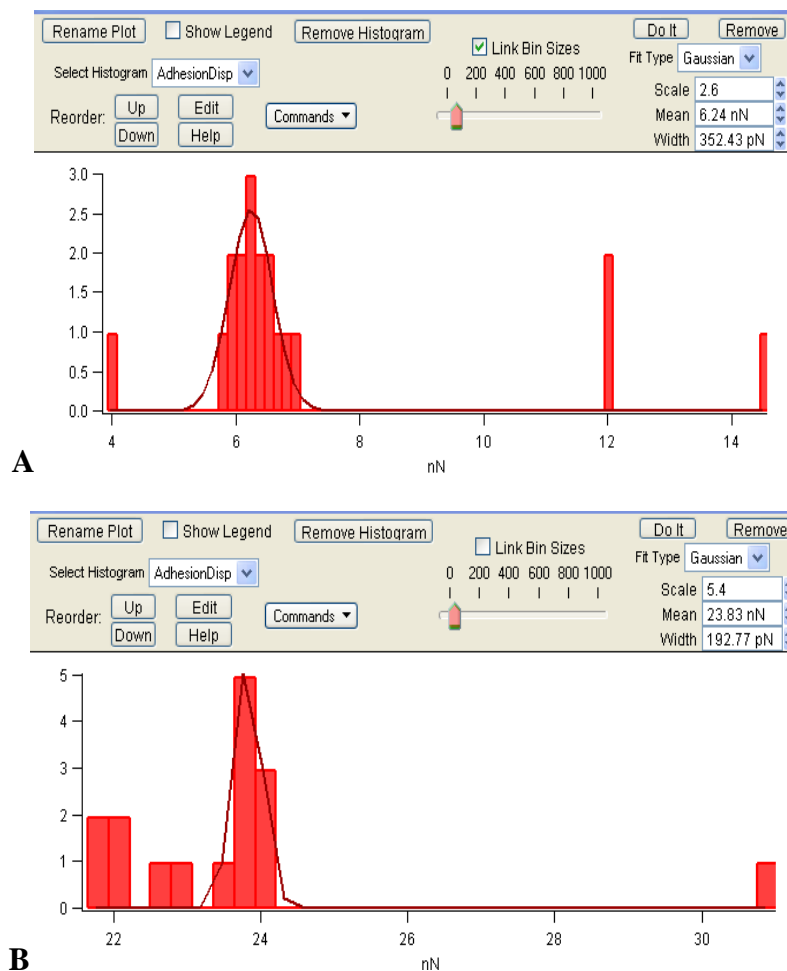


Fig. 44 Graphics show pull-off AFM force measurements using $N(\text{CH}_3)_3^+$ -SAM tips on cypris footprints of *B. amphitrite* (A) and *B. improvisus* (B). The means and standard deviations were calculated by fitting the histogram to a Gaussian distribution.

On the hydrophilic OH-SAMtip (Fig. 45), the adhesion was the lowest for *B. amphitrite* 2.3 ± 0.6 , while for *B. improvisus* was 47.1 ± 0.2 nN. Phanget *al.* (2009a) observed that the force required to detach the tip from the footprints not directly correlated with the length of extension of footprint but was probably the force to rupture inter-molecular sacrificial bonds emphasising the role of number of sites of footprints in contact with the tip.

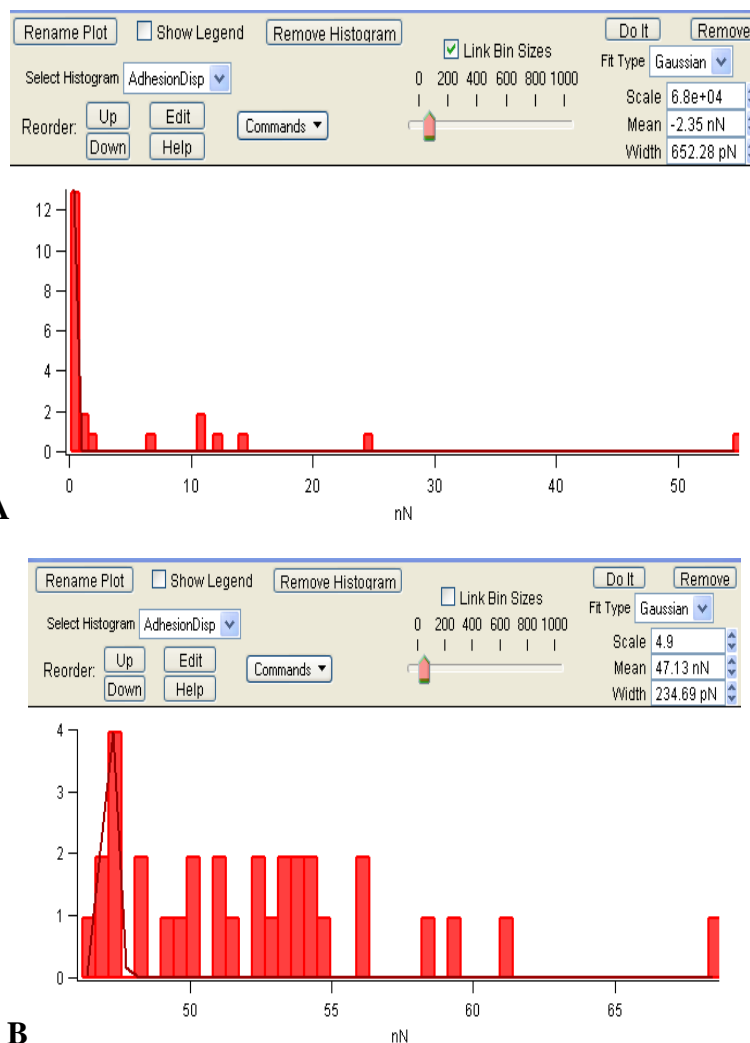


Fig. 45 Graphics show pull-off AFM force measurements using OH⁻-SAM tips on cypris footprints of *B. amphitrite* (A) and *B. improvisus* (B). The means and standard deviations were calculated by fitting the histogram to a Gaussian distribution.

The highest value of adhesion was recorded using the functionalised CH₃-SAMtip for both species, as also demonstrated by Phanget *al.* (2009a) for footprints of *S. balanoides* compared to a standard Si₃N₄ AFMtip. This result is in agreement with footprint investigations carried out by imaging ellipsometry (section 3.3) on different SAM surfaces, where spreading of proteinaceous material was higher on the hydrophobic surface, i.e. the protein had a high affinity for this surface.

The adhesion strength on the CO₂⁻ (MHA)-SAM tip was slightly higher for footprints of *B. amphitrite* than of *B. improvisus*. In contrast, the force curves recorded on positively (-N(CH₃)₃⁺) charged tips were higher for *B. improvisus*.

Phanget *al.* (2009a) explained differences in force curves between hydrophobic and Si₃N₄ tips by considering the number of protein chains adhering on the tip. On the

hydrophobic tip, the number of attached proteins was higher due to the fact that seawater was excluded from the protein interface (hydrophobic interactions), while on other hydrophilic tips the surface tension of seawater would prevent the attraction between footprint and tip by wetting both parts. The change in protein conformation and its denaturing process could enhance the contact between a hydrophobic tip and hydrophobic groups in the protein. The differences between hydrophobic and hydrophilic surfaces were found to be similar for SIPC and fibrinogen by Petrone *et al.* (2015), with broadly the same behaviour, both adsorbed irreversibly to negatively charged surfaces. Generally, with hydrophilic tips, the pull-off cycle leads to the rupturing of few sacrificial bonds, while with a hydrophobic tip the protein remains attached during the retraction cycle, continuously unfolding until the weakest link in its structure ruptures and the footprint loses its contact with the tip. The high values elaborated in the Gaussian distribution for the CH₃-functionalised tip (histograms in Fig.42) are probably due to the long stretching of protein chains correlated to the high number of attached sites. The values of force adhesion for the two species performed with the hydrophobic tip (see Table 5) showed differences greater than any other functionalised tips, confirming the results of Phanget *al.* (2009a) for another barnacle species.

	<i>B. amphitrite</i>	<i>B. improvisus</i>
SAM Tip		
-CH ₃	37.5 ± 0.9	71.9 ± 4.5
-CO ₂ ⁻ (MHA)	10.5 ± 0.1	6.2 ± 1.0
-N(CH ₃) ₃ ⁺	6.2 ± 0.3	23.8 ± 0.2
-OH	2.3 ± 0.6	47.1 ± 0.2

Table 5. Values of adhesion force (nN) recorded with functionalised tips for both species.

In this study the footprints were freshly deposited by cyprids and kept in filtered (0.22 μm) seawater to maintain the natural conditions of the proteins. The intricate morphology of footprint proteins, consisting of interconnected and aggregated nanofibrils, complicates the study of their mechanical properties in relation to adsorption on substrata. Explanations based only on forces measured with AFM (Phanget *al.*, 2010) may fail to comprehensively elucidate the viscoelastic, unfolding and folding mechanisms of proteins adhering to an AFM tip. The so-obtained

mechanical properties of footprints therefore afford the opportunity to mimic the natural process, namely the attachment of the antennular disc onto a surface with the subsequent adhesive spreading.

Besides hydrophobic interactions already highlighted by Phang et al. (2009b) and in this experiment, Noy et al. (1997) suggested that another weak force could be involved in attraction force for SAM surfaces, i.e. van der Waals forces. In contrast to other types of force, van der Waals forces (also known as dispersion forces) are always present in any phenomenon involving intermolecular forces, and arise from dipole-dipole interactions, and are in the range from >10 nm down to interatomic distances (0.2 nm) (Singh et al., 2006; Israelachvili 2011). Although these forces are considered weak, the collectivity of multiple weak forces and the fact that they are always present can become the driving force for adhesion/adsorption of adsorbates on surfaces, as also described in the Johnson–Kendall–Roberts (JKR) model (Johnson et al., 1971).

Another factor to take into account is the presence of villi on the attachment disc, which are believed to be involved in the adhesion process (Phanget *al.*, 2008). By close observations of the exploratory phase of cyprids of *S. balanoides*, Aldredet *al.* (2013) highlighted the importance of villi, proposing three functions for the antennular disc and the velum (the structure that encircles the third segment) in the adhesion mechanism: (1) their flexibility maximises adhesive spreading on the surface; (2) the presence of cuticular villi enables resistance to lateral shear and (3) subsequent torsion force applied on the cypris body during the close exploration. According to these points, the villi would act as a mechanical buffer from the moment that a force is applied onto a surface during the first contact with the substratum to the peeling at the adhesive interface. It therefore appears that cyprid temporary adhesion is affected by a combination of proteinaceous adhesive material and cuticular villi structures. Such a synergistic combination would represent a rare system in nature, worthy of future studies leading to its comprehensive elucidation.

However, for the purpose of this thesis, the focus of the investigations described above related to differences between the two species of barnacle. *B. amphitrite* and *B. improvisus* cyprids have long been thought to have different settlement behaviours in response to surface chemistry (*B. amphitrite* preferring hydrophilic surfaces and *B. improvisus* preferring hydrophobic surfaces) (see chapter 2). Considering this alleged difference in surface preference, it was hypothesised that there may be differences in the

interaction of their respective adhesive proteins on the same surface. In the present study, however, only slight differences were found in terms of the biophysics of the adhesives, which is perhaps not surprising in the light of recent studies suggesting an absence of surface selectivity for *B. amphitrite* on the basis of hydrophobicity. Thick and confined footprints (indicating low spreading and affinity) were found on positively charged surfaces, on which cyprid settlement was also low or negligible for both species (see chapter 2). In conclusion, the temporary adhesive of the two species has, contrary to previous models in the literature, a strong affinity to hydrophobic surfaces and, in agreement with contemporary settlement studies, a low affinity and surface preference for positively charged surfaces. These findings may be crucial for understanding the mechanism of surface selection by cyprids and for the development of future antifouling technologies.

Chapter 4. Effect of elastic modulus on surface selection and barnacle adhesion

4.1 Introduction

The development of antifouling strategies free from harmful substances has been the major challenge since restrictions were introduced by the IMO in the 2001 (reference). Although biocide-based coatings are likely to be the basis of marine antifouling technologies for the foreseeable future, new solutions require more environmentally friendly approaches. Fouling-release coatings (FRCs) are biocide-free coatings, which act in two ways, as an antifouling and as anti-adhesive. Laboratory assays of such surfaces usually involve either quantification of settlement of competent larvae (Aldred *et al.*, 2010a) or algae (Callow *et al.*, 2000), or mechanical removal of adult organisms. The mechanisms that underpin the effects on fouling organisms are based on the chemical and physical properties present between coating and water (see chapter 1). Functional groups of the adhesives secreted by marine fouling organisms may be prevented from adhering by a nonpolar and nonreactive surface, which reduces surface charge and van der Waals forces. In addition, surface topography (e.g. roughness and porosity) may play an important role in fouling control. Bioadhesives may penetrate into the surface irregularity, finding anchoring points once cured. In this regard, the smoothness of FRCs may have a key role in enhancing the removal of organisms from the surface (Candries and Atlar, 2003) by minimising mechanical interlocking (Brady, 1999; Brady and Singer, 2000). Other parameters such as roughness, thickness and elastic modulus may have a great impact on the adhesive tenacity and on the release of fouling organisms. Certainly, the combined effect of all these factors may be different depending on the organism, and the nature of its adhesive. Furthermore, the size, shape and type of base in contact with the surface may affect removal by shear forces (Buskens *et al.*, 2013).

Among the commercial FRCs, the main products are mostly elastomers of poly(dimethyl siloxane) (PDMS), which have the properties of: hydrophobicity, low surface energy, low glass transition temperature (Mera *et al.*, 1998) and low elastic modulus (Stein *et al.*, 2003b; Yebra *et al.*, 2004; Patwardhan *et al.*, 2006). These coatings work by weakening adhesion such that fouling is released under hydrodynamic shear (Waite, 1983; Kim *et*

al., 2007; Murosaki *et al.*, 2009), The coatings are much less effective in static conditions (Brady, 2000). As PDMS is mechanically weak (Beigbederet *et al.*, 2008), it must be cross-linked in order to obtain a stronger structure (Schmidt *et al.*, 2002). Among the silicone formulations brought to market, uncross-linked silicone polymer chains or silicone oils may affect the bond by interacting with bio-adhesives as they cure (Berglin and Gatenholm, 1999; Meyer *et al.*, 2006). In this context cross-linked PDMS does not affect barnacle (*B. amphitrite*) recruitment but it does affect the adhesion of adults, thereby increasing removal under shear (Beigbederet *et al.*, 2008).

The removal of adult barnacles from coatings is difficult since the adhesive used has high modulus; condition that do not allow the storing of sufficient elastic energy by deformation under external forces. Furthermore, many species of barnacle have a calcareous basis, which adds rigidity to the adhesive interface (Hui *et al.*, 2011). Conversely, adhesion on polymers of low elastic modulus releases hard fouling organisms easier by readily deformation (Ramsay *et al.*, 2008). Release is by peeling, which requires less energy than shear.

Elastic modulus is thus an important parameter in the formulation of coatings in that it influences the adhesion and removal of fouling organisms (Backa and Loeb, 1984; Swain and Schultz, 1996; Singer *et al.*, 2000; Sun *et al.*, 2004; Zhang *et al.*, 2011). Different methods have been developed to characterize the elastic modulus on soft surfaces, such as Dynamic mechanical analysis (DMA), through oscillating elongation mode with a temperature scan; elongation measurements, as elongation to break; nano-indentation measurements carried out with AFM by pressing the tip on the surface to be measured.

The modulus of barnacle adhesive differs from artificial adhesives and may be important for the efficiency of adhesion on different substrata (Sun *et al.*, 2004). Growth of barnacles is inhibited on soft surfaces because a higher amount of adhesive is produced (Ahmed *et al.*, 2011). The detachment of barnacles from silicone materials can, however, be affected by cohesive failure of the substratum (Berglin and Gatenholm, 1999).

The process of separating a solid body or a joint into two or more parts is known as fracture (Meyers and Chawla, 1984). The forced release of barnacles from a surface may

be considered a fracture process (Sun *et al.*, 2004). In terms of fracture mechanics, thickness plays a fundamental role in release of hard fouling (Wendt *et al.*, 2006). Thicker silicone elastomers require less energy to break bonds between the organism and the coating. (Chambers *et al.*, 2006). Moreover, the low modulus of the material results in coating deformation and a failure mode similar to peeling occurs (Lejarset *et al.*, 2012).

The first studies on adhesion and fracture utilised rigid studs, which were pulled normal to the surface (Kendall, 1971). The study employed the energy balance criteria elaborated by Griffith (1920). Since the detachment occurs by peeling along an ever-shrinking circle radius, Kendall derived that the total energy U_T of the strained system is the resultant of surface energy, strain energy in the elastomer, and potential energy applied by the load:

$$U_t = -\pi a^2 G - \frac{p^2 t}{2\pi k a^2} \quad (5)$$

The equation 5 explains the fracture mechanism, which combines thickness, modulus and strain energy in an elastomeric adhesive/coating where:

p = normal force

a = contact radius

t = film thickness

G = Griffith's fracture energy per unit area

G_c = critical fracture energy per unit area

k = bulk modulus

It is then possible to determine the critical force P_c by applying Griffith's failure criterion (Griffith 1920) to equation 5, obtaining:

$$P_c = \pi a^2 \left(\frac{2G_c K}{t} \right)^{1/2} \quad (6)$$

For coatings represented by a thick elastomeric adhesive film Kendall (1971) derived:

$$P_c = \sqrt{2\pi E G_c a^3 / (1 - \nu^2)} \quad (7)$$

where E is the elastic modulus and ν is the Poisson's ratio, highlighting the importance of elastic properties of the material in the fracture process (Brady and Singer, 2000).

With this contribution, a new frontier was open in the field of antifouling technologies, raising the possibility of investigating the release of marine fouling organisms (Brady and Singer, 2000; Singer *et al.*, 2000; Chaudhury *et al.*, 2005). It represents a new challenge in view of the difficulties in removing marine organisms from surfaces, even when there are weak interactions between the surface and the organism, in that they exploit the adhesion varying the mechanical and geometric properties of the adhesives (Chung and Chaudhury, 2005).

Further investigations examined the incorporation of oils into silicone elastomeric coatings (Truby *et al.*, 2000) for improvements in fouling release. For example, Hoipkemeier-Wilson *et al.* (2004) showed improved *Ulva* spore release compared to surfaces with lower load of oil. Others have attempted to improve FR efficacy of silicones with nanofillers (Beigbeder *et al.*, 2008), tethered antimicrobials (Majumdar *et al.*, 2008), biocides (Al-Juhni and Newby, 2006; Ruzga-Wijasa *et al.*, 2007) and polyurethane (Brooks, 1991), epoxy (Rath *et al.*, 2009; 2010), or fluorinated segments (Mera and Wynne, 2001; Grunlan *et al.*, 2006; Sommer *et al.*, 2010).

Tests to evaluate the performance of coatings for fouling release have been developed to be rapid and repeatable. Systems to achieve this aim have been designed mainly to remove fouling organisms under shear, as reported for bacteria (Ekblad *et al.*, 2008), microalgae (Finlay *et al.*, 2002; 2010; 2013; Shultz *et al.*, 2000; Stanley and Callow, 2007; Estarlich *et al.*, 2011) and cyprids of barnacles (Finlay *et al.*, 2010). While barnacle adhesion strength measurements are commonly used in the field, they have been used infrequently in the laboratory (Webster *et al.*, 2007). Recently, the adhesion strength of adult barnacles has been evaluated with automated instruments (Singer *et al.*, 2000; Marabotti *et al.*, 2009; Martinelli *et al.*, 2012). The advantage of such tests, is their relatively high precision and for an instrument used by Conlan *et al.* (2008) a significant time saving as smaller barnacles could be used.

A hand-held force gauge is used to test the efficacy of FR coatings by a standardised method (ASTM D5618 1994; Stein *et al.*, 2003a; Wiegemann and Watermann, 2004).

This standardised method was developed to evaluate the force needed to remove barnacles from the surface normalising the values to the basal area in order to calculate the critical removal stress.

Generally, elastomeric surfaces are prepared using PDMS, a crosslinker and catalyst. The elastic properties of the coating can be altered by adjusting the quantity of these components.

Barry (1946) described a relationship between the viscosity and molecular weight using methyl-terminated silicones. It was also possible using hydroxyl terminated silicones to work out the molecular weight of the different resins and define the stoichiometric amount of cross linker and catalyst required for each formulation.

In this chapter the influence of elastic modulus on the settlement behaviour of cyprids of *B. amphitrite* and *B. improvisus* has been compared. Surfaces were prepared by adding different amounts of PDMS, crosslinker and catalyst in order to achieve different values of elastic modulus for each surface.

The two species of barnacle were compared in order to understand whether they also behave differently in response to physical properties of surfaces in addition to the chemical properties investigated in the chapter 2. Furthermore, the same surfaces were employed to investigate the removal of juveniles, 7 days post settlement, under shear. Subsequently, barnacles were grown on the coatings for a further 3 months and the removal of adults, with a minimum basal diameter of 5 mm, were used to measure critical removal stress. This latter assay, made with an automated system, also entailed quantifying basis failure and whether adhesive remained on the surface after removal. The combination of data obtained with different stages of the barnacle life cycle allowed the affinity of the various adhesives for the surfaces to be compared. Finally the two species were compared with respect to the above parameters.

4.2 Material and methods

4.2.1 Settlement assay

Cyprids of *B. amphitrite* and *B. improvisus* were obtained following the procedure described in section 2.2.1.

Settlement assays with *B. amphitrite* and *B. improvisus* were conducted in drops of 0.22 µm filtered artificial seawater (ASW) (salinity 32 for *B. amphitrite* and 22 for *B. improvisus*) placed on coated microscope slides containing 20 cyprids and 15 replicates for each surface. The hydrophobic nature of the surfaces used in these experiments (contact angles between 80 and 94°, see table 6) allowed the beading of droplets onto the microscope slides. The resulting height of the droplet placed on the surface was of 0.5 - 0.8 cm (at the highest point of the meniscus) so that the cyprids were not overly constrained, as they would be on a hydrophilic surface. Furthermore, the incubation method used for this experiment (glass slides were housed within Quadriperm dishes, with their lids on, which were wrapped in wet paper and tin foil) avoided water evaporation from the surfaces; a crucial point for assays that last for more than 24 h at high temperature (28°C). To ensure that cyprids were in good health, polystyrene 24-well plates were used for *B. amphitrite* and Falcon 1006 Petri dishes for *B. improvisus*, as laboratory standards, in order to compare the settlement ratio with other tests carried out with the same surfaces. Settlement results were monitored after 48 hours using a stereomicroscope.

4.2.2 Removal of juveniles under shear using a flow cell

Subsequent to the settlement assay, barnacles were grown on the coated microscope slides for 7 days. The coated slides (6 replicates of each surface), were kept in the individual wells of Quadriperm dishes, which were filled with 25 ml of ASW (salinity was specific per each species, 32 for *B. amphitrite* and 22 for *B. improvisus*). The water was changed daily, whereupon 2 ml of *T. suecica* were added. The temperature was maintained at 25°C for both species. After 7 days post-settlement the basis of the juveniles had a diameter of 1-2 mm. The slides with the juvenile barnacles on were then inserted into the flow cell, held on frame-mounted panels, and exposed to shear.

The flow cell (Politis *et al.*, 2009) was designed to simulate a fully developed turbulent boundary layer developing over the hull of a ship. With a measurement section of 1500 x 292 x 20 mm, pump power rating of 15kW, pump capacity of 90 litres/s at 10m head, the system has the potential to simulate the boundary layers developing on a 140m vessel travelling at speeds of up to 40 knots.

The flow generated during this assay was fixed at 12m/s with a maximum pressure of 120 Pa applied for 60 seconds.

4.2.3 Removal of adults by push off

Computer-controlled instrumentation (Advanced Analysis and Integration Ltd, Manchester, UK), hereafter referred to as push-off machine - has been employed to measure the critical removal stress of adult barnacles (Conlan *et al.*, 2008). To calculate the adhesive strength of barnacles, the instrument normalises the removal force to the area of the barnacle basis (Fig. 46). Only barnacles with base plates >5 mm were considered for this test. The critical removal stress measurements were made according to Conlan *et al.* (2008).

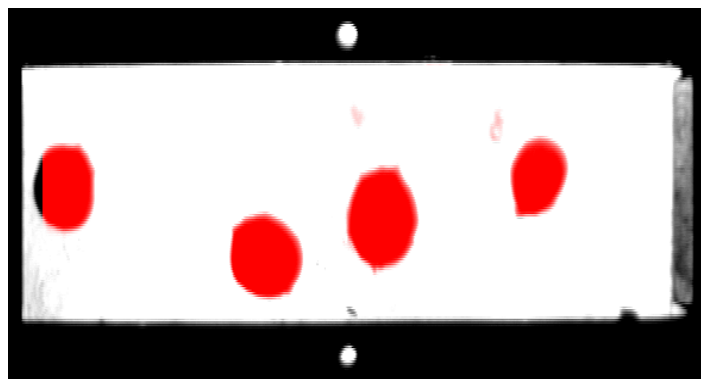


Fig.46 Screen grabs of barnacles that have been scanned and their basal areas measured using the automated methods' software.

4.2.4 Data analysis

Settlement, removal and area data are reported as means \pm standard error (SE). The effect of surface chemistry on settlement was examined by one-way analysis of variance (ANOVA) when the assumptions for parametric analysis were fulfilled. Post hoc Tukey's pairwise comparisons were done with Minitab 15 and an α level of 0.05 was used.

4.2.5 Surfaces for settlement assays

Settlement assays were conducted with a range of substrata. Nexterion Glass B slides (Schott, Germany), 76 mm x 25 mm, 1 mm thickness and sterile flat-bottom polystyrene 24-well plates for traditional tissue culture (TC Plate 24 Well F) (Sarstedt, USA) were used as internal laboratory standards. Removal assays were conducted only with coated microscope glass slides as described in the next section.

4.2.6 Surface preparation

Polydimethylsiloxane (PDMS) based surfaces were prepared with different quantities of hydroxyl terminated silicones (Fig. 47), tetraethyl orthosilicate – 40 crosslinker (TEOS) (Fig.48) and catalyst bis(2-ethylhexyl)hydrogenphosphate(BEHHP) (Fig. 49) as shown in table 6.

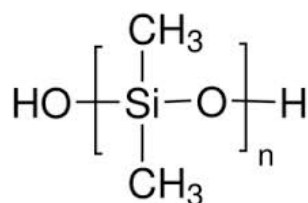


Fig. 47 General structure of hydroxyl terminated poly(dimethylsiloxane).

The preparation of surfaces with a range of elastic moduli has been carried out using different mixtures of the three substances listed above. The silicone's viscosity is a function of dimethylsiloxane repeating units ('n' in fig. 47); a high number of these groups gives longer chains with higher viscosity. Shorter chains, with lower numbers of 'n', have lower viscosity. Here after values of viscosity will be used for naming the coatings.

In order to extend the range of surfaces with different values of elastic modulus, an higher amount of TEOS was added to the mixture with a viscosity of 35 cSt, in order to increase the crosslinking density and therefore increase the elastic modulus of the coating. The surface so obtained was named '35 HT'; H referring to higher and T to TEOS (see table 6).

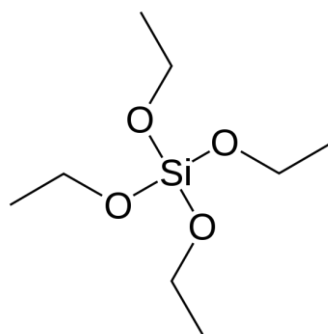


Fig. 48 General structure of tetraethyl orthosilicate–crosslinker (TEOS).

Upon addition of water, TEOS hydrolyses the silicon dioxide, which accounts for 28.8% of the initial mass of TEOS. Therefore, monomeric TEOS can be called TEOS 28, as opposed to TEOS 40, which has about 40% of silicon dioxide, meaning that TEOS 40 is an oligomeric version of TEOS 28 (i.e. molecules of TEOS28 condensed together). It is possible then to deduce that the TEOS40 used in this work was an oligomer of about 5 molecules of TEOS.

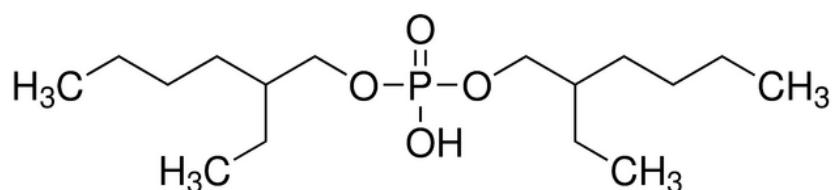


Fig. 49 General structure of bis(2-ethylhexyl)hydrogen phosphate (BEHHP).

Viscosity (cSt)	35HT	35	90	630	1000	4000	14000
Silicone (g)	40.137	46.792	61.951	67.941	68.560	69.141	69.461
Teos40 (g)	27.118	21.098	7.317	1.872	1.309	0.781	0.490
BEHHP (g)	2.715	2.110	0.732	0.187	0.131	0.078	0.049
Total (g)	70.000	70.000	70.000	70.000	70.000	70.000	70.000

Table 6. Properties of mixtures of silicone-based surfaces used for cyprid settlement assays and removal assays with juveniles and adults of *B. amphitrite* and *B. improvisus*.

Nexterion glass microscope slides were coated with silicone mixtures prepared as described previously. The coating procedure was performed using a paint roller to allow an homogenous distribution on the microscope slides, which avoided air bubble formation. Surfaces were stored overnight for drying and the following day contact angle measurements were made.

Subsequently, surfaces were transferred at Newcastle University for leaching in deionized water in order to free the coatings of residual chemicals that could affect the settlement of barnacles. The leaching procedure was carried out by immersing surfaces in a container with MilliQ water with a circulating system comprising a pump and filters (with activated carbon).

After three months of leaching, surfaces were gently cleaned using a sponge in order to remove biofilm and contact angle measurements were repeated to ensure that the period of immersion did not change the surface wettability.

4.2.7 Elastic modulus calculation

Dynamic mechanical analysis (DMA) was used to calculate the elastic modulus of surfaces prepared in the laboratory of International Paint (Felling). The calculation was made in an oscillating elongation mode with a temperature scan. A Perkin Elmer Diamond DMA was used with a temperature scan appropriate to the samples with MUSE Measurement and MUSE Standard Analysis v4.2 software from SII Technologies. The range of temperature used was -130°C to +100°C at a rate of 3°C/min.

The DMA settings were as follows: oscillation frequency - 1 Hz; longitudinal amplitude - 5 µm; minimum tension - 5 mN; tension gain - 1,25; and the force amplitude - 500 mN. The data recorded were storage modulus E' , loss modulus E'' and $\tan \delta$ (= the ratio of E'/E''). E' was used to measure the film's glass transition temperature (T_g) and the elastic modulus at 20°C.

Free films of coatings used for bioassays were cut in 1 x 4 cm samples and used for DMA. Measurements are presented with their 95% confidence interval (Fig 50).

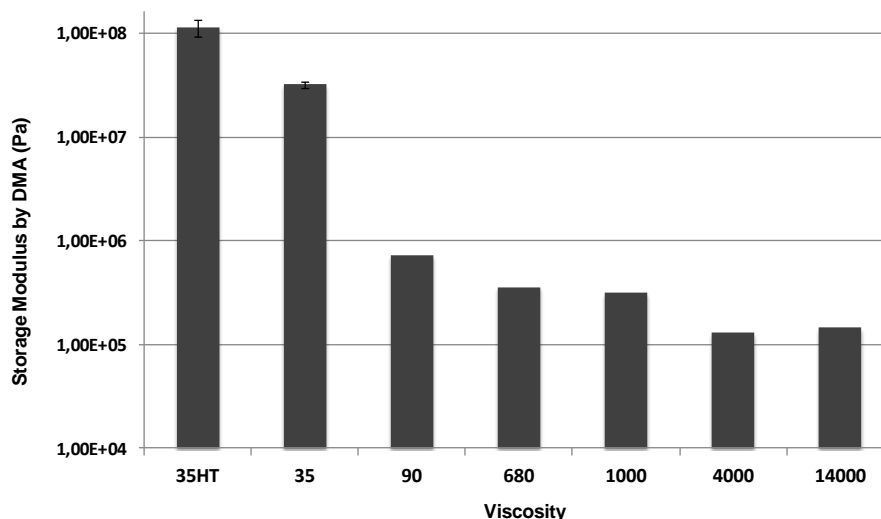


Fig. 50 Values of elastic modulus calculated using storage modulus at 20 degrees by dynamic mechanical analysis (DMA) with 95% confidence interval.

Elastic modulus was calculated also using an elongation measurement method: laser extensometer, Zwick Tensile Test Machine and Free Film Tensile v3-vi Front Panel software. Elongation to break has been used to calculate the tensile properties of silicone surfaces with very flexible behaviour. The test comprised stress/strain measurements of thin layers of coating approximately 0.6 mm thick (3 replicates). The size of the samples used for this characterisation was 80 x 12 mm. The loading speed was 50 mm min⁻¹; the width and the thickness were measured for each replicate before the experiment. Elastic modulus, here represented by the Young's modulus, was calculated by combining the tensile stress values (MPa) with the tensile strain (extension) (%).

4.2.8 Contact angle goniometry

Advancing contact angles of silicone surfaces were measured using Dataphysics OCA 35 system with SCA 22 software equipped with automatic liquid dispenser. Values of advancing and receding contact angles were the average of five measurements with water (Tab. 7). Surface free energy was calculated using values of advancing and receding contact angles obtained with water and diiodomethane.

Viscosity (cSt)	35HT	35	90	630	1000	4000	14000
Elastic modulus (MPa)	114±1.5	32±1.4	0.73±0.07	0.36±0.08	0.31±0.06	0.13±0.03	0.14±0.04
Contact angle (°)	87.2±2.1	83.6±4.6	92.4±4	87.6±2.6	80.4±6.2	83.6±6	90.8±4.1
Surface energy (mN/m)	31.36	33.1	31.98	32.87	30.12	28.63	30.39

Table 7. Values of viscosity, elastic modulus, contact angle and surface energy for each surface.

The approach used to calculate the free energy with two liquids was that of Owens and Wendt (1969). This method describes the polar and dispersive (i.e. non-polar) interactions at the interface between the surface and the environment for polymeric material.

4.3 Results

4.3.1 Settlement assay

Cyprid settlement varied on surfaces with different values of elastic modulus. *B. amphitrite* showed high settlement on surfaces with high values of elastic modulus. On surfaces denominated 35H and 35, with values of elastic modulus of 114 and 32 MPa respectively (which have three and two order of magnitude higher than the rest of surfaces used in this experiment), settlement was 40.9 ± 3 and $49.6 \pm 3.3\%$. On surfaces with elastic moduli of 0.73 (90), 0.36 (630) and 0.31 (1000) MPa, settlement decreased to 35.3 ± 3.7 and 31.5 ± 3.5 and $18.81 \pm 2.4\%$ respectively. Settlement on surfaces with elastic moduli 0.13 (4000) and 0.14 (14000) was 11.26 ± 2.8 and $19.41 \pm 3.7\%$ respectively. Data differed significantly between surfaces ($p < 0.05$, $F = 12.68$) at 95% confidence (ANOVA/Tukey test).

B. improvisus settlement was lower than that of *B. amphitrite*. Settlement on 35HT, 35 and 90 was respectively 14.2 ± 3 , 20 ± 3 and 14.2 ± 2.5 %. Settlement on the remaining four coatings - 630, 1000, 4000 and 14000 – was 6.3 ± 1.5 , 4.3 ± 1.3 , 5.3 ± 1.3 and 3.3 ± 2 %. Data differed significantly between surfaces ($p < 0.05$, $F = 8.22$) at 95% confidence (ANOVA, Tukey test).

Settlement of the two species was significantly different ($p < 0.05$, $F = 22.87$) at 95% confidence (ANOVA, Tukey test) (Fig.51).

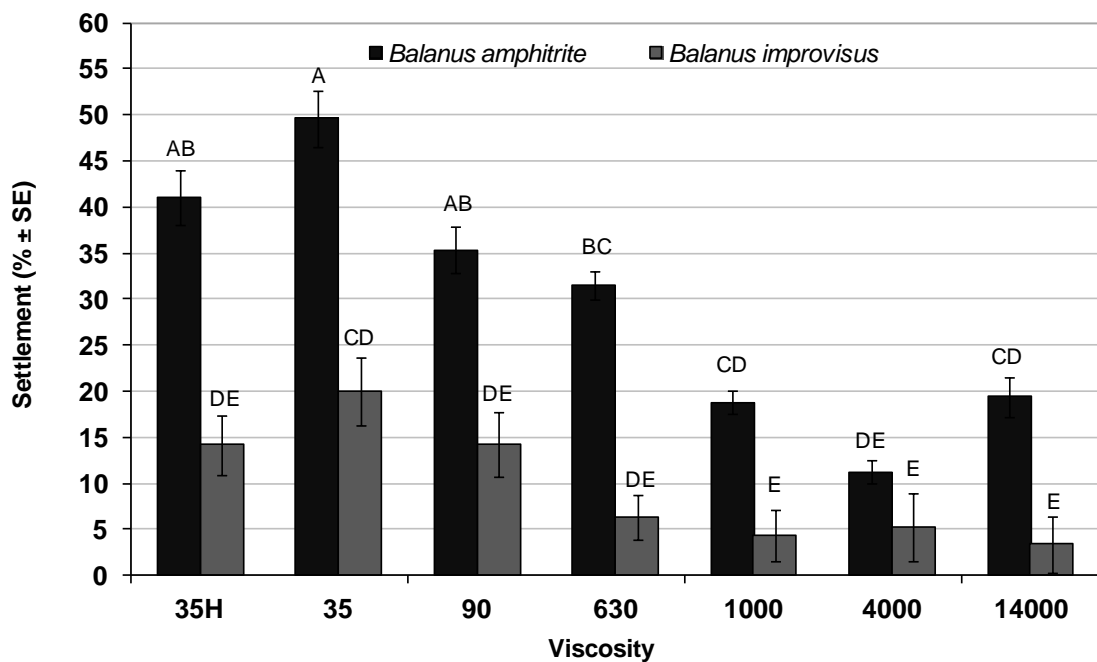


Fig. 51 Cyprid settlement (\pm standard error) after 48 h for *B. amphitrite* and *B. improvisus*. Data were obtained for 20 cyprids per surface and 15 replicates. Tukey pairwise comparisons are presented. Means that do not share a letter are significantly different.

4.3.2 Removal of juveniles by flow cell

Silicone-coated microscope slides, with 7-day-old juveniles, were inserted into the flow cell. Slides were exposed for 60 seconds at a flow rate of 12 m/s. Next, microscope slides were observed using a stereomicroscope and barnacles that were still attached were counted.

The percentage removal of juveniles of *B. amphitrite* from surfaces 35HT, 35, 90, 630 and 1000 were 11 ± 5 , 21.4 ± 5 , 22.6 ± 4 , 19.5 ± 5 and 16.9 ± 3 % respectively. Juveniles were more easily removed from coatings 4000 and 14000 with

values of 32.5 ± 7 and $36.7 \pm 5\%$. The removal data differed significantly between surfaces ($p < 0.05$, $F = 4.65$) at 95% confidence (ANOVA, Tukey test).

B. improvisus showed a different behaviour, percentage removal on 35HT, 35, 90, 630, 1000, 4000 and 14000 was 5.42 ± 2 , 2.3 ± 0.5 , 6.2 ± 1 , 10.2 ± 3 , 3.8 ± 1 , 9 ± 3 and $14.1 \pm 4\%$ respectively. These values were not significantly different. ($p > 0.05$, $F = 2.22$) at 95% confidence (ANOVA, Tukey test).

The two species did differ from each other with respect to ease of removal ($p < 0.05$, $F = 4.38$) at 95% confidence (ANOVA, Tukey test) (Fig. 52).

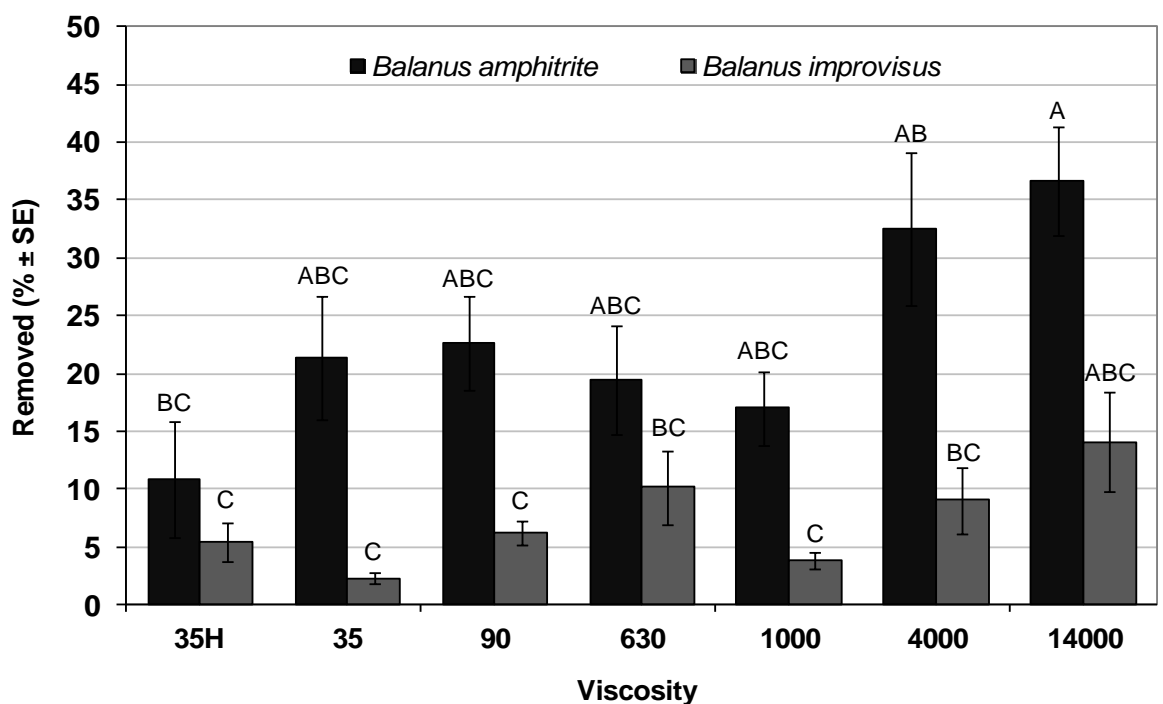


Fig. 52 Percentages (\pm standard error) of juveniles of *B. amphitrite* and *B. improvisus* removed from the surfaces under shear. Tukey pairwise comparisons are presented. Means that do not share a letter are significantly different.

4.3.3 Removal of adults using the push-off machine

The critical removal stress (CRS) for 3-month-old barnacles 3 was determined using the push-off machine. Surfaces with barnacles attached were quickly transferred from the aquarium to the holder of the machine in order to avoid water evaporation. They were then exposed to the push bar. Each slide had about 4 barnacles and 6 replicates were used for each surface.

The CRS values were significantly different between coatings ($p < 0.05$, $F = 16.71$) at 95% confidence (ANOVA). The peak forces appeared to fall into two groups (Fig. 53):

those for 35H, 35 and 90 were 8.06 ± 1.4 , 8.37 ± 0.6 and 7.6 ± 0.9 N. Corresponding values for 630, 1000, 4000 and 14000 were 2.09 ± 0.8 , 3.97 ± 0.6 , 1.22 ± 0.4 and 1.41 ± 0.5 N. Data differed significantly between surfaces ($p < 0.05$, $F = 16.71$) at 95% confidence (ANOVA, Tukey test).

Adults of *B. improvisus* showed differences between surfaces; on 35H, 35 and 90, values of peak force were 8 ± 1.5 , 5.5 ± 0.6 and 5.05 ± 0.5 N. On 630, 1000, 4000 and 14000 values of peak force were 0.5 ± 0.1 , 2.65 ± 0.6 , 0.87 ± 0.1 and 1 ± 0.1 N. Also in this case data differed significantly ($p < 0.05$, $F = 16.41$) at 95 % confidence (ANOVA, Tukey test).

When the data sets for the two species were combined, an ANOVA revealed that there were significant differences between surfaces ($p < 0.05$, $F = 17.45$) at 95% confidence (ANOVA, Tukey test). Data differed significantly with respect to the two species in regard only to the coating named 35.

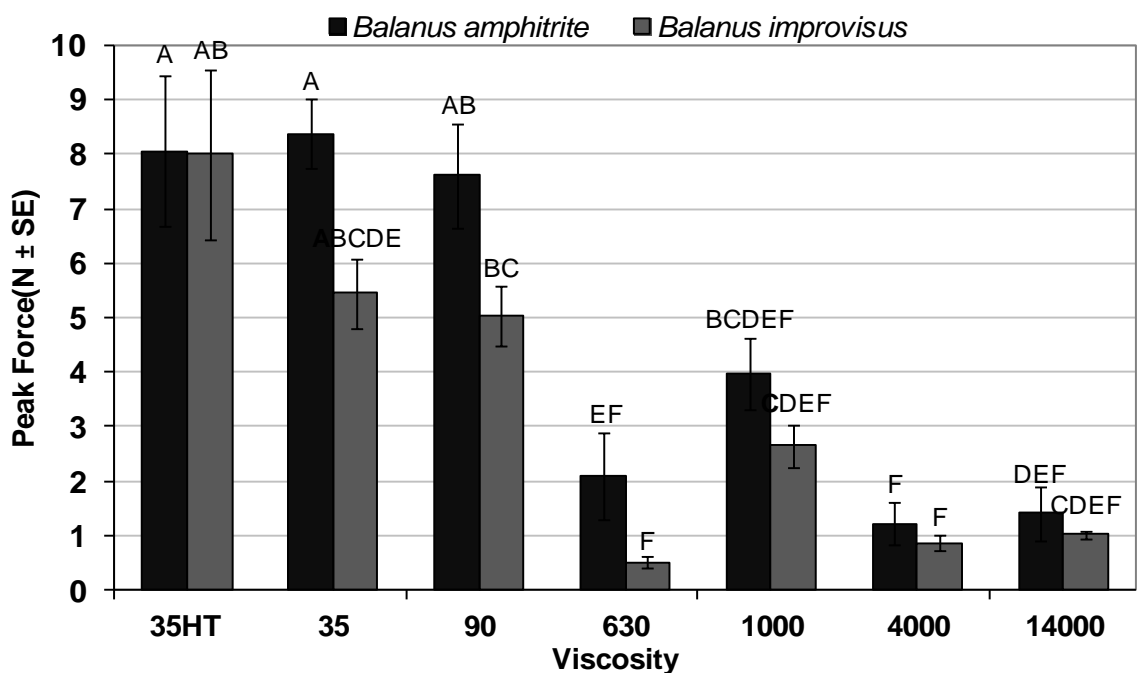


Fig. 53 Percentages (\pm standard error) of adults of *B. amphitrite* and *B. improvisus* removed from the surface by the push-off machine. Tukey pairwise comparisons are presented. Means that do not share a letter are significantly different.

4.3.4 Basal failure (percentage basis remaining on surface)

After the barnacles were removed by the push-off machine, all the coated microscope slides were photographed using a stereomicroscope in order to obtain digitised

images. Subsequently, the images were analysed using ImageJ in order to calculate the area of the basis that remained on the coating.

The area of the basis remaining was compared to the total basal area (prior to removal) in order to calculate the percentage of basis remaining. Figure 54 shows that both species were completely removed from coatings 1000, 4000 and 14000. For coating 630, *B. improvisus* were removed intact but there was a low percentage ($0.3 \pm 0.3\%$) of basal failure for *B. amphitrite*. On surfaces 35H, 35 and 90 the percentage of basis remaining for *B. amphitrite* was 58.01 ± 11.7 , 70.5 ± 7.8 , 11.4 ± 7.9 respectively. There were significant differences between coatings ($p < 0.05$, $F = 20.58$) at 95 % confidence (ANOVA, Tukey test).

For *B. improvisus*, bases remained only on 35H, 35 and 90, with percentage coverage values of 33.1 ± 10.9 , 55.1 ± 12.7 and $35.6 \pm 5.1\%$ respectively. Again there were significant differences between the surfaces ($p < 0.05$, $F = 19.59$) at 95 % confidence (ANOVA, Tukey test). Data differed significantly with respect to the two species in regard only to the coatings named 630 and 35 for *B. amphitrite*, while *B. improvisus* did not show basis left on the coating 630 (Fig. 54).

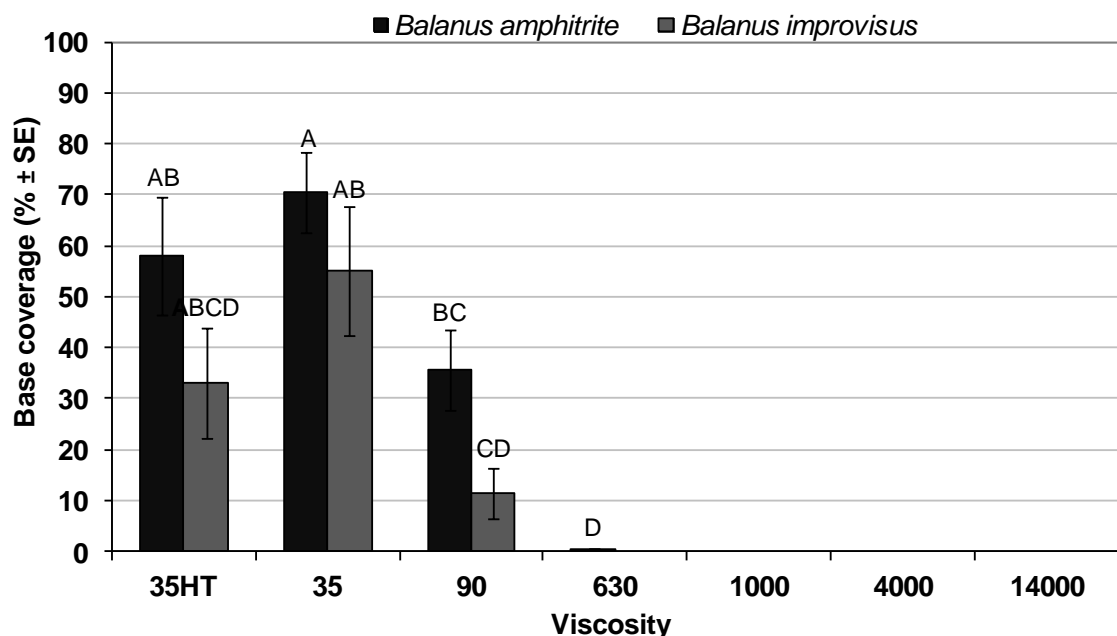


Fig. 54 Percentages (\pm standard error) of base coverage of *B. amphitrite* and *B. improvisus* remained on the surfaces after removal by push off. Tukey pairwise comparisons are presented. Means that do not share a letter are significantly different.

4.3.5 Percentage coverage by adhesive

Subsequent to the shell base coverage calculation, the same surfaces were used to evaluate the area covered by the barnacle adhesive. The barnacle base area was stained using Coomassie Brilliant Blue – G – Colloidal Blue-silver, prepared as described in section 3.4.2. The stain was left on the surface for three hours and rinsed using MilliQ water. The stained area was calculated using ImageJ. The area occupied by the basis (assuming adhesive was under the basis) was added to the value for the stained area to give total adhesive coverage.

The adhesive coverage for *B. amphitrite* was high on surfaces of high elastic modulus. 35H, 35 and 90 had percentage values of 91.8 ± 6 , 100 and 94.4 ± 2.6 % respectively. The lowest coverage - 36.7 ± 8.9 % - was observed on 14000. The coverage values differed significantly between surfaces ($p < 0.05$, $F = 11.40$) at 95 % confidence (ANOVA, Tukey test) (Fig. 55). Data differed significantly with respect in regard only to the coatings named 14000 for *B. amphitrite*.

Differences between surfaces were also observed for *B. improvises*. High percentage adhesive coverage was found on surfaces with high values of elastic modulus; on 35H, 35 and 90, the coverage was 92.7 ± 7.3 , 88.5 ± 14.1 and 98.5 ± 1.5 %. Lower values of 21.4 ± 3 , 56.2 ± 9.6 and 64.4 ± 7.6 % were calculated for 1000, 4000 and 14000 respectively. There were significant differences between surfaces ($p < 0.05$, $F = 7.57$) at 95 % confidence (ANOVA, Tukey test).

Differences between species were significantly different ($p < 0.05$, $F = 9.20$) at 95 % confidence (ANOVA, Tukey test).

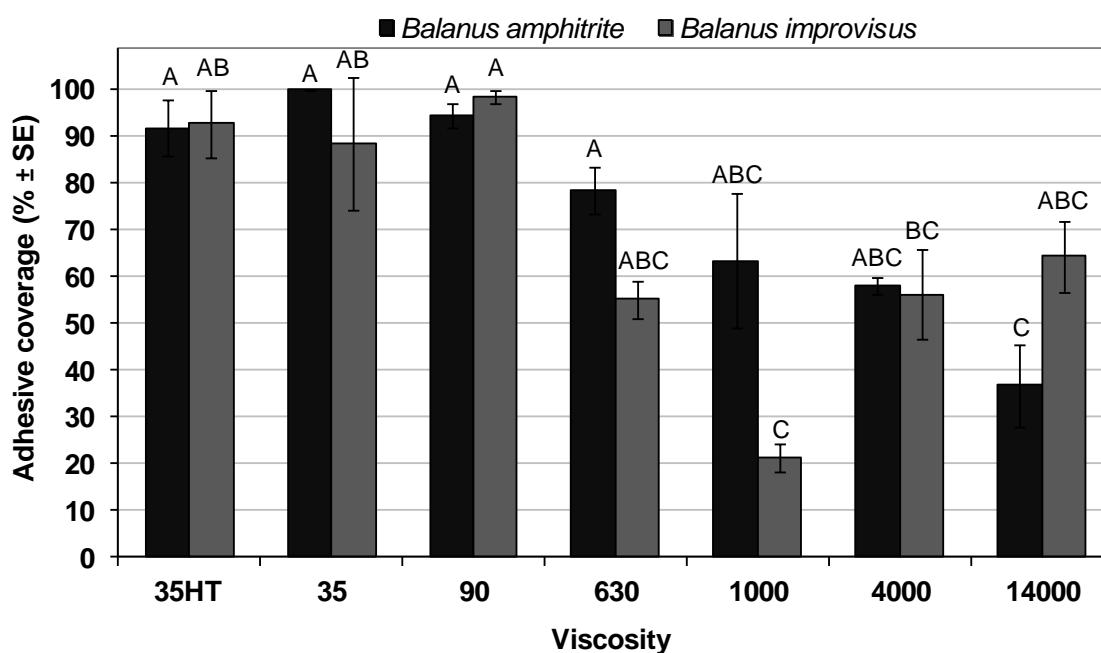


Fig. 55 Percentages (\pm standard error) of adhesive coverage of *B. amphitrite* and *B. improvisus* remained on the surfaces after removal by push off. Tukey pairwise comparisons are presented. Means that do not share a letter are significantly different.

4.4 Discussion

Silicone elastomers were employed in this investigation to understand the influence of elastic modulus on cyprid settlement and juvenile and adult adhesion for two species of barnacle, *B. amphitrite* and *B. improvisus*. These two species, as explained previously (chapter 2) were once considered to have different settlement behaviour. Following experiments carried out in more controlled manner (see chapter 2), however, it was concluded that the settlement behaviour of the two species did not differ, at least with respect to surface charge. In this chapter, rather than compare settlement in relation to chemistry, the aim is to examine a physical parameter, namely elastic modulus.

Elastic modulus has been considered, along with surface free energy, as one of the most important parameters in FR coating formulations. The most important determinant of success of FR is the ability to reduce the adhesion at the interface between the coating and the biofouling organism, rather than inhibiting settlement. So in addition to investigating the settlement preference of cyprids of both species, this study focused on evaluating the critical removal stress of barnacles post-metamorphosis in a controlled manner, employing instruments capable of producing accurate and precise force measurements.

Based on the study of Ahmed *et al.* (2011) a reasonable expectation was that settlement of both species would be higher on surfaces with high elastic modulus. However, it is unclear how cyprids can respond to differences in modulus, since they are relatively small, compliant organisms. Moreover the strength adhesion of adult barnacles should be compromised on coatings of low elastic modulus (Swain and Schultz, 1996; Swain *et al.*, 1998; Berglin and Gatenholm, 1999). In these experiments, values of surface free energy have been kept constant for all the surfaces in order to determine whether elastic modulus influences cyprid settlement and adhesion of juveniles and adults.

Settlement was affected by elastic modulus. *B. amphitrite* showed a clear preference for surfaces with high elastic modulus (Fig. 51). Although the differences were not so large, *B. improvisus* also preferred to settle on surfaces of relatively high elastic modulus. The differences between the species were significant with settlement on each surface always higher for *B. amphitrite*.

Compared to *B. amphitrite*, there have been few studies on *B. improvisus* adhesion on PDMS surfaces and even fewer settlement assays. The results reported here allow, for the first time, a direct comparison to be made between the two species. Although there were differences in the magnitude of settlement, the trend of higher settlement on high modulus surfaces was the same for both species.

The ease of release of juveniles 7 days post-settlement was measured using a fully turbulent flow cell. The shear force that impacted attached juveniles would be similar to conditions on a ship hull when underway.

Elastic modulus had a significant effect on the ease of removal of *B. amphitrite* juveniles. As expected based on previous studies (Holm *et al.*, 2005) higher removal was recorded on surfaces with low elastic modulus. In contrast, there was no significant effect of modulus for *B. improvisus* ($p > 0.05$, $F = 2.22$, fig. 41). The percentage removal was lower when compared with *B. amphitrite* and approximately homogenous across coatings. The latter was a surprising result. Unfortunately few studies have been attempted with this species and mainly on cyprids and recently metamorphosed barnacles. Berglin *et al.* (2001) found differences for release of these stages of development from surfaces of low (PDMS) and high (PMMA) elastic modulus. They working with new metamorphosed barnacles of *B. improvisus* have calculated the

force required to detach juveniles (base plate < 0.5mm) from the two surfaces, observing that the force required detaching juveniles from PMMA was significantly higher when compared with PDMS. Same observations were made with adults. At this regard, Berglin and Gatenholm (2003) found abnormal cementation, on low elastic modulus PDMS - the adhesive plaque was thick and rubbery, contrary to the hard adhesive plaque found on the high modulus PMMA. These differences affect adhesion strength of adult barnacles (Berglin and Gatenholm, 2003) but it cannot be assumed that the same applies to juveniles.

Measures of critical removal stress made with the automated method push-off machine clearly showed that elastic modulus affected both species. The force was applied to the bottom edge of the barnacle where the shell plates meet the basis. For this type of investigation, an important parameter is the size of barnacles attached on the surfaces. Whereas total cohesive failure commonly occurs for small *B. improvisus*, with the whole basis left on the surface, this becomes less frequent with age as the structural integrity of the basis increases with the growth (Berglin *et al.*, 2001). For this reason, only barnacles with a basal diameter of 4-6 mm were used in the present study. This exceeds the minimum size recommended by Conlan *et al.* (2008) for *B. amphitrite*. Furthermore, barnacles with shells in contact with each other were removed in order to avoid false CRS measurements (see Conlan *et al.*, 2008).

B. amphitrite adults were more easily (lower CRS) removed from low elastic modulus coatings compared to high elastic modulus coatings ($p < 0.05$, $F = 16.71$, fig. 42). The same trend was observed for *B. improvisus* adults ($p < 0.05$, $F = 16.41$), contrary to the results obtained with juveniles using the flow cell. Another difference between the species was that *B. improvisus* required a lower force for removal from all the surfaces tested compared to *B. amphitrite* ($p < 0.05$, $F = 17.45$).

Basal failure varied for the different coatings tested with the push-off machine (Fig. 54). The calculation of the area of the base plate remaining on the surface allowed more information to be obtained on the adhesive performance of the adults.

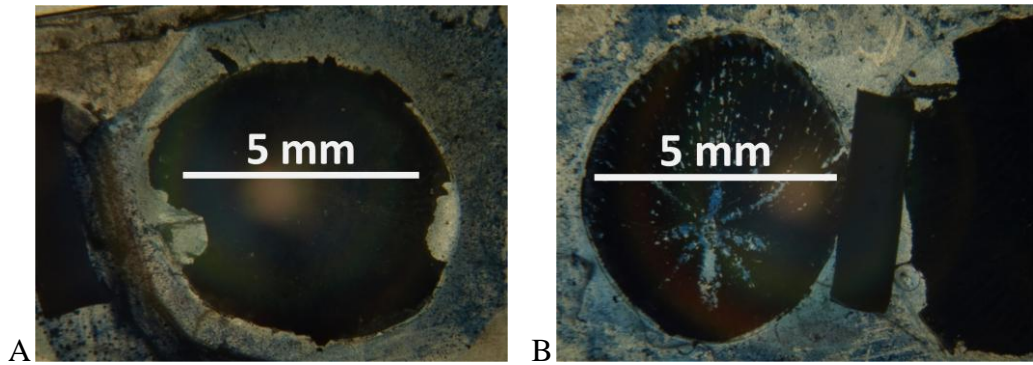


Fig. 56 Bases tended to remain intact on the surface with an elastic modulus of 32 MPa. (A) *B. amphitrite*, (B) *B. improvisus*.

The degree of basal failure (Fig. 57) for *B. amphitrite* was dependent on elastic modulus, decreasing as elastic modulus decreased (Figs. 54). Furthermore, no bases remained (i.e. no breakage of the basis) on coatings with an elastic modulus of 0.31 MPa or below. For *B. improvisus*, bases were completely removed from surfaces with an elastic modulus of 0.36 MPa or lower.

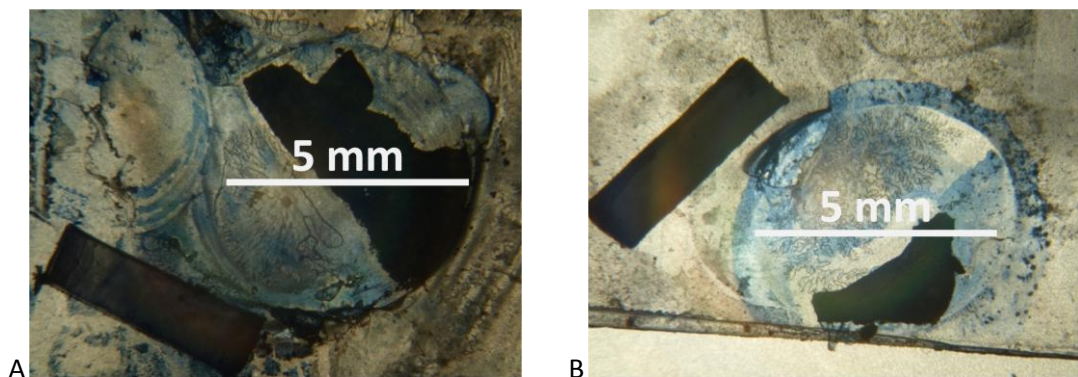


Fig. 57 Bases remaining on the surface with an elastic modulus 0.73 MPa (A) *B. amphitrite*, (B) *B. improvisus*.

The area remaining attached on the surfaces differed significantly between the two species ($p < 0,05$, $F = 19,32$, fig. 53). After the breakage caused by shear, the area of *B. amphitrite* bases remaining on the coatings was higher than for *B. improvisus*.

When the bases were completely removed, the area of adhesive was calculated by staining all the surfaces with CBB (Fig. 55). When partial bases were left on the coating, the calculation took into account the adhesive present under the bases with assumed even, total coverage of the basis.

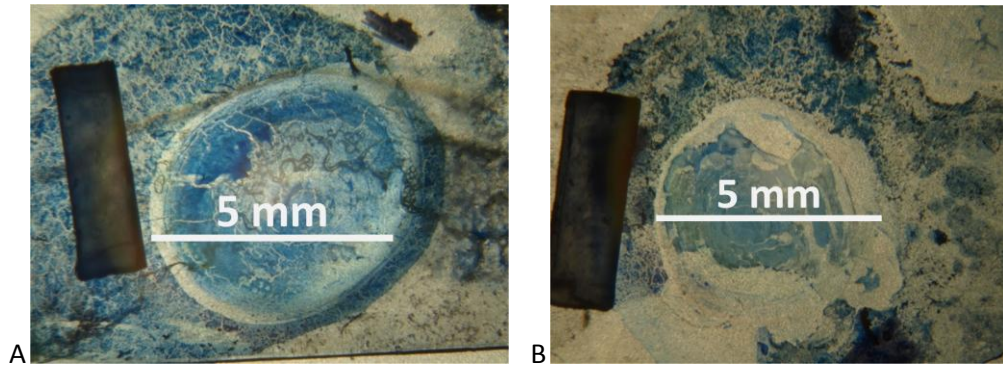


Fig. 58 Adhesive stained with CBB on the surface with anelastic modulus of 0.36 MPa (A) *B. amphitrite*, (B) *B. improvisus*.

There was higher adhesive coverage for *B. amphitrite* on coatings of high elastic modulus ($p < 0.05$, $F = 11.40$, fig. 54) as there was for *B. improvisus* ($p < 0.05$, $F = 7.57$). However, there was overall significantly less adhesive coverage for *B. improvisus* compared to *B. amphitrite* ($p < 0.05$, $F = 9.20$).

The adhesive secretion of barnacles is dependent on substratum characteristic. The expression of the thick adhesive plaque is dependent on substratum, lending credence to this hypothesis. Holm *et al.* (2005) used two different silicone-based surfaces to investigate variation in the characteristics of the adhesive of the barnacle. The adhesive plaque produced on a commercial fouling-release surface was thicker compared with silicone rubber. This highlights how PDMS-based surfaces can increase the adhesive secretion because there is a reduction in tenacity between barnacle and surface.

The analysis of the base plaques and the adhesive of adults left on the surfaces after barnacle detachment enhance the influence of elastic modulus of the surfaces tested on barnacle removal. Berglin *et al.* (2001) showed how occurs the breakage of barnacles of *B. improvisus* on surfaces with different hardness. The breakage was higher on surface with high elastic modulus (PMMA) and low on surfaces with low elastic modulus (PDMS).

The low coverage of adhesive on surfaces with low elastic modulus supports the importance of this parameter in surface performance evaluation. Sun *et al.* (2004) showed by staining the surface after barnacle detachment, that the shear strength of adhesion was strongly dependent on the mean Young's modulus for the adhesive plaque.

Based on these experiments it is evident that there is an effect of elastic modulus of elastomeric surfaces on barnacle settlement and adhesion, Indeed, Grayet *et al.* (2002) reported that this parameter affected the settlement of different species of invertebrates due to an influence of the surface on mechano-sensitive ion channels, even if the highest elastic modulus tested in their experiments was between 0.01 and 0.1 MPa (which are corrected values reported in an Erratum Note to the original 2002 paper (Biofouling 19(2), April 2003).

Ahmed *et al.* (2011) found that elastic modulus was more important than other parameters, such as wettability to ease of release of barnacles. They used PDMS and double-network hydrogels with different values of elastic modulus and hydrophobicity. Both settlement and release of adults were strongly affected by elastic modulus, and barnacles even became detached as they grew on surfaces. Most 'self-release' occurred on PDMS with an elastic modulus of approximately 0.09 MPa.

The fractures observed after the removal test by push off may be an unavoidable consequence on elastomeric surface as reported by Kamino (2013), who observed joint results in destruction of the peripheral shell, with all or part of the calcareous base shell remaining attached to the substratum.

Insert about normal condition of adhesive and then compare when adhesive in abnormal on low modulus coatings. Barnacles use relatively thick and high modulus adhesive, which makes it difficult to remove them because insufficient elastic energy is stored by deformation under external stress (Callow *et al.*, 2000). On the contrary, mussels are able to maximize adhesion by distributing the force to multiple attachment sites that act independently. Sun *et al.* (2004) showed changing in elastic modulus of adhesive plaque in barnacles freshly detached from PDMS surfaces, the adhesive found was structured in multi layers, the outer layer presented lower elastic modulus when compared with layers closer to the base plate. Furthermore they found a strong correlation between the elastic modulus of the outer layer and the shear strength of adhesion.

On elastomeric surfaces the release (fracture) of the barnacle basis can occur through both interfacial and cohesive failure of the adhesive (Sun *et al.*, 2004). In the present study, the partial release of the basis suggests that there may be differences in either adhesive cover and/or nature of the adhesive in different regions of the plaque, i.e. some regions of the basis are more firmly adhered than others. Regional differences have been

noted for abnormal ‘rubbery’ plaques produced by some barnacles grown on elastomeric coatings (Sun *et al.*, 2004). However, the morphology of the adhesive plaque was not examined in the present study and the relevance of this observation to the release characteristics from the elastic modulus series is unclear. Indeed, the fracture mechanics of live barnacles are poorly understood and Kendall’s model (1971) does not take account of the modulus of the adhesive or basal flexure (Ramsay *et al.*, 2008).

Surfaces with high elastic modulus, such as PMMA, with inflexible polymer chains and high glass transition temperature, may explain the stronger attachment of barnacles to this surface compared to PDMS, which has low intramolecular forces between the PDMS chains facilitating the failure (Berglin and Gatenholm, 1999).

Surface free energy, has long been considered an important parameter for good fouling release performance (Baier, 1972; Dexter *et al.*, 1975). Brady (1999) reported, however, that adhesion is not directly correlated with surface energy, as estimated theoretically and empirically for silicones (22 mJ m^{-2}), which performed better than very low-energy fluorocarbon-based coatings ($10\text{--}18 \text{ mJ m}^{-2}$). Evidence to suggest that SFE is not the most important parameter for fouling release has also been reported for other surfaces and barnacles: *Semibalanus balanoides* (Aldred *et al.*, 2011), *B. amphitrite* (Maki *et al.*, 1994; Petrone *et al.*, 2011) and *B. improvisus* (Di Fino *et al.*, 2013). In the present study, however, SFE was kept constant; the main variable was elastic modulus.

In conclusion, it is likely that a combination of factors including elastic modulus and SFE are responsible for the trends presented here for *B. amphitrite* and *B. improvisus*. Settlement, removal and adhesive coverage are all impacted by elastic modulus. Moreover, the results were comparable for two species of barnacle, which is encouraging in relation to the development of coatings with broad-spectrum efficacy.

Chapter 5. Discussion

5.1 Summary

This work has focused on improving our understanding of the mechanisms that influence settlement preferences and the adhesion of two species of barnacle - *Balanus amphitrite* and *B. improvisus* - in order to allow a direct comparison.

I have concentrated on evaluating settlement behaviour, characterising adhesive footprints and the strength of adhesion of the two species, which are the most widely used in laboratory and field antifouling tests. In a recent review Holm (2012) reported that the number of articles (Science Citation Index) related to these two species has increased significantly during the last three decades, compared to other fouling organisms. Although the number of studies has seen an increase, comparisons between the two species are scarce. Furthermore, *B. improvisus* remains poorly studied compared to *B. amphitrite*; which is considered a model organism in antifouling research.

There are studies that have attempted to explain, morphologically and physiologically, the mechanisms that control the surface exploration and adhesion of these species of fouling organism. Moreover, these studies, have mainly drawn comparison between different papers, which usually used different methods (or approaches), precluding an appropriate comparison.

The need to improve the knowledge of the behaviour of different species of fouling organisms has become important for hypothesis-driven coatings design.

The concentration of attention on a single problematic species may have been to the disadvantage of a broader understanding of barnacle fouling ecology. It is thus important to widen studies of other relevant fouling species to test further the assumption that *B. amphitrite* is a suitable model.

5.2 Settlement behaviour

Chapter one focused on understanding the settlement behaviour of cyprids. Tests were carried out on surfaces with characteristics, such as SFE, that in the literature have been reported to influence cyprid settlement in an opposite manner for the two species. Commonly the comparison between these two species has referred almost exclusively to tests conducted on glass (polar and high surface energy) and polystyrene (non-polar and low surface energy) surfaces (Rittschof and Costlow, 1989; Gerhart *et al.*, 1992; O'Connor and Richardson, 1994), assuming that these surfaces had the potential to clarify the different surface preference of the two species. Wettability and SFE were considered to have the greatest influence on settlement behaviour (Dahlström *et al.*, 2004). This approach, however, was not adequate for its aim. Indeed the number of surfaces used and the variability in the composition of glass may have affected SFE. In addition, better characterised surfaces, such as silanised glass, have been used to improve the assay conditions (Rittschof and Costlow, 1989; Roberts *et al.*, 1991; Gerhart *et al.*, 1992; Phang *et al.*, 2009). This is a treatment used to modify the surface properties of the glass and make the surface parameter more predictable. The limitations of this technique were found in their low level of surface coverage and the ability to change the surface charge under controlled conditions (Behrens and Grier, 2001). In this investigation, assays were carried out with well-defined surfaces under controlled conditions; SAM surfaces were employed varying the range of SFE and surface charge. Two assays were carried out using 24-well plates and Petri dishes. The results showed that, contrary to previous suggestions, both the species responded similarly to the surface charge.

5.3 Footprint characterisation

Chapter 3 described the temporary adhesive secretion (footprints) of both species in relation to different surface properties. The small quantity of material used by cyprids to explore the substratum precludes biochemical characterisation. Moreover, the investigation needs to be carried out on freshly released material without change in the natural conditions, such as wetting and temperature. Indeed, few studies have accomplished this. Recently, improvements in technology have allowed microscopic and other non-disruptive approaches (Andersson *et al.*, 2009; Aldred *et al.*, 2011). The

present investigations were carried out again using SAM surfaces in order to observe the morphological differences of footprints using imaging ellipsometry. This was a novel application of the technique, which revealed substantial differences in footprint deposition between different surfaces and between the quantity secreted by cyprids of the two species. Furthermore, the mechanical properties of footprints have been investigated using AFM in order to measure the adhesion force with different functionalised tips. Differences were found between surfaces. The highest adhesion was found for hydrophobic tips and the lowest with positively charged tips, an affinity in agreement with the results of settlement assays presented in this thesis.

5.4 Influence of elastic modulus

Chapter 4 addressed the settlement behaviour and strength of adhesion of both species on surfaces that are considered to be the basis of antifouling technologies since the ban on TBT, i.e. silicone-based FR surfaces. The aim was to determine if there were differences between the two species of barnacle, when only one parameter, elastic modulus, was tested and other potential variables were controlled.

Differences were observed between surfaces and between species. Surfaces with low elastic modulus showed a higher efficacy against the settlement of both species. *B. improvisus* settled in lower numbers than *B. amphitrite*. The same surfaces were used to investigate the strength of adhesion of juveniles under shear (flow cell). Results showed again a higher influence of surfaces with lower elastic modulus, where the juveniles were removed more easily from the surface. On the same basis, three-month-old barnacles were removed from surfaces using an automated push-off machine in order to measure the strength adhesion of permanent adhesive secreted by adults. Again, barnacles of both species were removed more easily from surfaces with low elastic modulus. *B. improvisus* registered lower adhesion strength than *B. amphitrite* when removed from the same surfaces.

These findings highlight the influence of elastic modulus on all stages of barnacles, from settlement to the adhesion of cyprids and adults. Settlement of *B. improvisus* was affected more than *B. amphitrite* and was weaker under shear conditions.

5.5 Final thoughts

Results showed how these two species are similar in their settlement behaviour in relation to surface charge. Similarities were also found in regard to the effect of elastic modulus, which inhibited the settlement of *B. improvisus* more than *B. amphitrite*.

This work was based largely on studies that in the past few decades have discussed whether different species of barnacle respond in differently to varying surface characteristics. SAMs provided a controlled way to improve knowledge of the mechanisms of surface selection and adhesion in relation to surface chemistry, while PDMS- based surfaces represented a material already in widespread use and therefore directly applicable to the real world.

Investigations of cyprid settlement behaviour could benefit greatly from modern methods that allow the investigation of physicochemical and mechanical processes at a size-scale relevant to the organism. SAM surfaces, with their highly conserved surface characteristics, were already employed for studies with spores of *Ulva* sp. and their beneficial features were here extended to barnacles. Compared with the spores, the cyprids require a different assay environment and the flat surface of a microscope slide was not suitable for all of the necessary experimental approaches. From the different approaches tested to overcome this issue, the most successful one was the full coating of Petri dishes and subsequent application of thiols, to produce the SAM. Cyprids were therefore not restricted in their pre-settlement behaviour to the extent seen on microscope slides with sessile water drop.

The employment of such techniques improved our understanding of the mechanisms of surface selection, settlement and adhesion of barnacle cyprids, as well as a comparison between both species. This represents only a small part of the larger picture of forces that govern fouling processes, and there is the need to expand the knowledge to other mechanisms. The approaches used in this study gave important results in view of adhesion mechanisms, but these do not cover completely the processes involved in the surface selection and surface adhesion. Other parameters, such as the bonding mode of functional groups involved in the adhesion process, have to be taken in consideration to allow a broader understanding of the this field. In this regard, the Langmuir adsorption constant, for the binding mode of hydrophilic surfaces to replace surface-bond water, or the competitive adsorption for other kind of adsorbate, should also be considered. It is

of paramount importance the improving of the surfaces used for bioassays, and refining and /or combing other instruments for surface investigation, such as attenuated total reflection-infrared (ATR-IR) spectroscopy.

Results obtained using SAMs revealed the importance of surface charge on settlement preference of cyprids of barnacles and the lower effect of SFE. Nevertheless, other marine organisms respond differently to surface properties. Diatoms, for example, are affected by SFE and it was proved using SAMs. In light of this fact, the surface chemistries of new coatings should have different properties capable to work at broad-spectrum, with the example given above, surface charge and SFE may be important aspects to deter cyprids and diatoms respectively. Thus coatings with even broader surface properties may be more effective against other types of fouling organisms and achieve the efficiency requires.

SAMs showed the importance of positively charged surfaces against settlement of both species of barnacles, as also for the spreading of cyprids temporary adhesive (demonstrated also for *S. balanoides*). The hypothesis is that this phenomenon may be caused by the presence of positively charged lysine found in the barnacle adhesives and from this the preference of negatively charged surfaces. These results suggest the importance of surface charge in surface preference and adhesion of *B. amphitrite* and *B. improvisus*, as also demonstrated for other species, such as *S. balanoides*, probably due to a natural adaptation to the predominance of negatively charged surfaces in the natural environment. Research should be extended to other species, in order to understand if this can be the base for broader efficiency of antifouling coatings. Furthermore, it has been demonstrated that organisms such as zoospores (*Ulva* sp.) respond differently to surface charge. In view of fouling control, there is the need to find the right combination of other factors which can be effective to a wider group of organisms, in order to decrease the impact of biofouling. This goal may be reached by improving the relation between surface charge and surface preferences to other marine organisms with the help of new instruments for the characterisation of both adhesive and surfaces.

Settlement and adhesion of different stages of barnacles have been already investigated on FR surfaces as PDMS-based coatings, which have showed high efficiency in the past and are still relevant to date. The experiments carried out in this thesis improved the understanding of the mechanisms of one of the parameters of FR coatings, the elastic modulus, to begin to explain the apparent antifouling efficacy of this fouling-release

material. In regard to this, the elastic modulus gave important indications on how two species of barnacle are influenced. The development of more efficient coatings is also dependent on the investigation of other parameters (i.e. dissociative coordination of water molecules and their influence surface charge) and needs to be tested with different types of organisms, not only with different species of the family, so that the final product may have a wider efficiency in fouling control.

Based on the results presented here, is clear that the surface preferences of marine organisms are as important in coating preparation as the mechanisms of adhesion. Future studies on antifouling should focus on both these two aspects in order to obtain products capable to work on all the stages of fouling colonization. The best coating fitness would be to stop the fouling organism from sticking to surfaces, instead of removing it from the surfaces after settlement, in order to avoid the load that will affect the marine structures. However, given that not all the organisms can be stopped from sticking, the combination with fouling release coatings is important. There are too many fouling adhesion strategies and may be impossible to control all of them, so coatings with multiple actions become essential.

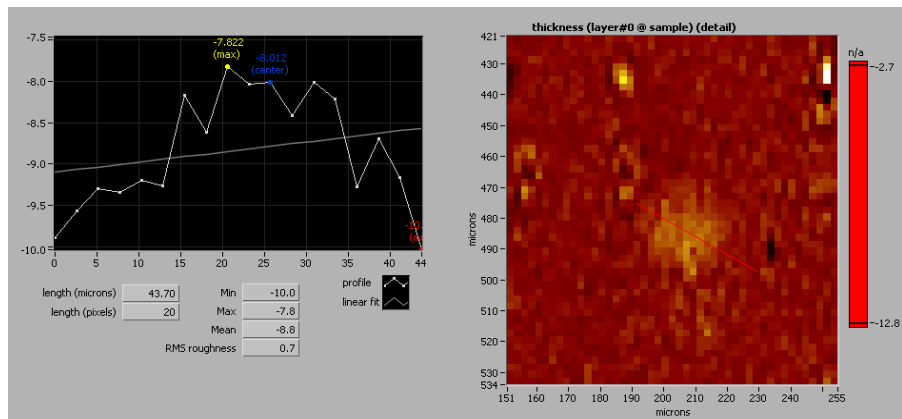
In conclusion this work was designed to indentify the antifouling and anti-adhesion characteristics of surfaces in a systematic way. To achieve these objectives, firstly the surface properties that can influence the barnacle behaviour and their adhesion were investigated. Secondly, methods were developed to obtain highly defined surfaces to test parameters potentially important to surface selection and adhesion, controlling for other potential variables that could confound interpretation of the results. SAMs and PDMS-based surfaces and the techniques employed here, many of which are novel in this field, may find wider application in antifouling research, particularly for the many other species that have yet to be investigated in such a controlled, systematic way. There is a pressing need for new solutions to control fouling given that the oceans are the engine of life and it must be preserved.

Appendix I

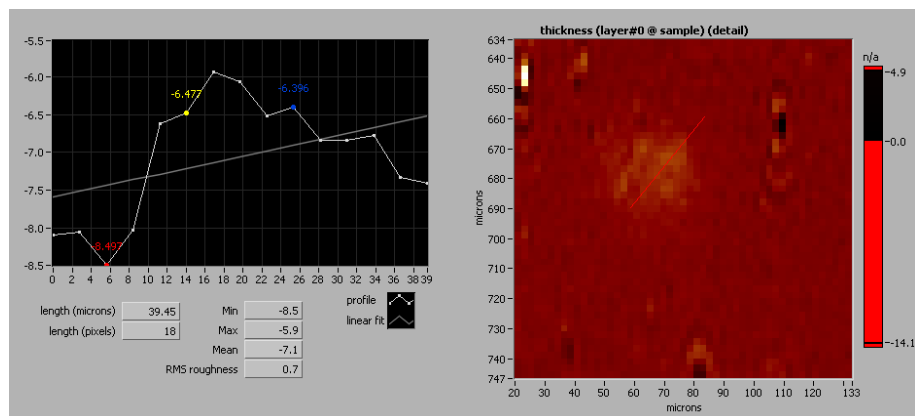
Profile diagrams and map windows of footprints investigated on different SAM surfaces obtained using imaging ellipsometry for *Balanus amphitrite* and *B. improvisus*.

Balanus amphitrite

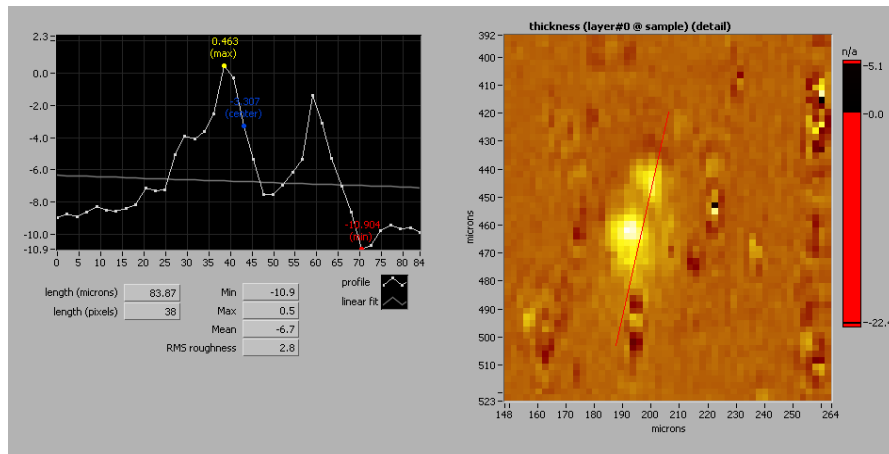
CH₃-SAM



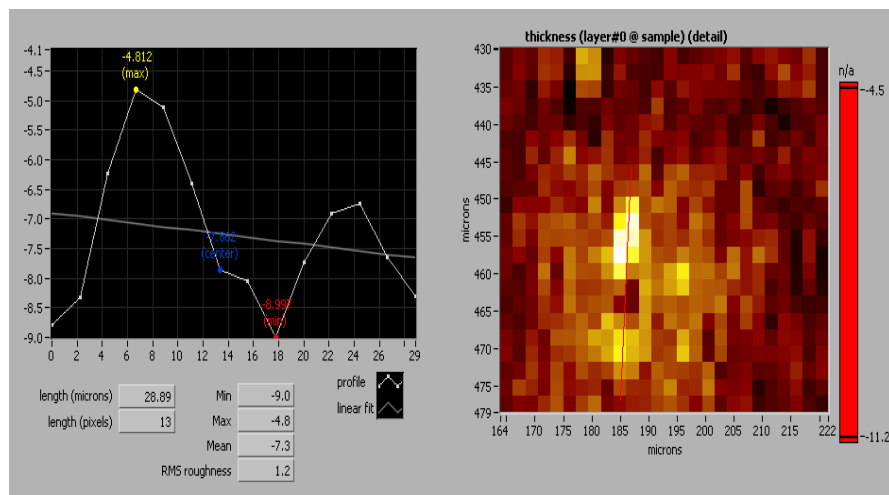
CO₂⁻(MHA)-SAM



$N(CH_3)_3^+$ -SAM

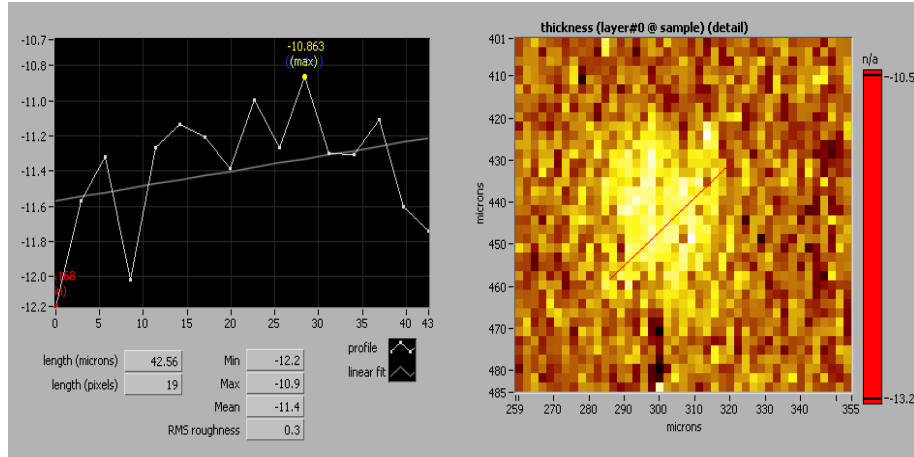


OH-SAM.

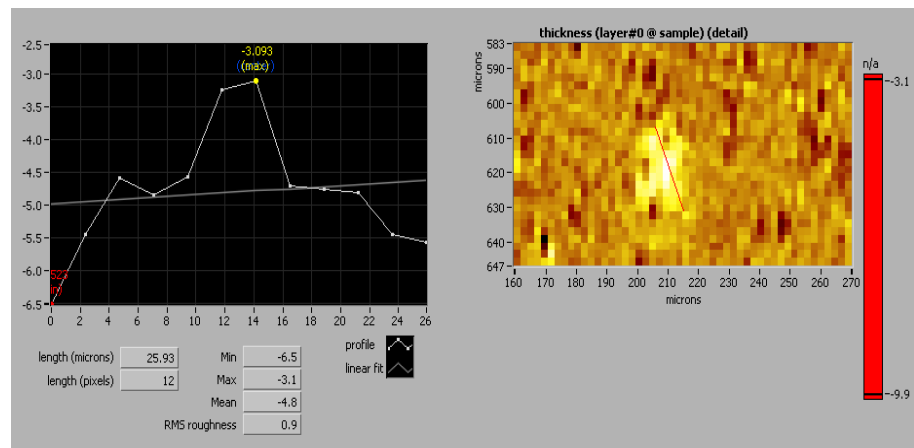


B. improvisus

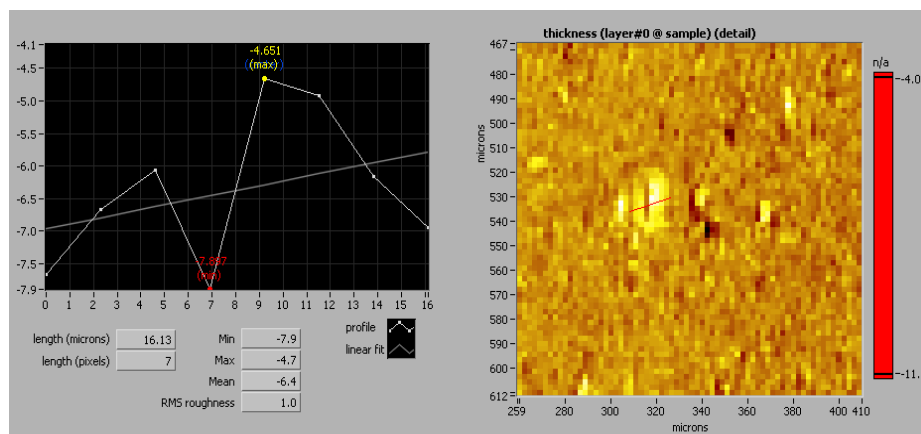
CH₃-SAM



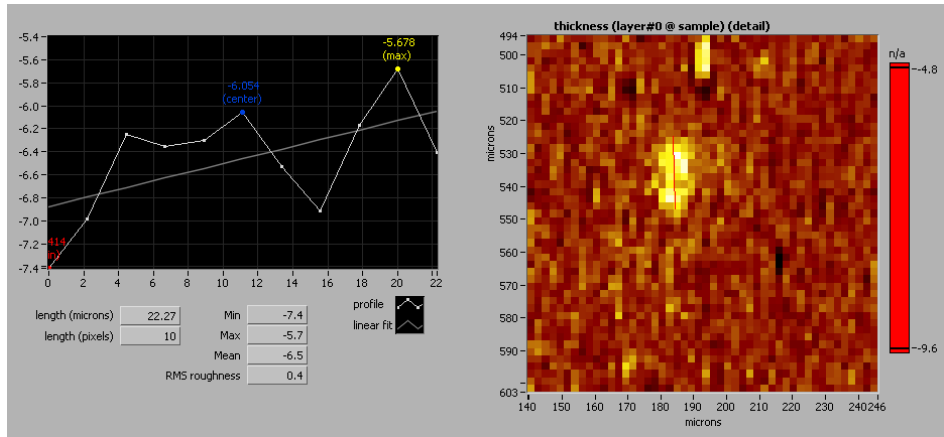
CO₂⁻(MHA)-SAM



N(CH₃)₃⁺-SAM



OH-SAM.



References

Abbott, A., Abel, P.D., Arnold, D.W. and Milne, A. 2000. Cost-benefit analysis of the use of TBT: the case for a treatment approach. *Science of the Total Environment* 258: 5-19.

Adamson, A.W. 1990. *Physical chemistry of surfaces*. New York: John Wiley & Sons. Chapter III, p. 53–105.

Ahmed, N., Murosaki, T., Kakugo, A., Kurokawa, T., Gong, J.P. and Nogata Y. 2011. Long-term in situ observation of barnacle growth on soft substrates with different elasticity and wettability. *Soft Matter* 7: 7281-7290.

Al-Juhni, A.A. and Newby, B.Z. 2006. Incorporation of benzoic acid and sodium benzoate into silicone coatings and subsequent leaching of the compound from the incorporated coatings. *Progress in Organic Coatings* 56: 135-145.

Aldred, N. and Clare, A.S. 2008. The adhesive strategies of cyprids and development of barnacle-resistant marine coatings. *Biofouling* 24: 351-363.

Aldred, N. and Clare, A.S. 2009. Mechanisms and principles underlying temporary adhesion, surface exploration and settlement site selection by barnacle cyprids: a short review. In: Gorb SN, editor. *Functional surfaces in biology*. Vol. 2. Adhesion related phenomena. Heidelberg (Germany): Springer-Verlag. p. 43-65.

Aldred, N., Ekblad, T., Andersson, O., Liedberg, B., Clare, A.S. 2011. Real-time quantification of micro-scale bioadhesion events in situ using imaging surface Plasmon resonance (iSPR). *ACS Applied Materials & Interfaces* 3: 2085-2091.

Aldred, N., Gohad, N.V., Petrone, L., Orihuela, B., Liedberg, B., Ederth, T., Mount, A., Rittschof, D. and Clare, A.S. 2013a. Confocal microscopy-based goniometry of barnacle cyprid permanent adhesive. *Journal of the Experimental Biology* 216: 1969-1972.

Aldred, N., Høeg, J.T., Maruzzo, D. and Clare, A.S. 2013b. Analysis of the behaviours mediating barnacle cyprid reversible adhesion. *Plos One* 8(7) DOI: 10.1371/journal.pone.0068085.

Aldred, N., Ista, L.K., Callow, M.E., Callow, J.A., Lopez, G.P. and Clare, A.S. 2006. Mussel (*Mytilus edulis*) byssus deposition in response to variations in surface wettability. *Journal of the Royal Society Interface* 3: 37-43.

Aldred, N., Li, G.Z., Gao, Y., Clare, A.S. and Jiang, S.Y. 2010a. Modulation of barnacle (*Balanus amphitrite* Darwin) cyprid settlement behavior by sulfobetaine and carboxybetaine methacrylate polymer coatings. *Biofouling* 26: 673-683.

Aldred, N., Phang, I.Y., Conlan, S.L., Clare, A.S. and Vancso, G.J. 2008. The effects of a serine protease, Alcalase1, on the adhesives of barnacle cyprids (*Balanus amphitrite*). *Biofouling* 24: 97-107.

Aldred, N., Scardino, A., de Nys, R. and Clare, A.S. 2010b. Attachment strength is a key factor in the selection of surfaces by barnacle cyprids (*Balanus amphitrite*) during settlement. *Biofouling* 26: 287-299.

Aldred, N., Scardino, A., Cavaco, A., de Nis, R. and Clare, A.S. 2010b. Attachment strength is a key factor in the selection of surfaces by barnacle cyprids (*Balanus amphitrite*) during settlement. *Biofouling* 26: 287-299.

Allinger, N.L., Cava, M.P., de Jongh, D.C., Johnson, C.P., Lebel, N.A. and Stevens, C.L. 1980. *Organic chemistry*. New York: Worth Publishers Inc. 260 pp.

Anderson D.T. 1994. *Barnacles: structure, function, development and evolution*. Chapman & Hall; London: Epizootic adaptations; pp. 292-306.

Anderson, C., Atlar M., Callow, M., Candries, M., Milne, A. and Townsin, R.L. 2003. The development of foul-release coatings for seagoing vessels. *Journal of Marine Design and Operations* B(4) 11-23.

Andersson, M., Berntsson, K., Jonsson, P. and Gatenholm, P. 1999. Microtextured surfaces: towards macrofouling resistant coatings. *Biofouling* 14: 167-178.

Andersson, O., Ekblad, T., Aldred, N., Clare, A.S. and Liedberg, B. 2009. Novel application of imaging surface plasmon resonance for in situ studies of the surface exploration of marine organisms. *Biointerphases* 4: 65-68.

ASTM D5618. 1994. Standard test method for measurement of barnacle adhesion strength in shear. American Standard for Testing and Materials. *Paint-Tests for formulated products and applied coatings* 06.01.

ASTM D1141-98. 2003. Standard practice for the preparation of substitute ocean water. West Conshohocken (PA): ASTM International.

Arwin, H. 1998. Spectroscopic ellipsometry and biology: recent developments and challenges. *Thin Solid Films* 313-314, 764-774.

Avelin Mary, S.R., Vitalina Mary, S.R., Rittschof, D. and Nagabhushanam, R. 1993. Bacterial barnacle interaction: Potential of using juncellins and antibiotics to alter structure of bacterial communities. *Journal of Chemical Ecology* 19: 2155-2167.

Azzam, R.M.A. and Bashara, N.M. 1977. *Ellipsometry and polarized light*. North-Holland, Amsterdam.

Backa, A. and Loeb, G. 1984. Ease of removal of barnacles from various polymeric materials. *Biotechnology and Bioengineering* 26 (10): 1245-1251.

Bain, C.D., Troughton, E.B., Tao, Y.T., Evall, J., Whitesides, G.M. and Nuzzo, R.G. 1988a. Formation of monolayer films by the spontaneous assembly of organic thiols from solution onto gold. *Journal of the American Chemical Society* 111: 321-335.

Bain, C.D. and Whitesides, G.M. 1988. Molecular-level control over surface order in self-assembled monolayer films of thiols on gold. *Science* 240: 62-63.

Bain, C.D. and Whitesides, G.M. 1989. Modelling organic surfaces with self-assembled monolayers. *Angewandte Chemie International Edition English* 28: 506-516.

Baier, R.E. and DePalma, V.A. 1971. The relation of the internal surface of grafts to thrombosis. In: Dale WA, editor. *Management of occlusive arterial disease*. Chicago (IL): Yearbook Medical Publishers. p. 147-163.

Baier, R.E. 1972. Influence of the initial surface condition of material on bioadhesion. P. 633-63 in *Proceeding Third International Congress on Marine Corrosion and Fouling*. National Bureau of Standards, Gaithersburg, Maryland.

Baier, R.E. and Meyer, A.E. 1992. Surface analysis of fouling resistant marine coatings. *Biofouling* 6: 165-180. Barlow, D.E. and Wahl, K.J. 2012. Optical spectroscopy of marine bioadhesives interfaces. *Annual Review of Analytical Chemistry* 5:2 29-251.

Barlow, D.E., Dickinson, G.H., Orihuela, B., Kulp, J.L., III, Rittschof, D. and Wahl, K.J. 2010. Characterization of the adhesive plaque of the barnacle *Balanus amphitrite*: Amyloid-like nanofibrils are a major component. *Langmuir*. 26: 6549-6556.

Barlow, D.E. and Wahl, K.J. 2012. Optical spectroscopy of marine bioadhesives interfaces. *Annual Review of Analytical Chemistry* 5: 229-51.

Barnes, H. 1970. A review of some factors affecting settlement and adhesion of some common barnacles. In: Manly RS, editor. *Adhesion in biological systems*. New York, London: Academic Press. p. 89-111.

Barnes, J., Goodwyn, P., Nokhbatolfoghahai, M. and Gorb, S. 2011. Elastic modulus of tree frog adhesive toe pads. *Journal of Comparative Physiology A* 197: 969-978.

Barnes, H. and Powell, H. 1950. The development, general morphology, and subsequent elimination of barnacle populations after heavy initial settlement. *Journal of Animal Ecology* 19: 175-179.

Barry, A.J. 1946. Viscometric investigation of dimethylsiloxane polymers. *Journal of Applied Physics* 17: 1020-1024.

Baty, A.M., Leavitt, P.K., Siedlecki, C.A., Tyler, B.J., Suci, P.A., Marchant, R.E. and Geesey, G.G. 1997. Adsorption of adhesive proteins from the marine mussel, *Mytilus edulis*, on polymer films in the hydrated state using angle dependent X-ray photoelectron spectroscopy and atomic force microscopy. *Langmuir* 13: 5702-5710.

Bayne, B.L. 1969. The gregarious behavior of the larvae of *Ostrea edulis* L. at settlement. *Journal of the Marine Biological Association of the United Kingdom*. 49:327-356.

Becker, K., Siriratanachai, S. and Hormchong, T. 1997. Influence initial substratum surface tension on marine micro- and macro-fouling in the Gulf of Thailand. *Helgoland Marine Research* 51: 445-461.

Behrens, S.H. and Greyer, D.G. 2001. The charge of glass and silica surfaces. *Journal of Chemical Physics* 115: 6716-6721.

Beigbeder, A., Degee, P., Conlan, S.L., Mutton, R., Clare, A.S., Pettitt, M.E., Callow, M.E., Callow, J.A. and Dubois, P. 2008. Preparation and characterization of silicone-based coatings filled with carbon nanotubes and natural sepiolite and their application as marine fouling-release coatings. *Biofouling* 24: 291-302.

Bennett, S.M., Finlay, J.A., Gunari, N., Wells, D.D., Meyer, A.E., Walker, G.C., Callow, M.E., Callow, J.A., Bright, F.V. and Detty, M.R. 2010. The role of surface energy and water wettability in aminoalkyl/fluorocarbon/hydrocarbonmodified xerogel surfaces in the control of marine biofouling. *Biofouling* 26: 235-246.

Berglin, M. and Gatenholm, P. 1999. The nature of bioadhesive bonding between barnacles and fouling-release silicone coatings. *Journal of Adhesion Science and Technology* 13: 713-727.

Berglin, M. and Gatenholm, P. 2003. The barnacle adhesive plaque: morphological and chemical differences as a response to substrate properties. *Colloids and Surfaces B: Biointerfaces* 28: 107-117.

Berglin, M., Hedlund, J., Fant, C. and Elwing, H. 2005. Use of surface-sensitive methods for the study of adsorption and cross-linking of marine bioadhesives. *The Journal of Adhesion* 81: 805-822.

Berglin, M., Larsson, A., Jonsson, P.R. and Gatenholm, P. 2001. The adhesion of the barnacle, *Balanus improvisus*, to poly(dimethylsiloxane) fouling-release coatings and poly(methyl methacrylate) panels: The effect of barnacle size on strength and failure mode. *Journal of Adhesion Science and Technology* 15: 1485-1502.

Berglin, M., Pinori, E., Sellborn, A., Andersson, M., Hulander, M. and Elwing, H. 2009. Fibrinogen adsorption and conformational change on model polymers: novel aspects of mutual molecular rearrangement. *Langmuir*. 25(10): 5602-5608.

Berntsson, K.M., Andreasson, H., Jonsson, P.R., Larsson, L., Ring, K., Petronis, S. and Gatenholm, P. 2000a. Reduction of barnacle recruitment on micro-textured surfaces: Analysis of effective topographic characteristics and evaluation of skin friction. *Biofouling* 16: 245-261.

Berntsson, K.M. and Jonsson, P.R. 2003. Temporal and spatial patterns in recruitment and succession of a temperate marine fouling assemblage: A comparison of static panels and boat hulls during the boating season. *Biofouling* 19: 187-195.

Berntsson, K.M., Jonsson, P.R., Larsson, A.I. and Holdt, S. 2004. Rejection of unsuitable substrata as a potential driver of aggregated settlement in the barnacle *Balanus improvisus*. *Marine Ecology Progress Series*. 275: 199-210.

Berntsson, K.M., Jonsson, P.R., Lejhall, M. and Gatenholm, P. 2000b. Analysis of behavioural rejection of micro-textured surfaces and implications for recruitment by the barnacle *Balanus improvisus*. *Journal of the Experimental Marine Biology and Ecology* 251: 59-83.

Bielecki, J., Chan, B.K.K., Hoeg, J.T. and Sari, A. 2009. Antennular sensory organs in cyprids of balanomorphan cirripedes: standardizing terminology using *Megabalanus rosa*. *Biofouling* 25: 203-214.

Blomsterberg, M., Høeg, J.T., Jeffries, W.B., and Lagerström, N.C., 2004. Antennular sensory organs in cyprids of *Octolasmis angulata* and three species of *Lepas* (Crustacea: Thecostraca: Cirripedia: Thoracica): a scanning electron microscopy study. *Journal of Morphology* 200: 141-153.

Brady, R.F. 1999. Properties which influence marine fouling resistance in polymers containing silicon and fluorine. *Progress in Organic Coatings* 35: 31-35.

Brady, R.F. 2000. No more tin: what now for fouling control? *Journal of Protective Coatings & Linings* 17: 42-48.

Brady, R.F. 2001. A fracture mechanical analysis of fouling release from nontoxic antifouling coatings. *Progress in Organic Coatings*, 43(1-3):188-192.

Brady, R.F. and Singer, I.L. 2000. Mechanical factors favoring release from fouling release coatings. *Biofouling* 15: 73-81.

Bressy, C., Hellio, C., Marechal, J.P., Tanguy, B. and Margaillan, A. 2010. Bioassays and field immersion tests: a comparison of the antifouling activity of copper-free poly(methacrylic)-based coatings containing tertiary amines and ammonium salt groups. *Biofouling* 26: 769-777.

Bressy, C., Margaillan, A., Fay, F., Linossier, I. and Réhel, K. 2009. Tin-free self-polishing marine antifouling coatings. In: Hellio, C., Yebra, D.M., editors. *Advances in marine antifouling coatings and technologies*. Cambridge, UK: Woodhead Publishing. p. 445-491.

Brooks, R.R. 1991. Process for inhibiting fouling of an underwater surface. US5017322.

Brown, A.E.X., Litvinov, R.I., Discher, D.E. and Weisel, J.W. 2007. Forced Unfolding of Coiled-Coils in Fibrinogen by Single-Molecule AFM. *Biophysical Journal*. 92(5): L39-L41.

Burden, D.K., Barlow, D.E., Spillmann, C.M., Orihuela, B., Rittschof, D., Everett, R.K. and Wahl, K.J. 2012. Barnacle *Balanus amphitrite* adheres by a stepwise cementing process. *Langmuir*. 28:13364-13372.

Buskens, P., Wouters, M., Rentrop, C. and Vroon, Z. 2013. A brief review of environmentally benign antifouling and foul-release coatings for marine applications. *Journal of Coatings Technology and Research* 10: 29-36.

Brubaker, C.E., Kissler, H., Wang, L.J., Kaufman, D.B. and Messersmith, P.B. 2010. Biological performance of mussel-inspired adhesive in extrahepatic islet transplantation. *Biomaterials* 31: 420-7.

Brubaker, C.E. and Messersmith, P.B. 2012. The present and future of biologically inspired adhesive interfaces and materials. *Langmuir* 28: 2200-5.

Callow, M. 1990. Ship fouling: problems and solutions. *Chemistry and Industry (London)* 1990 No. 5 pp. 123-127.

Callow, J.A. and Callow, M.E. 2006. The *Ulva* Spore Adhesive System. In: Biological adhesive, eds. Smith, A.M. and Callow, J.A. Springer-Verlag, Berlin and Heidelberg, Germany, pp 63-78.

Callow, J.A. and Callow, M.E. 2011. Trends in the development of environmentally friendly fouling-resistant marine coatings. *Nature Communication* 2: 244, 1-10.

Callow, M.E., Callow, J.A., Ista, L.K., Coleman, S.E., Nolasco, A.C. and Lopez, G.P. 2000. The use of self-assembled monolayers of different wettabilities to study surface selection and primary adhesion processes of green algal (*Enteromorpha*) zoospores. *Applied and Environmental Microbiology* 66: 3249-3254.

Callow, J.A., Callow, M.E., Ista, L.K., Lopez, G. and Chaudhury, M.K. 2005. The influence of surface energy on the wetting behaviour of the spore adhesive of the marine alga *Ulva linza* (synonym *Enteromorpha linza*). *Journal of the Royal Society Interface* 2: 319-325.

Callow, J.A., Crawford, S.A., Higgins, M.J., Mulvaney, P. and Wetherbee, R. 2000b. The application of atomic force microscopy to topographical studies and force measurements on the secreted adhesive of the green alga *Enteromorpha*. *Planta* 211, 641-647.

Callow, M.E., and Fletcher, R.L. 1994. The influence of low surface-energy materials on bioadhesion - a review. *International Biodeterioration & Biodegradation* 34: 333-348.

Candries, M. and Atlar, M. 2003. On the drag and roughness characteristics of antifoulings. *International Journal of Maritime Engineering*. 145(A2). p.36-60.

Carrè, A., Lacarrière, V. and Birch, W. 2003. Molecular interactions between DNA and an aminated glass substrate. *Journal of Colloid and Interface Science* 260: 49-55.

Carrion-Vazquez, M., Oberhauser, A.F., Fisher, T.E., Marszalek, P.E., Li, H.B. and Fernandez, J.M. 2000. Mechanical design of proteins studied by single-molecule force spectroscopy and protein engineering. *Progress in Biophysics and Molecular Biology* 74: 63-91.j

Cerne, L., Simoncic, B. and Zeljko, M. 2008. The influence of repellent coatings on surface free energy of glass plate and cotton fabric. *Applied Surface Science* 254: 6467-6477.

Chambers, L.D., Stokes, K.R., Walsh, F.C. and Wood, R.J.K. 2006. Modern approaches to marine antifouling coatings. *Surface and Coatings Technology*. 201: 3642-3652.

Chan, Y.H.M., Schweiss, R., Werner, C. and Grunze, M. 2003. Electrokinetic characterization of oligo- and poly(ethyleneglycol)-terminated self-assembled monolayers on gold and glass surfaces. *Langmuir* 19: 7380-7385.

Chaudhury, M.K., Finlay, J.A., Chung, J.Y., Callow, M.E. and Callow, J.A. 2005. The influence of elastic modulus and thickness on the release of the soft-fouling green alga *Ulva linza* (syn. *Enteromorpha linza*) from poly(dimethylsiloxane) (PDMS) model networks. *Biofouling* 21(1): 41-48.

Choresch, O., Bayarmagnai, B. and Lewis, R.V. 2009. Spider web glue: two proteins expressed from opposite strands of the same DNA sequence. *Biomacromolecules* 10: 2852–2856.

Christie, A.O. and Dalley, R. 1987. Barnacle fouling and its prevention. In: Southward, A.J., editor. *Crustacean issues: barnacle biology*. Rotterdam (the Netherlands): AABalkema. p. 419-433.

Chung, J.Y. and Chaudhury, M.K. 2005. Soft and hard adhesion. *The Journal of Adhesion* 81: 1119-1145.

Clare, A.S. 1995 Chemical signals in barnacles: old problems, new approaches. In: Schram FR, Høeg JT (eds) *New frontiers in barnacle evolution*. A.A. Balkema, Rotterdam, pp 49-67.

Clare, A.S. 1998. Towards nontoxic antifouling. *Journal of Marine Biotechnology* 6: 3-6.

Clare, A.S. 2011. Toward a characterization of the chemical cue to barnacle gregariousness. In: Breithaupt, T., Thiel, M. editors. *Chemical communication in crustaceans*. New York: Springer. 431-450.

Clare, A.S. and Aldred, N. 2009. Surface colonisation by marine organisms and its impact on antifouling research. In: Hellio, C. and Yebra, D., editors. *Advances in marine antifouling coatings and technologies*. Oxford (UK): Woodhead Publishing. p. 46-79.

Clare, A.S., Freet, R.K. and McClary, M. 1994. On the antennular secretion of the cyprid of *balanus amphitrite amphitrite*, and its role as a settlement pheromone. *Marine Biological Association of the UK* 74: 243-250.

Clare, A.S. and Høeg, J.T. 2008. *Balanus amphitrite* or *Amphibalanus amphitrite*? A note on barnacle nomenclature. *Biofouling* 24: 55-57.

Clare, A.S. and Matsumura, K. 2000. Nature and Perception of Barnacle Settlement Pheromones. *Biofouling* 15: 57-71.

Clare, A.S. and Nott, J.A. 1994. Scanning-electron-microscopy of the 4th antennular segment of *Balanus amphitrite*. *Journal of the Marine Biological Association of the United Kingdom* 74: 967-970.

Clare, A.S., Rittschof, D., Gerhart, D.J. and Maki, I. 1992. Effects of the nonsteroidal ecdysone mimic RH 5849 on larval crustaceans. *Journal of Experimental Zoology* 262: 436-440.

Clare, A.S., Thomas, R.F. and Rittschof, D. 1995. Evidence for the involvement of cyclic AMP in the pheromonal modulation of barnacle settlement. *Journal of Experimental Biology* 198: 655-664.

Conlan, S.L., Mutton, R.J., Aldred, N. and Clare, A.S. 2008. Evaluation of a fully automated method to measure the critical removal stress of adult barnacles. *Biofouling* 24: 471-481.

Crisp, D.J., 1960. Factors influencing growth-rate in *Balanus balanoides*. *Journal of Animal Ecology* 29: 95-116.

Crisp, D.J. 1967. Chemical factors inducing settlement in *Crassostrea virginica* (Gmelin). *Journal of Animal Ecology*. 36(2): 329-335.

Crisp, D.J. 1974. Factors influencing the settlement of marine invertebrate larvae. In: P. T. Grant and A. M. Mackie (eds) *Chemoreception in marine organisms*. Academic Press, New York, pp. 177-265.

Crisp, D.J. 1976. Settlement responses in marine organisms. In: Newell RC editor. *Adaptations to the Environment*. London: Butterworth. 83-124.

Crisp, D.J. 1984. Overview of research on marine invertebrate larvae 1940–1980. In: Costlow JD, Tipper RC, editors. *Marine biodeterioration: an interdisciplinary study*. Annapolis (MD): Naval Institute Press. p. 103-126.

Crisp, D.J. and Barnes, H. 1954. The orientation and distribution of barnacles at settlement with particular reference to surface contour. *Journal of Animal Ecology* 23: 142-162.

Crisp, D.J. and Meadows, P.S. 1962. The chemical basis of gregariousness in cirripedes. *Proceedings of the Royal Society B* 156: 500-520.

Crisp, D.J. and Meadows, P.S. 1963. Adsorbed layers: the stimulus to settlement in barnacles. *Proceedings of the Royal Society B* 158: 364-387.

Crisp, D.J., Walker, G., Young, G.A., Yule, A. 1985. Adhesion and substrate choice in mussels and barnacles. *Journal of Colloid and Interface Science* 104: 40-50.

Dahlström, M., Jonsson, H., Jonsson, P.R. and Elwing, H. 2004. Surface wettability as a determinant in the settlement of the barnacle *Balanus Improvisus* (Darwin). *Journal of the Experimental Marine Biology and Ecology* 305: 223-232

Dahlström, M., Martensson, L.G.E., Jonsson, P.R., Arnebrant, T. and Elwing H. 2000. Surface active adrenoceptor compounds prevent the settlement of cyprid larvae of *Balanus improvisus*. *Biofouling* 16: 191-203.

Dann, J.R. 1965. Forces involved in the adhesive process. 1. Critical surface tensions of polymeric solids as determined with polar liquids. *Journal of Colloid and Interface Science* 32: 302-320.

Darwin, C.R. 1854. A monograph on the sub-class Cirripedia, with figures of all the species. The Balanidæ, (or sessile cirripedes); the verucidae, etc., vol. 2. London, UK: The Ray Society.

Debe M.K. 1987. Optical probes of organic thin films: photon-in and photon-out. *Progress in Surface Science* 24, 1.

del Campo, A., Schwotzer, W., Gorb, S.N., Alderd, N., Santos, R. and Flammang, P. Preface in Santos, R., Aldred, N., Gorb, S. and Flammang P. 2013. Biological and biomimetic adhesive challenges and opportunities. RSC Publishing, Croydon UK.

Dexter, S.C. 1979. Influence of substratum critical surface tension on bacterial adhesion in situ studies. *Journal of Colloid and Interface Science* 70: 346-354.

Dexter, S.C., Sullivan, J.D., Iii, J.W. and Watson, S.W. 1975. Influence of substrate wettability on the attachment of marine bacteria to various surfaces. *Journal of Applied Microbiology* 30: 298-308.

Dicke, C. and Hähner, G. 2002. pH-dependent force spectroscopy of tri(ethylene glycol)- and methyl-terminated selfassembled monolayers adsorbed on gold *Journal of the American Chemical Society* 124: 12619-12625.

Dickinson, G.H., Vega, I.E., Wahl, K.J., Orihuela, B., Beyley, V., Rodriguez, E.N., Everett, R.K., Bonaventura, J. and Rittschof, D 2009. Barnacle cement: a

polymerization model based on evolutionary concepts. *Journal of the Experimental Biology* 212: 3499-510.

Di Fino, A., Petrone, L., Aldred, N., Ederth, T., Liedberg, B. and Clare, A.S. 2013. Correlation between surface chemistry and settlement behaviour in barnacle cyprids (*Balanus improvisus*). *Biofouling* 30: 143-152.

Directive 98/8/EC and its new replacement:

http://ec.europa.eu/environment/chemicals/biocides/regulation/regulation_en.htm

Dobretsov, S., Abed, R.M.M. and Teplitski, M. 2013 Mini-review: Inhibition of biofouling by marine microorganisms. *Biofouling* 29: 423-441.

Dobretsov, S. and Thomason, J.C. 2011. The development of marine biofilms on two commercial non-biocidal coatings: a comparison between silicone and fluoropolymer technologies. *Biofouling* 27: 869–880.

Dreanno, C., Kirby, R.R. and Clare, A.S. 2006a. Locating the barnacle settlement pheromone: spatial and ontogenetic expression of the settlement-inducing protein complex of *Balanus amphitrite*. *Proceeding of the Royal Society B* 273: 2721-2728.

Dreanno, C., Kirby, R.R. and Clare, A.S. 2006b. Smelly feet are not always a bad thing: the relationship between cyprid footprint protein and the barnacle settlement pheromone (SIPC). *Biology Letters* 2: 423-425.

Dubois, L.H. and Nuzzo, R.G. 1992. Synthesis, structure, and properties of model organic surfaces. *Annual Review of Physical Chemistry* 43: 437-473.

Ducret, A., Valignat, M.P., Mouhamar, F., Mignot, T. and Theodoly, O. 2012. Wet-surface-enhanced ellipsometric contrast microscopy identifies slime as a major adhesion factor during bacterial surface motility. *Proceedings of the National Academy of Sciences of the United States of America*. 109(25): 10036-41.

Ederth, T., Claesson, P. and Liedberg, B. 1998. Self-assembled monolayers of alkanethiolates on thin gold films as substrates for surface force measurements. Long-range hydrophobic interactions and electrostatic double-layer interactions. *Langmuir* 14: 4782-4789.

Ederth, T., Ekblad, T., Pettitt, M.E., Conlan, S.L., Du, C.X., Callow, M.E., Callow, J.A., Mutton, R., Clare, A.S., D'Souza F, Donnelly, G., Bruin, A., Willemsen, P.R., Su, X.J.S., Wang, S., Zhao, Q., Hederos. M., Konradsson. P. And Liedberg, B. 2011. Resistance of galactoside-terminated alkanethiol self-assembled monolayers to marine fouling organisms. *ACS Applied Materials & Interfaces* 3: 3890-3901.

Ekblad, T., Bergström, G., Ederth, T., Conlan, S.L., Mutton, R., Clare, A.S., Wang, S., Liu, Y., Zhao, Q., D'Souza, F., Donnelly, G.T., Willemsen, P.R., Pettitt, M.E., Callow, M.E., Callow, J.A. and Liedberg, B. 2008. Poly(ethylene glycol)-containing hydrogel surfaces for antifouling applications in marine and freshwater environments. *Biomacromolecules* 9: 2775-2783.

Elbourne, P.D. and Clare, A.S. 2010. Ecological relevance of a conspecific, waterborne settlement cue in *Balanus amphitrite* (Cirripedia). *Journal of Experimental Marine Biology and Ecology* 392: 99-106.

Elbourne, P.D., Veater, R.A. and Clare, A.S. 2008. Interaction of conspecific cues in *Balanus amphitrite* Darwin (Cirripedia) settlement assays: continued argument for the singlelarva assay. *Biofouling* 24: 87-96.

Estarlich, F., Eaton, P., Fletcher, B., Lewey, S., Nevell, T., Smith, J. and Tsibouklis, J. 2011. The effects of incorporated silicone oils and calcium carbonate on the resistance to settlement and the antifouling performance of a silicone elastomer. *Journal of Adhesion Science and Technology* 25(17): 2183-2198.

Faimali, M., Garaventa, F., Terlizzi, A., Chiantore, M. and Cattaneo-Vietti, R. 2004. The interplay of substrate nature and biofilm formation in regulating *Balanus amphitrite* Darwin, 1854 larval settlement. *Journal of Experimental Marine Biology and Ecology* 306: 37-50.

Finlay, J.A., Bennett, S.M., Brewer, L.H., Sokolova, A., Clay, G., Gunari, N., Meyer, A.E., Walker, G.C., Wendt, D.E., Callow M.E., Callow, J.A. and Detty, M.R. 2010. Barnacle settlement and the adhesion of protein and diatom microfouling to xerogel films with varying surface energy and water wettability. *Biofouling* 26: 657-666.

Finlay, J.A., Callow, M.E., Ista, L.K., Lopez, G.P. and Callow, J.A. 2002. The influence of surface wettability on the adhesion strength of settled spores of the green alga *Enteromorpha* and the diatom *Amphora*. *Integrative and Comparative Biology* 42: 1116-1122.

Finlay J.A., Schultz, M.P., Cone, G., Callow, M.E. and Callow, J.A. 2013. A novel biofilm channel for evaluating the adhesion of diatoms to non-biocidal coatings. *Biofouling* 29: 401-411.

Fisher, T.E., Oberhauser, A.F., Carrion-Vazquez, M., Marszalek, P.E. and Fernandez, J.M. 1999. The study of protein mechanics with the atomic force microscope. *Trends in Biochemical Sciences* 24(10): 379-384.

Flammang, P. and Walker, G. 1997. Measurement of the adhesion of the podia in the Asteroid *Asterias rubens* (Echinodermata). Journal of the Marine Biological Association U. K. 77: 1251-1254.

Fyhn, U.E. and Costlow, J.D. 1976. A histological study of cement secretion during the intermolt cycle in barnacles. The Biological Bulletin 150(1): 47-56.

Flynn, N.T., Tran, T.N.T., Cima, M.J. and Langer, R. 2003. Long-term stability of self-assembled monolayers in biological media. Langmuir 19: 10909-10915.

Fraenkel, G., Rudall, K.M. 1947. The structure of insect cuticles. Proceedings of the Royal Society B 134: 111-144.

Gabbott, P.A.; Larman, V.N. 1987. The chemical basis of gregariousness in cirripedes: a review (1953-1984), in: Southward, A.J. 1987. Barnacle biology. Crustacean Issues, 5: pp. 377-388.

Garaventa, F., Centanni, E., Pellizzato, F., Faimali, M., Terlizzi, A. and Pavoni, B. 2007. Imposex and accumulation of organotin compounds in populations of *Hexaplex trunculus* (Gastropoda, Muricidae) from the Lagoon of Venice (Italy) and Istrian Coast (Croatia). Marine Pollution Bulletin 54: 615-622.

Gee, J.M., 1965. Chemical stimulation of settlement in larvae of *Spirorbis rupestris* (Serpulidae). Animal Behaviour 13: 181-186.

Gerhart, D.J., Rittschof, D., Hooper, I.R., Eisenman, K., Meyer, A.E., Baier, R.E. and Young, C. 1992. Rapid and inexpensive quantification of the combined polar components of surface wettability: application to biofouling. Biofouling 5: 251-259.

Giannotti, M.I. and Vansco, G.J. 2007. Interrogation of single synthetic polymer chains and polysaccharides by afm-based force spectroscopy. ChemPhysChem 8: 2290-2307.

Gibbs, J.W. 1928. The collected works. Thermodynamics Vol. 1. New York City: Longmans, Green and Co. p. 33.

Gibson, P. and Nott, J.A. 1971. Concerning the fourth antennular segment of the cypris larva of *Balanus balanoides*. In: Crisp, D.J., ed. Fourth European marine biology Symposium. Cambridge University Press, 227-236

Glenner, H. and Høeg, J.T. 1995. Scanning electron microscopy of cyprid larvae in *Balanus amphitrite* (Crustacea: Cirripedia: Thoracica: Balanomorpha). Journal of Crustacean Biology 15(3): 523-536.

- Goldberg, E.D. 1986. TBT: an environmental dilemma. *Environment* 28: 17-44.
- Good, R.J. 1993. Contact angle, wetting and adhesion: a critical review. In: Mittal KL, editor. *Contact angle, wettability and adhesion*. Utrecht (the Netherlands): VSP. p. 3–36.
- Gorb, S. 2008. Biological attachment devices: exploring nature's diversity for biomimetics. *Philosophical Transactions of the Royal Society A* 366: 1557-1574.
- Gray, J.S. 1966. The attractive factor of intertidal sands to *Protodrilus symbioticus*. *Journal of the Marine Biological Association of the United Kingdom* 46: 627-645.
- Gray, J.S. 1967a. Substrate selection by the archianellid *Protodrilus hypoleucus* Armenante. *Journal of Experimental Marine Biology and Ecology* 1: 47-54.
- Gray, J.S. 1967b. Substrate selection by the archianellid *Protodrilus rubropharyngeus* Jagersten. *Helgolander wissenschaftliche Meeresuntersuchungen*, 15: 253-269.
- Gray, N.L., Banta, W.C. and Loeb, G.I. 2002. Aquatic biofouling larvae respond to differences in the mechanical properties of the surfaces on which they settle. *Biofouling* 18: 269-273.
- Greco, G., Lanero, T.S., Torrassa, S., Young, R., Vassalli, M., Cavaliere, A., Rolandi, R., Pelucchi, E., Faimali, M. and Davenport, J. 2013. Microtopography of the eye surface of the crab *Carcinus maenas*: an atomic force microscope study suggesting a possible antifouling potential. *Journal of the Royal Society Interface* 10:20130122.
- Griffith, A.A. 1920. *The Phenomena of Rupture and Flow in Solids*. *Philosophical Transactions of the Royal Society of London* 221A: 163-198.
- Grigson, C.W.B. 1992. Drag losses of new ships caused by hull finish. *Journal of Ship Research* 36:182-196.
- Grunlan, M.A., Lee, N.S., Mansfeld, F., Kus, E., Finlay, J.A., Callow, J.A., Callow, M.E. and Weber, W.P.J. 2006. Minimally adhesive polymer surfaces (maps) prepared from star oligosiloxanes and star oligofluorosiloxanes. *Journal of Polymer Science Part A*: 44: 2551-2566.
- Gunari, N., Brewer, L.H., Bennett, S.M., Sokolova, A., Kraut, N.D., Finlay, J.A., Meyer, A.E., Walker, G.C., Wendt, D.E., Callow, M.E., Callow, J.A., Bright, F.V. and
- Hadfield, M. 2011. Biofilms and marine invertebrate larvae: what bacteria produce that larvae use to choose settlement sites. *Annual Review of Marine Science* 3: 453-470.

- Hanein, D., Geiger, B. and Addai, L. 1993. Fibronectin adsorption to surfaces of hydrated crystals. An analysis of the importance of bound water in protein–substrate interactions. *Langmuir* 9: 1058-65.
- Hallberg, E., Johansson, K.U.I. and Elofsson, R. 1992. The aesthetasc concept: structural variations of putative olfactory receptor cell complexes in Crustacea. *Microscopy Research and Technique* 22: 325-35.
- He, L-S., Zhang, G. and Qian, P-Y. 2013. Characterization of two 20kda-cement protein (cp20k) homologues in *Amphibalanus amphitrite*. *PLOSE ONE* 8(5) doi:10.1371/journal.pone.0064130.g001
- Head, R.M. Berntsson, K.M. Dahlstrom, M. Overbeke, K. and Thomason, J.C. 2004. Gregarious settlement in cypris larvae: The effects of cyprid age and assay duration. *Biofouling*. 20: 123-128.
- Higgins, M.J., Molino, P., Mulvaney, P. and Wetherbee, R. 2003. The structure and nanomechanical properties of the adhesive mucilage that mediates diatom-substratum adhesion and motility *Journal of Phycology*. 39: 1181-1193.
- Hinterdorfer, P., Baumgartner, W., Gruber, H. J., Schilcher, K., Schindler, H. 1996. Detection and localization of individual antibody-antigen recognition events by atomic force microscopy. *Proceedings of the National Academy of Sciences of the United States of America* 93: 3477-3481.
- Hoipkemeier-Wilson, L., Schumacher, J.F., Carman, M.L., Gibson, A.L., Feinberg, A.W., Callow, M.E., Finlay, J.A., Callow, J.A. and Brennan, A.B. 2004. Antifouling potential of lubricious, micro-engineered, PDMS elastomers against zoospores of the green fouling alga *Ulva* (Enteromorpha). *Biofouling* 20: 53-63.
- Holm, E.R. 2010. Barnacles and biofouling. *Integrative and Comparative Biology* 52: 348–355
- Holm, E.R. 2012. Barnacles and biofouling. *Integrative and Comparative Biology* 52: 348-355.
- Holm, E.R., Cannon, G, Roberts D., Schmidt, A.R., Sutherland, J.P. and Rittschof, D. 1997. The influence of initial surface chemistry on development of the fouling community at Beaufort, North Carolina. *Journal of the Experimental Marine Biology and Ecology* 215: 189-203.

Holm, E.R., Orihuela, B., Kavanagh, C.J. and Rittschof, D. 2005. Variation among families for characteristics of the adhesive plaque in the barnacle *Balanus amphitrite*. *Biofouling*. 21:121-126.

Höök, F., Kasemo, B., Nylander, T., Fant, C., Sott, K. and Elwing, H. 2001. variations in coupled water, viscoelastic properties, and film thickness of a mefp-1 protein film during adsorption and cross-linking: a quartz crystal microbalance with dissipation monitoring, ellipsometry, and surface plasmon resonance study. *Analytical Chemistry* 73: 5796-5804.

Horber, J.K.H. and Miles, M.J. 2003. Scanning probe evolution in biology. *Science* 302: 1002-1005.

Huggett, M.J., Nedved, B.T. and Hadfield, M.G. 2009. Effects of initial surface wettability on biofilm formation and subsequent settlement of *Hydroides elegans*. *Biofouling* 25: 387-399.

Hui, C.Y., Long, R., Wahl, K.J. and Everett, R.K. 2011. Barnacles resist removal by crack trapping. *Journal of the Royal Society Interface*. 8: 868-879.

Hung, O.S., Thiyagarajan, V. and Qian, P.Y. 2008. Preferential attachment of barnacle larvae to natural multi-species biofilms: does surface wettability matter? *Journal of Experimental Marine Biology and Ecology* 361: 36-41.

Ito, T., and Grygier, M.J. 1990. Description and complete larval development of a new species of *Baccalaureus* (Crustacea: Ascothoracida) parasitic in a Zoanthid from Tanabe Bay, Honshu, Japan. *Zoological Science* 7: 485-515.

Janshoff, A., Neitzert, M., Oberdorfer, Y., and Fuchs, H. 2000. Force spectroscopy of molecular systems-single molecule spectroscopy of polymers and biomolecules. *Angewandte Chemie International Edition*. 39: 3213-3237.

Janovjak, H., Kessler, M., Oesterhelt, D., Gaub, H. and Muller, D.J. 2003. Unfolding pathways of native bacteriorhodopsin depend on temperature. *EMBO Journal* 22: 5220-5229.

Jin, G., Jansson, R. and Arwin, H. 1996. Imaging ellipsometry revisited: Developments for visualization of thin transparent layers on silicon substrates. *Review of Scientific Instruments* 67: 2930-2936.

Johnson, K.L., Kendall, K., and Roberts, A.D. 1971. Surface energy and the contact of elastic solids. *Proceeding of the Royal Society London A* 324: 301-313.

Jonker, J.L., von Byern, J., Flammang, P., Klepal, W. and Power, A.M. 2012. Unusual adhesive production system in the barnacle *Lepas anatifera*: an ultrastructural and histochemical investigation. *Journal of Morphology* 273: 1377-1391.

Jonsson, P.R., Berntsson, K.M. and Larsson, A.I. 2004. Linking larval supply to recruitment: Flow-mediated control of initial adhesion of barnacle larvae. *Ecology* 85: 2850-2859.

Ikai, A., Mitsui, K., Tokuoka, H. and Xu, X.M. 1997 Mechanical measurements of a single protein molecule and human chromosomes by atomic force microscopy. *Materials Science and Engineering. C* 4: 233-240.

Ista, L.K., Callow, M.E., Finlay, J.A., Coleman, S.E., Nolasco, A.E., Simons, R.H., Callow, J.A. and Lopez, G.P. 2004. Effect of substratum surface chemistry and surface energy on attachment of marine bacteria and algal spores. *Applied and Environmental Microbiology* 70: 4151-4157.

Kamino, K. 2001. Novel barnacle underwater adhesive protein is a charged amino acid-rich protein constituted by a Cys-rich repetitive sequence. *Biochemical Journal* 356: 503-507.

Kamino, K. 2006. Barnacle underwater attachment. In: Smith, A.M., Callow, J.A., editors. *Biological adhesives*. Berlin, Heidelberg: Springer-Verlag. p. 145–166.

Kamino, K. 2010. Molecular design of barnacle cement in comparison with those of mussel and tubeworm. *The Journal of Adhesion* 86: 96-110-

Kamino, K. 2012. Diversified molecular design in the biological underwater adhesives. In: Thomopoulos, S., Birman, V., Genin, G.M. editors. *Structural interfaces and attachments in biology*. New York (NY): Springer-Verlag; p. 175–199.

Kamino, K. 2013. Mini-review: Barnacle adhesives and adhesion. *Biofouling* 29: 735-749.

Kamino, K., Inoue, K., Maruyama, T., Takamatsu, N., Harayama, S. and Shizuri, Y. 2000. Barnacle cement proteins: importance of disulfide bonds in their insolubility. *The Journal of Biological Chemistry* 275: 27360-27365.

Kamino, K., Nakano, M. and Kanai, S. 2012. Significance of the conformation of building blocks in curing of barnacle underwater adhesive. *FEBS Journal* 279: 1750-60.

Kamino, K., Odo, S. and Maruyama, T. 1996. Cement proteins of the acorn barnacle, *Megabalanus rosa*. *The Biological Bulletin*. 190: 403-409.

Kamino, K. and Shizuri, Y. 1998. Structure and function of barnacle cement proteins. In: LeGal Y, Halvorson HO, editors. New developments in marine biotechnology. New York: Plenum Press. p. 77-80.

Katsikogianni, M., Amanatides, E., Mataras, D. and Missirlis, Y.F. 2008. *Staphylococcus epidermidis* adhesion to He, He/O₂ plasma treated PET films and aged materials: contributions of surface free energy and shear rate. Colloids and Surfaces B: Biointerfaces 65: 257-268.

Kavanagh, C.J., Quinn, R.D. and Swain, G.E. 2005. Observations of barnacle detachment using high-speed video. Journal of the Adhesion 81: 843-850.

Kempf, G. 1937. On the effect of roughness on the resistance of ships. Trans INA 79: 109-119. Kesel, A.B., Martin, A., and Seidl, T. (2003). Adhesion measurements on the attachment devices of the jumping spider *Evarcha arcuata*. Journal of the Experimental Biology 206: 2733-2738.

Kendall, K. 1971. The adhesion and surface energy of elastic solids. Journal of Physics D: Applied Physics 4: 1186-1195.

Kim, J., Chisholm, B. J. and Bahr, J. 2007. Adhesion study of silicone coatings: the interaction of thickness, modulus and shear rate on adhesion force. Biofouling, 23: 113-120.

Kim, N.S., Shim, W.G., Yim, U.H., Ha, S.Y., An, J.G. and Shin, K.H. 2011. Three decades of TBT contamination in sediments around a large scale shipyard. Journal of Hazardous Materials 192(2): 634-642.

Knight-Jones, E.W., 1953. Laboratory experiments on gregariousness during setting in *Balanus balanoides* and other barnacles. Journal of Experimental Biology 30: 584-59.

Knight-Jones, E.W. and Stevenson J.P. 1950. Gregariousness during settlement in the barnacle *Elminius modestus* Darwin. Journal of the Marine Biological Association of the United Kingdom 28: 281-297.

Knight-Jones, E.W. and Crisp, D.J. 1953. Gregariouness in barnacles in relation to the fouling of ship and to anti-fouling research. Nature 171: 1109-1110.

Kreuzer, H.J., Wang, R.L.C. and Grunze, M. 2003. Hydroxide ion adsorption on self-assembled monolayers. Journal of the American Chemical Society 125: 8384-8389.

- Kugele, M., Yule, A. B., 1993. Short communications: Mobility in lepadomorph barnacles. *Journal of the Marine Biological Association of the United Kingdom* 73: 719-722.
- Kunz, W. In: Kunz, W. editor. *Specific ion effects*. Singapore: World Scientific Publishing; 2010. 325.
- Kwok, D.Y. and Neumann, A.W. 1999. Contact angle measurements and contact angle interpretation. *Advances in Colloid and Interface Science* 81: 167-249.
- Lacombe, D. 1970. A comparative study of the cement glands in some balanid barnacles (cirripedia, balanidae). *The Biological Bulletin* 139: 164-179.
- Lagersson, N.C., Garm, A. and Høeg, J.T. 2003. Notes on the ultrastructure of the setae on the fourth antennular segment of the *Balanus amphitrite* cyprid (Crustacea: Cirripedia: Thoracica). *Journal of the Marine Biological Association of the United Kingdom* 83: 361-365
- Lagersson, N.C. and Høeg, J.T. 2002. Settlement behaviour and antennular biomechanics in cypris larvae of *Balanus amphitrite* (Crustacea: Thecostraca: Cirripedia). *Marine Biology* 141: 513-526.
- Larman, V.N., Gabbott, P.A. and East, J. 1982. Physico-chemical properties of the settlement factor proteins from the barnacle *Balanus balanoides*. *Comparative Biochemistry and Physiology* 72B: 329-338.
- Lee, G.U., Chrisey, L.A., Colton, R.J. 1994. Direct measurement of the forces between complementary strands of DNA. *Science* 266: 771-773.
- Lee, B.P., Messersmith, P.B., Israelachvili, J.N and, Waite, J.H. 2011. Mussel-inspired adhesives and coatings. *Annual Review of Material Research* 41: 99-132.
- Lejars, M., Margaillan, A. and Bressy, C. 2012. Fouling release coatings: a nontoxic alternative to biocidal antifouling coatings. *Chemical Reviews* 112: 4347-4390.
- Lemire, M. and Bourget, E. 1996. Substratum heterogeneity and complexity influence micro-habitat selection of *Balanus* sp. and *Tubularia crocea* larvae. *Mar Ecol Prog Ser* 135: 77-87.
- Le Tourneux, F. and Bourget, E. 1988. Importance of physical and biological settlement cues used at different spatial scales by the larvae of *Semibalanus balanoides*. *Marine Biology* 97: 57-66.

Lewandowski, Z. 2000. Structure and function of biofilms. In: Evans LV, editor. Biofilms: recent advances in their study and control. Amsterdam (The Netherlands): Harwood Academic Publishers. p. 1-17.

Li, Y., Gao, Y.H., Li, X.S., Yang, J.Y. and Que, G.H. 2010. Influence of surface free energy on the adhesion on marine benthic diatom *Nitzschia closterium* MMDL533. Colloids and Surfaces B: Biointerfaces 75: 550-556.

Li, H.B., Linke, W.A., Oberhauser, A.F., Carrion-Vazquez, M., Kerkvliet, J.G., Lu, H., Marszalek, P.E., and Fernandez, J.M., 2002. Reverse engineering of the giant muscle protein titin. Nature 418, 998-1002.

Lindner, E. 1992. A low surface free energy approach in the control of marine biofouling. Biofouling 6: 193-205.

Lindner, E. and Dooley, C.A. 1972. Chemical bonding in cirriped adhesive; Proc. 3rd Int. Cong. Marine Corrosion and Fouling USA 653-673.

Majumdar, P., Lee, E., Patel, N., Ward, K., Stafslie, S.J., Daniels, J., Boudjouk, P., Callow, M.E., Callow, J.A. and Thompson, S.E.M. 2008. Combinatorial materials research applied to the development of new surface coatings IX: an investigation of novel anti-fouling/fouling-release coatings containing quaternary ammonium salt groups. Biofouling 24: 185-200.

Maki, J.S., Rittschof, D., Costlow, J.D. and Mitchell, R. 1988. Inhibition of attachment of larval barnacles, *Balanus amphitrite*, by bacterial surface films. Marine Biology. 97(2): 199-206.

Maki, J.S., Rittschof, D. and Mitchell, R. 1992. Inhibition of larval barnacle attachment to bacterial films: an investigation of physical properties. Microbial Ecology. 23(1): 97-106.

Maki, J. S., Rittschof, D., Samuelsson, M-O, Szewzyk, U., Yule, A.B., Kjelleberg, S., Costlow, J.D. and Mitchell, R. 1990. Effect of marine bacteria and their exopolymers on the attachment of barnacle cypris larvae. Bulletin of Marine Science. 46(2): 499-511.

Maki, J.S., Yule, A.B., Rittschof, D. and Mitchell, R. 1994. The effect of bacterial films on the temporary adhesion and permanent fixation of cyprid larvae, *Balanus amphitrite* Darwin. Biofouling 8: 121-131.

Maleschlijski, S., Sendra, G.H., Di Fino, A., Leal-Taixe, L., Thome I., Terfort, A., Aldred, N., Grunze, M., Clare, A.S., Rosenhahn, B., Rosenhahn, A. 2012. Three dimensional tracking of exploratory behavior of barnacle cyprids using stereoscopy.

Biointerphases 7: 50.

Marinova, K.G., Alargova, R.G., Denkov, N.D., Velev, O.D., Petsev, D.N., Ivanov, I.B. and Borwankar, R.P. 1996. Charging of oil–water interfaces due to spontaneous adsorption of hydroxyl ions. *Langmuir* 12: 2045-2051.

Marabotti, I., Morelli, A., Orsini, L.M., Martinelli, E., Galli, G., Chiellini, E., Lien, E.M., Pettitt, M.E., Callow, M.E., Callow, J.A., Conlan, S.L., Mutton, R.J., Clare, A.S., Kocijan, A., Donik, C. and Jenko, M. 2009. Fluorinated/siloxane copolymer blends for fouling release: chemical characterisation and biological evaluation with algae and barnacles. *Biofouling*. 25: b481-93.

Marechal, J-P., Matsumura, K., Conlan, S. and Hellio, C. 2012. Competence and discrimination during cyprid settlement in *Amphibalanus amphitrite*. *International Biodeterioration & Biodegradation*, 72: 59-66.

Martinelli, E., Sarvothaman, M.K., Galli, G., Pettitt, M.E., Callow, M.E., Callow, J.A., Conlan, S.L., Clare, A.S., Sugiharto, A.B., Davies, C. and Williams, D. 2012. Poly(dimethyl siloxane) (PDMS) network blends of amphiphilic acrylic copolymers with poly(ethylene glycol)-fluoroalkyl side chains for fouling-release coatings. II. Laboratory assays and field immersion trials. *Biofouling* 28: 571-82.

Maruzzo, D., Conlan, S., Aldred, N., Clare, A.S. and Høeg, J.T. 2011. Video observation of surface exploration in cyprids of *Balanus amphitrite*: the movements of antennular sensory setae. *Biofouling* 27: 225-239.

Matos-Pérez, C.R., White, J.D. and Wilker, J.J. 2012. Polymer composition and substrate influences on the adhesive bonding of a biomimetic, cross-linking polymer. *Journal of the American Chemical Society* 134: 9498-505.

Matsumura, K., Mori, S., Nagano, M. and Fusetani, N. 1998a. Lentil lectin inhibits adult extract-induced settlement of the barnacle, *Balanus amphitrite*. *Journal of the Experimental Zoology* 280: 213-219.

Matsumura, K., Nagano, M. and Fusetani, N. 1998b Purification of a settlement-inducing protein complex (SIPC) of the barnacle, *Balanus amphitrite*. *Journal of the Experimental Zoology* 281: 12-20.

Matsumura, K., Nagano, M., Kato-Yoshinaga, Y., Yamazaki, M., Clare, A.S. and Fusetani, N. 1998c. Immunological studies on the settlement-inducing protein complex (SIPC) of the barnacle *Balanus amphitrite* and its possible involvement in larva-larva interactions. *Proceedings of the Royal Society B* 265: 1825-1830.

- McQuillan, A.J. 2002. From adsorption to bioadhesion at hydrous metal (oxide) surfaces. What does in situ infrared spectroscopy reveal? *Chemistry in New Zealand*. 66: 34-7.
- Mera, A.E., Fox, R.B., Bullock, S. and Wynne, K.J. 1998. Surface properties and fouling release behavior of poly(dimethylsiloxane) networks. In: Proc 21st Ann Meeting of the Adhesion Society, pp 138-140.
- Mera, A.E. and Wynne, K.J. Fluorinated silicone resin fouling release composition. US6265515, 2001.
- Meyer, A., Baier, R., Darkangelo Wood, C., Stein, J., Truby, K., Holm, E., Montemarano, J., Kavanagh, C., Nedved, B., Smith, C., Swain, G. and Wiebe, D. 2006. Contact angle anomalies indicate that surface-active eluates from silicone coatings inhibit the adhesive mechanisms of fouling organisms. *Biofouling* 22: 411-423.
- Meyers, M.A. and Chawla, K.K. 1984. *Mechanical metallurgy: Principles and applications*. Prentice-Hall, Englewood Cliffs, N.J. P. 761.
- Mignucci-Giannoni, A.A., Beck, C.A., Montoya-Ospina, R.A., Williams, E.H. 1999. Parasites and commensals of the West Indian manatee from Puerto Rico. *Journal of the Helminthological Society of Washington* 66(1): 67-69.
- Mitsui, K., Hara, M. and Ikai, A. 1996. Mechanical unfolding of alpha2-macroglobulin molecules with atomic force microscope. *FEBS Letters* 385: 29-33.
- Moore, H.B. and Frue, A.C. 1959. The settlement and growth of *Balanus improvisus*, *B. eburneus* and *B. amphitrite* in the Miami area. *Bulletin of Marine Science* 9: 421-440.
- Mori, Y., Urushida, Y., Nakanom M., Uchiyama, S. and Kamino, K. 2007. Calcite-specific coupling protein in barnacle underwater cement. *FEBS Journal* 274: 6436-6446.
- Murosaki, T., Noguchi, T., Kakugo, A., Putra, A., Kurokawa, T., Furukawa, H., Osada, Y., Gong, J.P., Nogata, Y., Matsumura, K., Yoshimura, E. and Fusetani, N. 2009. Antifouling activity of synthetic polymer gels against cyprids of the barnacle (*Balanus amphitrite*) in vitro. *Biofouling* 25: 313-320.
- Nakano, M., Shen, J-R. and Kamino, K. 2007. Self-assembling peptide inspired by a barnacle underwater adhesive protein. *Biomacromolecules* 8: 1830-1835.

Naldrett, M.J. 1993. The importance of sulphur cross-links and hydrophobic interactions in the polymerization of barnacle cement. *Journal of the Marine Biological Association of the United Kingdom* 73: 689-702.

Naldrett, M.J. and Kaplan, D.L. 1997. Characterization of barnacle (*Balanus eburneus* and *B. crenatus*) adhesive proteins. *Maine Biology*. 127: 629-635.

Nanofilm Technologie, Nanofilm EP3 ellipsometry GmbH, Göttingen, Germany.

Netz, R.R. 2004. Water and ions at interfaces. *Current Opinion in Colloid & Interface Science* 9: 192-197.

Nicklisch, S.C.T. and Waite JH. 2012. Mini-review: The role of redox in DOPA-mediated marine adhesion. *Biofouling* 28: 865-877.

Norde, W. And Lyklema, J. 1978. The adsorption of human plasma albumin and bovine pancreas ribonuclease at negatively charge polystyrene surfaces. *Journal of Colloid and Interface Science* 66: 257-265.

Nott, J.A. 1969. Settlement of barnacle larvae: surface structure of the antennular attachment disc by scanning electron microscopy. *Marine Biology* 2: 248-251.

Nott, J.A. and Foster, B.A. 1969. On the structure of the antennular attachment organ of the cypris larva of *Balanus balanoides* (L.). *Philosophical Transactions of the Royal Society, B* 256: 115-134.

Noy, A., Vezenov, D.V., and Lieber, C.M. 1997. *Annual Review of Material Science* 27: 381-421.

Nuzzo, R.G., Fusco, F.A. and Allara, D. 1987. Spontaneously organized molecular assemblies. 3. Preparation and properties of solution adsorbed monolayers of organic disulfides on gold surfaces. *Journal of the American Chemical Society* 109: 2358-2368.

Nuzzo, R.G., Dubois, L.H. and Allara, D. 1989. Fundamental studies of microscopic wetting on organic surfaces. 1. Formation and structural characterization of a self-consistent series of polyfunctional organic monolayers. *Journal of the American Chemical Society* 112: 558-569.

O'Connor, N.J. and Richardson, D.L. 1994. Comparative attachment of barnacle cyprids (*Balanus amphitrite* Darwin, 1854, *B. improvisus* Darwin, 1854, and *B. eburneus* Gould, 1841) to polystyrene and glass substrata. *Journal of Experimental Marine Biology and Ecology* 183: 213-225.

- O'Connor, N.J. and Richardson, D.L. 1996. Effects of bacterial films on attachment of barnacle (*Balanus improvisus* Darwin) larvae: Laboratory and field studies. *Journal of Experimental Marine Biology and Ecology* 206: 69-81.
- O'Connor, N.J. and Richardson, D.L. 1998. Attachment of barnacle (*Balanus amphitrite* Darwin) larvae: responses to bacterial films and extracellular materials. *Journal of the Experimental Marine Biology and Ecology* 226: 115-129.
- Ödling, K., Albertsson, C., Russell, J.T. and Mårtensson, L.G.E. 2006. An in vivo study of exocytosis of cement proteins from barnacle *Balanus improvisus* (D.) cyprid larva. *Journal of the Experimental Biology* 209: 956-964.
- Ohsawa, K., Murata, M. and Ohshima, H. 1986. Zeta potential and surface charge density of polystyrene-latex; comparison with synaptic vesicle and brush border membrane vesicle. *Colloid and Polymer Science* 264: 1005-1009.
- Okano, K., Shimizu, K., Satuito, C.G. and Fusetani, N. 1996. Visualization of cement exocytosis in the cypris cement gland of the barnacle *Megabalanus rosa*. *The Journal of Experimental Biology*. 199: 2131-2137.
- Okano, K., Shimizu, K., Satuito, C.G. and Fusetani, N. 1998. Enzymatic isolation and culture of cement secreting cells from cypris larvae of the barnacle *Megabalanus rosa*. *Biofouling*. 12: 149-159.
- Olivier, F., Tremblay, R., Bourget, E. and, Rittschof, D. 2000. Barnacle settlement: field experiments on the influence of larval supply, tidal level, biofilm quality and age of *Balanus amphitrite* cyprids. *Marine Ecology Progress Series* 199: 185-204.
- Owens, D.K. and Wendt, R.C. 1969. Estimation of the surface free energy of polymers. *Journal of Applied Polymer Science* 13: 1741-1747.
- Patwardhan, S.V., Taori, V.P., Hassan, M., Agashe, N.R., Franklin, J.E., Beaucage, G., Mark, J.E. and Clarson, S.J. 2006. An investigation of the properties of poly (dimethylsiloxane)-bioinspired silica hybrids. *European Polymer Journal* 42: 167-178.
- Petrone, L. 2013. Molecular surface chemistry in marine bioadhesion. *Advances in Colloid and Interface Science* 195-196: 1-18.
- Petrone, L., Aldred, N., Emami, K., Enander, K., Ederth, T. and Clare, A.S. 2015. Chemistry-specific surface adsorption of the barnacle settlement-inducing protein complex. *Interface focus*. 5:20140047.

Petrone, L., Di Fino, A., Aldred, N., Sukkaew, P., Ederth, T., Clare, A.S. and Liedberg, B. 2011. Effects of surface charge and Gibbs surface energy on the settlement behaviour of barnacle cyprids (*Balanus amphitrite*). *Biofouling* 27: 1043-1055.

Petrone, L., Lee, S.S.C., Teo, S.L.M. and Birch, W.R. 2013. A novel geometry for a laboratory-based larval settlement assay. *Biofouling* 29: 213-221.

Petrone, L., Ragg, N.L.C., Girvan, L. and McQuillan, A.J. 2009. Scanning electron microscopy and energy dispersive Xray microanalysis of *Perna canaliculus* mussel larvae adhesive secretion. *Journal of Adhesion* 85: 78-96.

Petrone, L., Ragg, N.L.C. and McQuillan, A.J. 2008 In situ infrared spectroscopic investigation of *Perna canaliculus* mussel larvae primary settlement. *Biofouling* 24: 405-413.

Petronis, S., Berntsson, K., Golde, J. and Gatenholm, P. 2000. Design and microstructuring of PDMS surfaces for improved marine biofouling resistance. *Journal of Biomaterials Science, Polymer Edition* 11: 1051-1072.

Phang, I.Y., Aldred, N., Clare, A.S., Callow, J.A. and Vancso, G.J. 2006. An in situ study of the nanomechanical properties of barnacle (*Balanus amphitrite*) cyprid cement using atomic force microscopy (AFM). *Biofouling* 22: 245–250.

Phang, I.Y. Aldred, N. Clare, A.S. and Vancso, G.J. 2007. Development of effective marine antifouling coatings - studying barnacle cyprid adhesion with atomic force microscopy. *NanoS*. 01: 35-39.

Phang, I.Y. Aldred, N. Clare, A.S. and Vancso, G.J. 2008. Towards a nanomechanical basis for temporary adhesion in barnacle cyprids (*Semibalanus balanoides*). *Journal of the Royal Society Interface*. 5: 397-401.

Phang, I.Y, Aldred, N., Ling, X.Y, Huskens, J., Clare, A.S. and Vancso, G.J. 2010. Atomic force microscopy of the morphology and mechanical behaviour of barnacle cyprid footprint proteins at the nanoscale. *Journal of the Royal Society Interface* 7: 285-296.

Phang, I.Y., Aldred, N., Ling, X.Y., Tomczak, N., Huskens, J., Clare, A.S. and Vancso, G.J. 2009a. Chemistry-specific interfacial forces between barnacle (*Semibalanus balanoides*) cyprid footprint proteins and chemically functionalised AFM tips. *The Journal of Adhesion* 85: 616-630

Phang, I.Y., Chaw, K.C., Choo, S.S.H., Kang, R.K.C., Lee, S.S.C., Birch, W.R., Teo, S.L.M. and Vancso, C.J. 2009b. Marine biofouling field tests, settlement assay and

footprint micromorphology of cyprid larvae of *Balanus amphitrite* on model surfaces. *Biofouling* 25: 139-147.

Pinori, E., Elwing, H. and Berglin, M. 2013. The impact of coating hardness on the anti-barnacle efficacy of an embedded antifouling biocide. *Biofouling* 29: 763-773.

Pletikapić, G., Berquand, A., Mišić Radić, T. and Svetličić, V. 2012. Quantitative nanomechanical mapping of marine diatom in seawater using peak force tapping atomic force microscopy. *Journal of Phycology*. 48(1): 174-185.

Politis, G., Downie, M. and Atlar, M. 2009. Design of a turbulent channel flow facility for antifouling coating research. *Proceeding 1st Advanced Model Measurement Technology Nantes* 12-17.

Pyefinch, K.A. and Mott, J.C. 1948. The sensitivity of barnacles and their larvae to copper and mercury. *The Journal of Experimental Biology* 25: 276-298.

Qian, P.Y., Rittschof, D. and Sreedhar, B. 2000. Macrofouling in unidirectional flow: miniature pipes as experimental models for studying the interaction of flow and surface characteristics on the attachment of barnacle, bryozoans and polychaete larvae. *Marine Ecology Progress Series* 207: 109-121.

Qiu, J.W., Hung, O.S. and Qian, P.Y. 2008. An improved barnacle attachment inhibition assay. *Biofouling* 24: 259-266.

Raman, S. and Kumar, R. 2011. Interfacial morphology and nanomechanics of cement of the barnacle, *Amphibalanus reticulatus*, on metallic and non-metallic substrata. *Biofouling*. 27: 569-577.

Ramsay, D.B., Dickinson, G.H., Orihuela, B., Rittschof, D. and Wahl, K.J. 2008. Base plate mechanics of the barnacle *Balanus amphitrite* (= *Amphibalanus amphitrite*). *Biofouling* 24: 109-118.

Rasmussen, K., Willemsen, P.R. and Østgaard, K. 2002. Barnacle settlement on hydrogels. *Biofouling* 18: 177-191.

Rath, S.K., Chavan, J.G., Sasane, S., Srivastava, A., Patri, M., Samui, A.B., Chakraborty, B.C. and Sawant, S.N. 2009. Coatings of PDMS-Modified Epoxy via Urethane Linkage: Segmental Correlation Length, Phase Morphology, Thermomechanical and Surface Behavior *Progress in Organic Coatings* 65: 366-374.

Rath, S. K., Chavan, J. G., Sasane, S., Jagannath, Patri, M., Samui, A.B. and Chakraborty, B. C. 2010. Two component silicone modified epoxy foul release

coatings: Effect of modulus, surface energy and surface restructuring on pseudobarnacle and macrofouling behaviour. *Applied Surface Science* 256: 2440-2446.

Regulation (EU) No 528/2012 of the European Parliament and of the Council of 22 May 2012 concerning the making available on the market and use of biocidal products
Text with EEA relevance

Rittschof, D. and Costlow, J.D. 1989. Bryozoan and barnacle settlement in relation to initial surface wettability: a comparison of laboratory and field studies. *Scientia Marina* 53: 411-416.

Rittschof, D., Branscomb, E. S. and Costlow, J. D. 1984. Settlement and behavior in relation to flow and surface in larval barnacles, *Balanus amphitrite* Darwin. *Journal of Experimental Marine Biology and Ecology* 82(2-3): 131-146.

Ritz, D.A. 1974. Factors influencing the settlement of marine invertebrate larvae. In *Chemoreception in Marine Organisms* (ed. P. T. Grant and A. M. Mackie), pp. 177-265. Academic Press.

Roberts, D., Rittschof, D., Holm, E. and Schmidt, A.R. 1991. Factors influencing initial larval settlement: temporal, spatial and surface molecular components. *Journal of Experimental Marine Biology and Ecology* 150: 203-221.

Rodahl M, Hook F, Krozer A, Brzezinski P and Kasemo B. 1995. Quartz crystal microbalance setup for frequency and Q-factor measurements in gaseous and liquid environments. *Review of Scientific Instruments* 66: 3924-3930.

Rothenhausler, B. and Knoll, W. 1988. Surface-plasmon microscopy. *Nature* 332: 615-617.

Ruzga-Wijas, K., Mirerska, V., Fertuniak, W., Chojnowski, J., Halska, R. and Werel, W. 2007. Quaternary ammonium salts (QAS) modified polysiloxane biocide supported on silica materials. *Journal of Inorganic Organometallic Polymers* 17: 605-613.

Salta, M., Wharton, J.A., Stoodley, P., Dennington, S.P, Goodes, L.R, Werwinski, S., Mart, U., Wood, R.J.K and Stokes, K.R. 2010. Designing biomimetic antifouling surfaces. *Philosophical Transactions of the Royal Society, B* 368: 4729-4754.

Santos, R., Aldred, A., Gorb, S. N., and Flammang, P. (Eds.) 2013. *Biological and biomimetic adhesives - challenges and opportunities*. 208 pp. RSC publishing, Cambridge, UK.

Saroyan, J.R., Lindner, E. and Dooley, C.A. 1968. Attachment mechanism of barnacles, in Proc. 2nd Int. Congr. on Marine Corrosion and Fouling. Technical Chamber of Greece, Athens, 495.

Saroyan, J.R., Lindner, E. and Dooley, C.A. 1970. Repair and reattachment in the balanidae as related to their cementing mechanism. The Biological Bulletin. 139: 333-350.

Satuito, C.G., Shimizu, K., Natoyama, K., Yamazaki, M. and Fusetani, N. 1996. Age-related settlement success by cyprids of the barnacle *Balanus amphitrite*, with special reference to consumption of cyprid storage protein. Marine Biology 127: 125-130.

Scardino, A.J. and de Nys, R. 2011. Mini review: Biomimetic models and bioinspired surfaces for fouling control. Biofouling 27: 73-86.

Shibata, M., Yamashita, H., Uchihashi, T., Kandori, H. and Ando, T. 2010. High-speed atomic force microscopy shows dynamic molecular processes in photoactivated bacteriorhodopsin. Nature Nanotechnology 5: 208-212.

Shimizu, K., Saikawa, W. and Fusetani, N. 1996. Identification and partial characterization of vitellin from the barnacle *Balanus amphitrite*. Comparative Biochemistry and Physiology Part B: Biochemistry and Molecular Biology 115(1): 111-119.

Schmidt, M., Cavaco, A., Gierlinger, N., Aldred, N., Fratzl, P., Grunze, M. and Clare, A.S. 2009. In situ imaging of barnacle (*Balanus amphitrite*) cyprid cement using confocal Raman microscopy. The Journal of Adhesion 85: 139-51.

Schmitt, F.J., Ederth, T., Weidenhammer, P., Claesson, P. and Jacobasch, H.J. 1999. Direct force measurements on bulk polystyrene using the bimorph surface forces apparatus. Journal of Adhesion Science and Technology 13: 79-96.

Schmidt, D., Shah D. and Giannelis, E.P. 2002. New advances in polymer/layered silicate nanocomposites. Current Opinion in Solid State and Materials Science 6: 205-212.

Schonhorn, H. 1981. Adhesion in Cellulosic and Wood-Based Composites NATO Conference Series Volume 3, pp 91-111 Adhesion and Adhesives: Interactions at Interfaces.

Schultz, M.P. 2004. Frictional resistance of antifouling coating systems. ASME Journal of Fluids Engineering 126: 1039-1047.

- Schultz, M.P., Bendick, J.A, Holm, E.R. and Hertel, W.M. 2011. Economic impact of biofouling on a naval surface ship. *Biofouling* 27: 87-98.
- Schultz, M.P., Finlay, J.A., Callow, M.E., and Callow J.A. 2000. A turbulent channel flow apparatus for the determination of the adhesion strength of microfouling organisms. *Biofouling* 15: 243-251.
- Singer, I. L., Kohl, J.G. and Patterson, M. 2000. Mechanical aspects of silicone coatings for hard foulant control. *Biofouling* 16: 301-309.
- Singh, S., Houston, J., van Swol, F., and Brinker, C.J. 2006. Drying transition of confined water. *Nature* 442: 526-526.
- Smith, J.M., Barnes, W.J.P., Downie, J.R. and Ruxton, G.D. 2006. Adhesion and allometry from metamorphosis to maturation in hylid tree frogs: a sticky problem. *Journal of Zoology* 270: 372--83.
- Sommer, S., Ekin, A., Webster, D.C., Stafslie, S.J., Daniels, J., Van der Wal, L.J., Thompson, S.E.M., Callow, M.E. and Callow, J.A. 2010. A preliminary study on the properties and fouling-release performance of siloxane-polyurethane coatings prepared from poly(dimethylsiloxane) (PDMS) macromers. *Biofouling* 26: 961-972.
- Stanley, M.S. and Callow, J.A. 2007. Whole cell adhesion strength of morphotypes and isolates of *Phaeodactylum tricornutum* (Bacillariophyceae). *European Journal of Phycology* 42(2): 191-197.
- Stein, J., Truby, K., Darkangelo Wood, C., Takemori, M., Vallance, M., Swain, G., Kavanagh, C., Kovach, B., Schultz, M., Weibe, D., Holm, E., Montemarano, J., Wendt, D., Smith C., and Meyer, A. 2003a. Silicone foul release coatings: effect of the interaction of oil and coating functionalities on the magnitude of macrofouling attachment strengths. *Biofouling*. 19: 71-82.
- Stein, J., Truby, K., Darkangelo Wood, C., Takemori, M., Vallance, M., Swain, G., Kavanagh, C., Kovach, B., Schultz, M., Weibe, D., Holm, E., Montemarano, J., Wendt, D., Smith C., and Meyer, A. 2003b. Structure-property relationships of silicone biofouling-release coatings: effect of silicone network architecture on pseudobarnacle attachment strengths. *Biofouling* 19: 87-94.
- Stewart, R.J., Ransom, T.C. and Hlady, V. 2011. Natural underwater adhesives. *Journal of Polymer Science Part B: Polymer Physics* 49: 757-771.

- Strand, J. and Jacobsen, J. 2005 Accumulation and trophic transfer of organotins in a marine food web from the Danish coastal waters. *Science of The Total Environment* 350: 72-85.
- Strausberg, R.L. and Link, R.P. 1990. Protein-based medical adhesives. *Trends in Biotechnology* 8: 53-7.
- Sun, Y., Guo, S., Walker, G.C., Kavanagh, C.J. and Swain, G.W. 2004. Surface Elastic Modulus of Barnacle Adhesive and Release Characteristics from Silicone Surfaces. *Biofouling* 20: 279-289.
- Svetličić V, Žutić V, Pletikapić G, Mišić Radić T. 2013. Marine polysaccharide networks and diatoms at the nanometric scale. *International Journal of Molecular Sciences*. 14(10): 20064-20078.
- Swain, G.W. and Schultz, M.P. 1996. The testing and evaluation of nontoxic antifouling coatings. *Biofouling*. 10: 187-197.
- Swain, G.W., Nelson, W.G. and Preedeekanit, S. 1998. The influence of biofouling adhesion and biotic disturbance on the development of fouling communities on non-toxic surfaces. *Biofouling*. 12: 257-269.
- Tang, Y., Finlay, J.A., Kowalke, G.L., Meyer, A.E., Bright, F.V., Callow, M.E., Callow, J.A., Wendt, D.E. and Detty, M.R. 2005. Hybrid xerogel films as novel coatings for antifouling and fouling release. *Biofouling* 21: 59-71.
- Thompson, R.C., Hawkins, S.J. and Norton, T.A. 1998. The influence of epilithic microbial films on the settlement of *Semibalanus balanoides* cyprids a comparison between laboratory and field experiments. *Hydrobiologia* 375/376: 203-216.
- Toonen, R.J. and Pawlik, J.R. 1994. Foundations of gregariousness. *Nature* 370: 511-512.
- Townsin, R.L. 2003. The ship hull fouling penalty. *Biofouling* 19(Suppl):9-16. Conference: 11th International Congress on Marine Corrosion and Fouling Location: SAN DIEGO, CALIFORNIA Date: JUL, 2002 Sponsor(s): COIPM; USN Off Naval Res; Rohm & Hass Co; Florida Inst Technol; European Copper Antifouling Task Force; Arch Chem Inc; Hempels Marine Paints AS; Int Paint Inc; Jotun Paints AS; Sherwin Williams Co; US Coast Guard; Taylor & Francis Ltd; Poseidon Ocean Sci Inc Source: *Biofouling* 19(S): 9-15.

- Tremblay, R., Olivier, F., Bourget, E. and Rittschof, D. 2007. Physiological condition of *Balanus amphitrite* cyprid larvae determines habitat selection success. *Marine Ecology Progress Series*. 340: 1-8.
- Truby, K., Wood, C., Stein, J., Cella, J., Carpenter, J., Kavanagh, C., Swain, G., Wiebe, S., Lapota, D., Meyer, A., Holm, E., Wendt, D., Smith, C. and Montemarano, J. 2000. Evaluation of the performance enhancement of silicone biofouling-release coatings by oil incorporation. *Biofouling* 15: 141-150.
- Urushida, Y., Nakano, M., Matsuda, S., Inoue, N., Kanai, S., Kitamura, N., Nishino, T. and Kamino, K. 2007. Identification and functional characterization of a novel barnacle cement protein. *FEBS Journal* 274: 4336-4346.
- van Oss, C.J. 1994. *Interfacial forces in aqueous media*. New York: Marcel Dekker. p. 170-185.
- Vansant, E.F., Van der Voort, P. and Vranken, K.C. 1995. Characterization and chemical modification of the silica surface. In: Delmon B, Yates JT, editors. *Studies in surface science and catalysis*. Vol. 93. Amsterdam: Elsevier Science. 560 pp.
- Varenberg, M., Pugno, M. and Gorb, S. 2010 Spatulate structures in biological fibrillar adhesion. *Soft Matter* 6: 3269-3272.
- Viegas, J. 2009. Natural super glue found on asparagus spears. *Discovery News*. <http://news.discovery.com/earth/asparagus-glue-beetle.html>
- Voigt, D. and Gorb, S. 2010. Egg attachment of the asparagus beetle *Crioceris asparagi* to the crystalline waxy surface of *Asparagus officinalis*. *Proceedings of the Royal Society B* 22(277): 895-903.
- Wahl, M. 1989. Marine epibiosis. I. Fouling and antifouling: some basic aspects. *Mar Ecol Prog Ser* 58: 175-189.
- Waite, J.H. 1983. Evidence for a repeating 3,4-dihydroxyphenylalanine- and hydroxyproline-containing decapeptide in the adhesive protein of the mussel, *Mytilus edulis* L. *The Journal of Biological Chemistry*. 258: 2911-2915.
- Waite, J.H. 2002. Adhesion à la Moule. *Integrative and Comparative Biology*., 42: 1172-1180.
- Walker G. 1970. The histology, histochemistry and ultrastructure of the cement apparatus of three adult sessile barnacles, *Elminius modestus*, *Balanus balanoides* and *Balanus hameri*. *Marine Biology* 7: 239-248.

Walker G. 1971. A study of the cement apparatus of the cypris larva of the barnacle *Balanus balanoides*. *Marine Biology* 9: 205-212.

Walker, G. 1972. The biochemical composition of the cement of two barnacle species, *Balanus hameri* and *Balanus Crenatus*. *Journal of the Marine Biological Association of the United Kingdom* 52: 429-435

Walker, G. 1973. The early development of the cement apparatus in the barnacle, *Balanus balanoides* (L.) (Crustacea: Cirripedia). *Journal of the Experimental Marine Biology and Ecology* 12: 305-314.

Walker, G., 1995. Larval settlement: historical and future perspective. In: Schram, F.R., Høeg, J.T. (Eds.), *New Frontiers in Barnacle Evolution*. A.A. Balkema, Rotterdam, pp. 69-85.

Walker, G. and Yule, A.B. 1984a. Temporary adhesion of the barnacle cyprid: the existence of an antennular adhesive secretion. *Journal of the Marine Biological Association of the United Kingdom* 64: 679-686.

Walker, G. and Yule, A.B. 1984b. The temporary adhesion of barnacle cyprids: effects of some differing surface characteristics. *Journal of the Marine Biological Association of the United Kingdom* 64: 429-439.

Walker, G., Yule, A.B. and Nott, J.A. 1987. Structure and function in balanomorph larvae, in: Southward, A.J. *Barnacle biology*. *Crustacean Issues*, 5: 307-328.

Walley, L. 1969. Studies on the larval structure and metamorphosis of *Balanus balanoides* (L.). *Philosophical Transactions of the Royal Society B* 256: 237-280.

Wang, C.S. and Stewart, R.J. 2012. Localization of the bioadhesive precursors of sandcastle worm, *Phragmatopoma californica*. *Journal of the Experimental Biology* 15: 351-61.

Webster, D.C., Chisholm, B.J. and Stafslie, S.J. 2007. Mini-review: Combinatorial approaches for the design of novel coatings systems. *Biofouling*. 23: 179-192.

Wendt, D.E., Kowalke, G.L., Kim, J. and Singer, I.L. 2006. Factors that influence elastomeric coating performance: the effect of coating thickness on basal plate morphology, growth and critical removal stress of the barnacle *Balanus amphitrite*. *Biofouling*. 22: 1-9.

Wiegemann M. 2005. Adhesion in blue mussels (*Mytilus edulis*) and barnacles (genus *Balanus*): Mechanisms and technical applications. *Aquatic Sciences*. 67: 166-176.

Wiegemann, M., Kowalik, T. and Hartwig, A. 2006. Noncovalent bonds are key mechanisms for the cohesion of barnacle (*Balanus crenatus*) adhesive proteins. *Marine Biology* 149: 241-46.

Wiegemann, M. and Watermann, B. 2003. Peculiarities of barnacle adhesive cured on non-stick surfaces. *Journal of the Adhesion Science and Technology* 17(14): 1957-1977.

Wiegemann, M. and Watermann, B. 2004. The impact of desiccation on the adhesion of barnacles attached to non-stick coatings. *Biofouling*. 20: 147-153.

Williams, G.B., 1964. The effects of extracts of *Fucus serratus* in promoting the settlement of larvae of *Spirorbis borealis* (Polychaeta). *Journal of the Marine Biological Association of the United Kingdom* 44: 397-414.

Williams, G.B. 1965. Observations on the behaviour of the planulae of *Clava squamata*. *Journal of the Marine Biological Association of the United Kingdom* 45: 257-273.

Wilson, D.P., 1968. The settlement behaviour of the larvae of *Sabellaria alveolata* (L.). *Journal of the Marine Biological Association of the United Kingdom* 48: 387-435.

Wilson, D.P., 1970a. Additional observations on larval growth and settlement of *Sabellaria alveolata*. *Journal of the Marine Biological Association of the United Kingdom* 50: 1-31.

Wilson, D.P., 1970b. The larvae of *Sabellaria spinulosa* and their settlement behaviour. *Journal of the Marine Biological Association of the United Kingdom* 50: 33-52.

Woods Hole Oceanographic Institution (1952). *Marine fouling and its prevention*. Naval Institute Press, Annapolis, MD, p 97.

Yebra, D.M., Kiil, S. and Dam-Johansen, K. 2004. Antifouling technology - past, present and future steps towards efficient and environmentally friendly antifouling coatings. *Progress in Organic Coatings* 50: 75-104.

Yule, A.B. and Walker, G. 1985 Settlement of *Balanus balanoides*: the effect of cyprid antennular secretion. *Journal of the Marine Biological Association of the United Kingdom* 65: 707-712.

Yule, A.B. and Walker, G. 1987. In *Barnacle Biology*; Southward, A. J., Ed.; *Crustacean Issues*; A.A. Balkema: Rotterdam, Germany 5: 389-402.

Zaera, F. 2012. Probing liquid/solid interfaces at the molecular level. *Chemical Reviews* 112: 2920-86.

Zhang, J., Lin, C., Wang, L., Zheng, J., Peng, W. and Duan, D. 2011. The influence of elastic modulus on the adhesion of fouling organism to poly(dimethylsiloxane) (PDMS). *Advanced Materials Research* 152-153: 1466-1470.

Zhao, Q., Wang, S. and Müller-Steinhagen, H. 2004. Tailored surface free energy of membrane diffusers to minimize microbial adhesion. *Applied Surface Science* 230: 371-378.

Zhao, Q., Su, X., Wang, S., Zhang, X., Navabpour, P. and Teer, D. 2009. Bacterial attachment and removal properties of silicon- and nitrogen-doped diamond-like carbon coatings. *Biofouling* 25: 377-385.

Zardus, J.D., Nedved, B., Huang, Y., Tran, C. and Hadfield, M.G. 2008. Microbial biofilms facilitate adhesion in biofouling invertebrate. *The Biological Bulletin* 14(1): 91-8.

Zisman, W.A. and Fowkes, F. 1964. Relation of the equilibrium contact angle to liquid and solid constitution. Contact angle, wettability and adhesion. *Advances in Chemistry Series* 43: 1-51.

Zisman, W.A. 1972. Surface energetics of wetting, spreading and adhesion. *Journal of Paint Technology* 44: 41-57.